

## ABSTRACT

Title of Thesis:                   ENHANCED PRODUCTION OF  
  BIOSOLIDS BY IMPROVED ACTIVATED  
  SLUDGE CLARIFICATION AND  
  STRUCTURED WATER ANALYSIS

Xiaocen Liu, Master of Science, 2017

Thesis Directed By:            Dr. Birthe V. Kjellerup  
  Department of Civil and Environmental  
  Engineering, University of Maryland

Biosolids contain high contents of soil-required nutrients, so that have been widely applied in land application. The production of the biosolids depends on the clarification performance and dewaterability of the sludge, which are influenced by bioflocculation and structured water content, respectively. Therefore, research on sludge bioflocculation improvement and structured water content determination were proposed in this study. The result indicated that different activated sludge exhibited various bioflocculation limitations. Influence of the sludge characteristics such as the extracellular polymeric substances (EPS) composition, viscosity and floc size on the structured water content were also investigated. The results indicated that no significant correlation was observed between the EPS composition and the structured water content, however, the sludge floc size was positively correlated with it. The bioflocculation limitations

were pinpointed, and how floc size influenced the structured water content needed further studies to improve sludge dewaterability, therefore, enhance the biosolids production quantitatively and qualitatively.

ENHANCED PRODUCTION OF BIOSOLIDS BY IMPROVED  
ACTIVATED SLUDGE CLARIFICATION AND STRUCTURED WATER  
ANALYSIS

by

Xiaocen Liu

Thesis submitted to the Faculty of the Graduate School of the  
University of Maryland, College Park, in partial fulfillment  
of the requirements for the degree of  
[Master of Science]  
[2017]

Advisory Committee:  
Professor Birthe Kjellerup, Chair  
Dr. Alba Torrents  
Dr. Haydée De Clippeleir

© Copyright by  
[Xiaocen Liu]  
[2017]

## Acknowledgements

This project carried out during May, 2016 to August, 2017 in the research laboratory of the Blue Plains Advanced Wastewater Treatment Plant (DC Water). I want to express my gratitude to the Blue Plains Advanced Wastewater Treatment Plant for funding the entire project. Without this support, the research would not have been performed.

I also want to thank The Department of Civil and Environmental Engineering at the University of Maryland at College Park for the support that made this project possible.

I own my deepest gratitude to my advisor at the University of Maryland Dr. Birthe Venø Kjellerup for her guidance and support on my study and research, and I learnt a lot from her. She gave me valuable suggestions on how to lead a graduate project and encouraged me to be curious about all the observations about my project. She made significant contribution on the completion of this thesis.

I am deeply grateful to my supervisor at DC Water Dr. Haydée De Clippeir. Her suggestions and advice were important and helped me carry out the project. Without her help, I would not have been able to complete this project.

# Table of Contents

Acknowledgements.....	ii
Table of Contents.....	iii
List of Tables.....	v
List of Figures.....	vi
List of Abbreviations.....	viii
Chapter 1: Introduction.....	1
1.1 Problem Statement.....	1
1.2 Objectives.....	2
Chapter 2: Literature Review.....	4
2.1 Biosolids.....	4
2.2 Sludge Clarification and Bioflocculation.....	5
2.3 Anaerobic Digestion.....	7
2.4 Dewatering Process.....	7
2.5 Structured Water.....	8
2.6 Extracellular Polymeric Substances (EPS).....	12
Chapter 3: Manuscript 1: Identification of coagulation, flocculation and floc strength limitations in activated sludge using modified jar tests.....	14
Abstract.....	14
3.1 Introduction.....	15
3.2 Materials and Methods.....	19
3.2.1 Sample location and acquirement.....	19
3.2.2 Polymer types and preparation.....	19
3.2.3 Modified Jar test.....	20
3.2.4 Classic and novel settling metrics.....	22
3.2.5 Extracellular polymeric substances.....	22
3.3 Results.....	23
3.3.1 High-rate activated sludge.....	23
3.3.2 Bioaugmented high-rate activated sludge.....	26
3.3.3 Biological nutrient removal sludge.....	28
3.4 Discussion.....	34
3.4.1 Evaluation of modified jar tests.....	34
3.4.2 Limitations in HRAS sludge.....	35
3.4.3 Impact of bioaugmentation of HRAS on floc formation limitations.....	39
3.4.4 Impact of SRT and organic loading rate on floc formation limitations.....	41
3.5 Conclusion.....	42
3.6 References.....	42
Chapter 4: Manuscript 2: Influence of extracellular polymeric substance (EPS) on the structured water content in the sludge and objective measurements of the structured water content.....	45
Abstract.....	45
4.1 Introduction.....	46
4.2 Materials and Methodology.....	53
4.2.1 Sample locations and acquisition.....	53

4.2.2 Determination of the structured water content.....	54
4.2.3 Extracellular polymeric substances (EPS) extraction .....	56
4.2.4 Extracellular polymeric substances (EPS) Composition .....	57
4.2.5 Floc Size quantification .....	60
4.2.6 Approaches for Determination of the Structured Water Content .....	60
4.3 Results and Discussion .....	61
4.3.1 Determination of the Structured Water Content .....	61
4.3.2 Structured Water Content Values .....	71
4.3.3 Impact of EPS on the Structured Water Content .....	77
4.3.4 Impact of Dynamic Viscosity on the Structured Water Content .....	94
4.3.5 Impact of Floc Size on the Structured Water Content .....	96
4.3.6 Assessment of the approaches for determination of the Structured Water Content .....	97
4.4 Conclusion .....	101
4.5 Acknowledgements.....	103
4.6 References.....	103
Chapter 5: Conclusion.....	107
References (Chapter 1, 2 and 5, excluding manuscript references).....	114

## List of Tables

Table 3.1. Intrinsic characteristics of the tested sludge types -----	30
Table 4.1. EPS analysis for five sludge types -----	78
Table 4.2. Floc sizes for four sludge types -----	97

## List of Figures

Figure 2.1. Wastewater treatment process diagram-----	4
Figure 2.2. Moisture distribution in a sewage sludge floc-----	9
Figure 2.3. Drying curve-----	11
Figure 3.1. Orthokinetic and gravitational flocculation curves for activated sludge -----	31
Figure 3.2. Settling velocity distribution (line) -----	31
Figure 3.3. Polymer response curves -----	32
Figure 3.4. Orthokinetic flocculation curve -----	33
Figure 3.5. Settling velocity distribution (scatter) -----	34
Figure 4.1. Moisture distribution in a sewage sludge floc-----	49
Figure 4.2. Drying curve-----	50
Figure 4.3. Drying test set up -----	56
Figure 4.4. Drying rate curve for the THP sludge (forward rolling average) -----	64
Figure 4.5. Weight curve for the THP sludge (forward rolling average) -----	69
Figure 4.6. Structured water content from the drying rate curve and Monod model -----	73
Figure 4.7. Structured water content from the weight curve -----	75
Figure 4.8. Cake TS of five sludge types-----	77
Figure 4.9. Relationship between the COD and the structured water content -----	80
Figure 4.10. The structured water content and EPS composition (baseline A)	84-85
Figure 4.11. The structured water content and EPS composition (baseline B)	86-87
Figure 4.12. The structured water content and EPS composition (baseline C)	88-89

Figure 4.13. The structured water content and EPS composition (baseline D)90-91  
Figure 4.14. The structured water content and EPS composition (Monod) ---92-93  
Figure 4.15. Dynamic viscosity of the primary sludge -----95  
Figure 4.16. Flocs of five sludge types under microscope view -----96

## List of Abbreviations

AWWTP - advanced wastewater treatment plant  
Bio-HRAS - Bioaugmented high-rate activated sludge  
BNR - Biological nutrient removal sludge  
BP – Branched polymer  
C - PolyDADMAC  
COD – Chemical oxygen demand  
CSV - Critical settling velocity  
DLVO - Derjaguin-Landau-Verwey-Overbeek  
EPS - Extracellular polymeric substances  
HRAS – High-rate activated sludge  
ISV - Initial settling velocity  
LB-EPS – Loosely bound extracellular polymeric substances  
LOSS - Limit of Stokesian settling  
LP – Linear polymer  
M/D ratio - monovalent to divalent ratio  
PN – Protein  
PRC – Polymer response curve  
PS – Polysaccharides  
OFC – Orthokinetic flocculation curve  
SRT- Solis retention time  
SWC – Structured water content  
SVD - Settling velocity distribution  
SVI - Sludge volume index  
TB-EPS – Tightly bound extracellular polymeric substances  
TOF - Threshold of flocculation  
TS – Total solids  
TSS – Total suspended solids  
VSS – Volatile suspended solids  
WWTP – Wastewater treatment plant

# 1 **Chapter 1: Introduction**

## 2 **1.1 Problem Statement**

3           In wastewater treatment plants, sludge from different treatment stages  
4           confluences in the anaerobic digestion tank, where the final treatment process of  
5           the sludge produces biogas (methane) for energy recovery. Thereafter, the treated  
6           sludge is dewatered, and the solids collected after the dewatering process is  
7           referred to as biosolids. Biosolids contain high concentrations of nitrogen and  
8           phosphorus, and the material is subsequently used for land applications such as  
9           farming, silviculture, soil reclamation and others (Esteller et al., 2009; Wang,  
10          Shammas and Hung, 2007).

11           The total amount of the sludge that is separated in various treatment  
12          processes is the source for the biosolids. Therefore, the sludge clarification is an  
13          important process that influences the biosolids production. However, activated  
14          sludge (secondary sludge) is considered as clarification limited (Li et al., 2016),  
15          where metal salts and high molecular weight polymers are added to improve the  
16          separation. Floc formation is an important process that determines the activated  
17          sludge clarification. Therefore, a study that investigates the limitations that  
18          prevent the floc formation in the activated sludge is proposed (Chapter 3).

19           Reduction of the moisture content from the biosolids can reduce the  
20          volume and total weight, which reduces the need for biosolids storage and  
21          transportation requirements thus reducing the costs for biosolids handling and  
22          therefore also environmental foot print including a reduction of greenhouse gases  
23          from handling and transportation. The dewatering process aims to remove as

24 much water as possible to achieve a small biosolids volume. However, the  
25 dewatering process also has limitations (Vaxelaire, 2001). A proportion of the  
26 water in the biosolids cannot be removed by traditional dewatering treatments,  
27 and this part of water is referred to as structured water. Measurements of the  
28 structured water content in various sludge types served as a good estimate of the  
29 dewatering ability and biosolids quality (Neyens, 2004; Lee, Lai and Mujumdar,  
30 2006). However, current measurements of the structured water content are either  
31 dependent on subjective evaluations or require complicated approaches (Smith  
32 and Vesilind, 1995). Therefore, objective measurements of the structured water  
33 content using the drying test are proposed (Chapter 4).

34

## 35 **1.2 Objectives**

36 The objective of this research was to study the biosolids production  
37 considering both sludge sources and dewatering ability. Pinpointing the  
38 clarification limitations of the activated sludge paves for further studies aiming at  
39 improving the clarification capacity, so that increased volumes of sludge can be  
40 treated in the anaerobic digestion process. Sludge dewaterability determines the  
41 moisture content in the biosolids (Murthy, Novak and Holbrook, 2000). Objective  
42 measurements of the structured water content in the sources of sludge can provide  
43 information about the dewaterability of these sludge types.

44 The objectives of the study were:

45 (1) Pinpoint bioflocculation limitations for the activated sludge;

46 (2) Determine objective measurements of the structured water content for  
47 different sludge types and study the sludge characteristics influences  
48 on the structured water content;

49 (3) Provide suggestions for further study in this field that aiming to  
50 increase the biosolids production and quality.

51 In this study, a manuscript titled: “Identification of coagulation,  
52 flocculation and floc strength limitations in activated sludge using modified jar  
53 tests” evaluating bioflocculation limitations in high–rate activated sludge is  
54 shown in Chapter 3 for objective (1).

55 A second manuscript titled: “Influence of extracellular polymeric  
56 substance (EPS) on the structured water content in the sludge and objective  
57 measurements of the structured water content” evaluated objective measurements  
58 of structured water content and the influence of sludge characteristics on the  
59 structured water was present in Chapter 4 for objective (2). Suggestions on further  
60 studies about biosolids production was shown in Chapter 5 for objective (3).

61

62

63

64

65

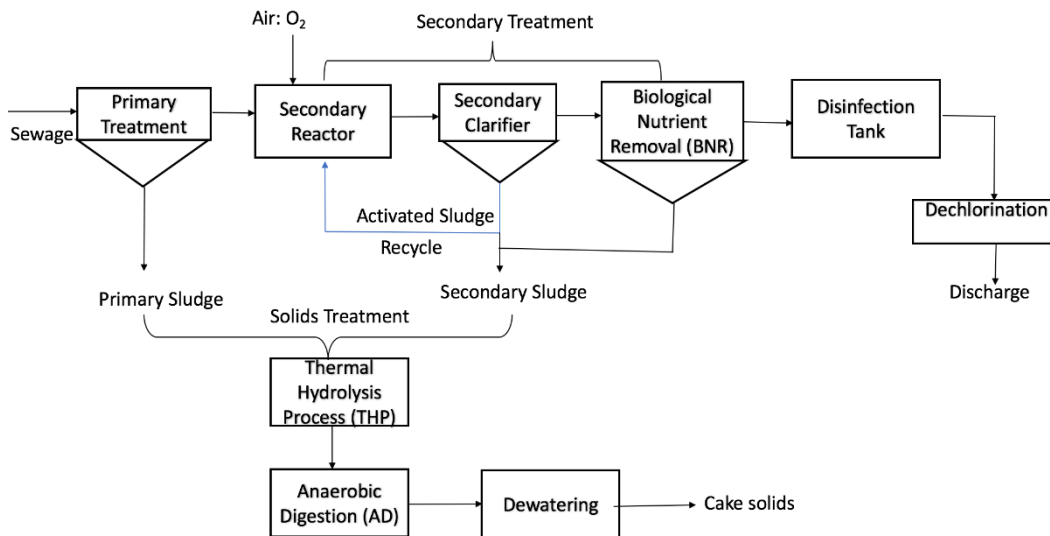
66

67

68 **Chapter 2: Literature Review**

69 **2.1 Biosolids**

70 Municipal sewage is treated through various types of wastewater treatment  
71 plants, where a series of biological processes remove or transform the organic  
72 matter, nutrients, and pathogenic bacteria to meet the regulatory requirements for  
73 the effluent enabling discharge to receiving water systems (Wang et al., 2008)  
74 (Figure 2.1).



75

76 **Figure 2.1.** Wastewater treatment process diagram.

77

78 The wastewater is constituted of two main parts: 1) the liquid part, which  
79 contains water and soluble organic or inorganic matters, while 2) makes up the  
80 solid part, which contains insoluble particles including organic matter and  
81 bacteria (Painter and Viney, 1959). In the wastewater, these two parts are mixed  
82 together, and one objective in wastewater treatment is to separate them to obtain  
83 clean effluent. During gravitational separation, the solids settle to the bottom of

84 the sedimentation tank as sludge, and the sludge from each treatment stage is  
85 collected for further treatment referred to as the solids treatment process. First, the  
86 thermal hydrolysis process makes the sludge more biodegradable under high  
87 temperature and pressure, the sludge will then be stabilized through the anaerobic  
88 digestion process, where anaerobic bacteria and archaea decompose the organic  
89 compounds in the sludge to produce biogas for energy recovery and thereby  
90 reduce the sludge volume (Wang, Shammas and Hung, 2007). The sludge from  
91 the anaerobic digestion tank will then be dewatered to reduce the water content,  
92 whereby the volume will be further reduced in addition to limiting potential issues  
93 with odor during storage and transportation for land application purposes (Parkin  
94 and Owen, 1986). The biosolids contains a high concentration of nutrients such as  
95 carbon, nitrogen, phosphorous as well as micro nutrients such as zinc, copper and  
96 nickel (Esteller et al., 2009). This content makes biosolids applicable as fertilizer  
97 and for soil amendment in land application such as farming, silviculture, soil  
98 reclamation and others (Wang, Shammas and Hung, 2007; EPA, 2002).

99 As the increase in the population takes place, more municipal sewage will  
100 be produced (Vorosmarty, 2000). Therefore, evaluation of the solids treatment  
101 process and biosolids production will become increasingly important and invite  
102 more public attention.

103

## 104 **2.2 Sludge Clarification and Bioflocculation**

105 Sludge clarification refers to the solid separation in gravitational  
106 sedimentation tanks in each treatment process (Chao and Keinath, 1979). Floc

107 formation and settlement are the most important processes that determine the  
108 sludge clarification efficiency. Bioflocculation is a complicated process that refers  
109 to the floc formation that takes place in the activated sludge. The two processes  
110 coagulation and flocculation are important for bioflocculation (Amuda and Amoo,  
111 2007). In coagulation, discrete particles in the wastewater combine into  
112 aggregates, whereas these aggregates attach to each other and form microflocs  
113 during the flocculation process. These interactions can be described by the  
114 Derjaguin-Landau-Verwey-Overbeek (DLVO) theory, considering both molecular  
115 interactions, attractive Van De Waals forces, repulsive electrostatic forces, and  
116 solid particle electrification (Derjaguin & Landau, 1993; Verwey et al., 1999). In  
117 wastewater treatment, charge neutralization and polymer addition are commonly  
118 applied for improving the bioflocculation process. Solids particles of the sludge  
119 are negatively charged (Jin, Wilén and Lant, 2003) thus they can combine with  
120 positively charged cations to form electroneutral flocs. Therefore, decreasing the  
121 monovalent/divalent cation ratio (M/D ratio) by dosing divalent cations such as  
122 calcium and magnesium ions can increase the efficiency of the electroneutral floc  
123 formation thus improving bioflocculation (Higgins, Tom and Sobeck, 2004).  
124 Polymers, on other hand, can have linear or branched structures to provide  
125 junctions for solid particles to attach thus increasing the floc size and strength  
126 (Poduska and Hicks, 1979; Singh et al., 2003). Activated sludge from the  
127 secondary treatment process is an important source of biosolids. However, it is  
128 considered as bioflocculation limited (Li et al., 2016), and the limitation would  
129 originate from both coagulation and flocculation steps (Busch and Stumm, 1968;

130 Urbain, Block and Manem, 1993). Therefore, pinpointing the limitation can  
131 inform potential solutions that can improve the sludge clarification process.

132

### 133 **2.3 Anaerobic Digestion**

134 Anaerobic digestion is a biological process, where anaerobic bacteria and  
135 archaea transform organic material in the sludge and form biogas that is mainly  
136 composed of methane, carbon dioxide, water vapor and trace hydrogen sulfide  
137 (Lastella et al., 2002). Removal of carbon dioxide, water vapor and other  
138 produced gases from the raw biogas results in improved quality of biogas thus  
139 mainly methane. Biogas production is applied as a means of energy recovery from  
140 the wastewater treatment process and can be used by the facilities for producing  
141 mechanical energy, heating the anaerobic digester, supplying electricity (Deng et  
142 al., 2014). The volume of the sludge is reduced after anaerobic digestion due to  
143 the production of methane and the remaining biomass (called digestate) will be  
144 dewatered to produce biosolids.

145

### 146 **2.4 Dewatering Process**

147 Dewatering involves the solid-liquid separation process that removes  
148 moisture from the sludge (Stasta et al., 2006). Digestate from the anaerobic  
149 digestion process is dewatered, and the water content often decreases from 95% in  
150 anaerobic digestion to 70-85% in the dewatered solids (Wang et al., 2008). Water  
151 is commonly removed from the sludge by filtration and centrifugation (Wakeman,  
152 2007). The water that is removed through this process is called filtrate and is

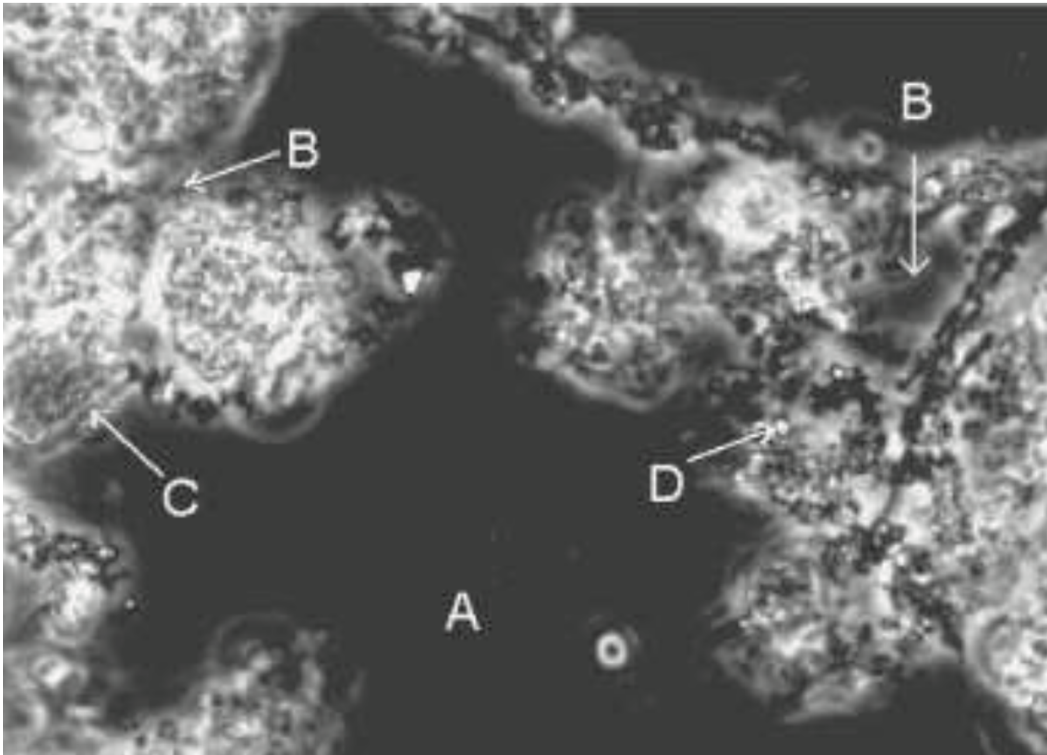
153 commonly returned to secondary treatment processes. Dewatered solids are  
154 referred to as “cake solids”. The moisture content in the cake solids varies and is  
155 influenced by both sludge characteristics and the applied dewatering technology  
156 (Novak, 2006). Various dewatering technologies result in different total solids  
157 (TS) content of the cakes. The cake TS can range from 24-42% for pressure and  
158 vacuum filtered sludge, while the TS content ranges from 20-40% for belt and  
159 centrifuge filtered solids (Werther and Ogada, 1999). The cake solids obtained  
160 could be applied for land application as biosolids. As the population continues to  
161 increase, increased cake solids production is expected due to increased volumes of  
162 municipal wastewater. Therefore, issues with storage, transportation and  
163 management of these cake solids will require solutions. As a result, it is important  
164 to study the mechanisms of different dewatering technologies to achieve higher  
165 dewaterability and less moisture content in the cake solids.

166

## 167 **2.5 Structured Water**

168 As mentioned above, dewatered biosolids have high moisture contents,  
169 since not all water can be removed with current mechanical dewatering  
170 technologies (Werther and Ogada, 1999; Tsang and Vesilind, 1990). Four types of  
171 water have been identified in sludge (Vesilind, 1994): (1) Free water: water that is  
172 unaffected by the capillary force and moves freely in the sludge; (2) Interstitial  
173 water: water that is trapped into interstitial places between the sludge flocs due to  
174 capillary forces; (3) Surface water: water that is attached to the surface of the  
175 sludge flocs due to adhesive forces; (4) Chemically bound water: water that is

176 tightly bound to the sludge flocs due to chemical interactions such as hydration  
177 water (Figure 2.2) (Kopp and Dichtl, 2000). There is a continuous debate about  
178 the determination of the structured water content, and different approaches for  
179 measuring the structured water content have been applied (Vaxelaire and Cézac,  
180 2004).



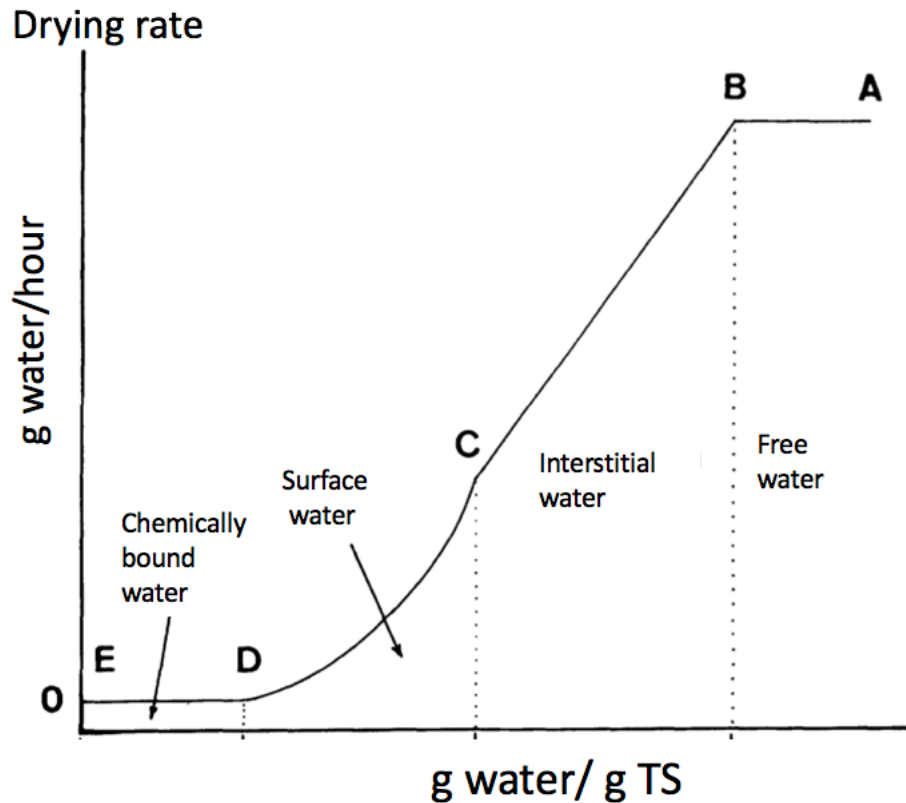
181  
182 **Figure 2.2.** Moisture distribution in a sewage sludge floc: A: free water; B:  
183 interstitial water; C: surface water; D: chemically bound water (Kopp and Dichtl,  
184 2000).

185  
186 One operational determination of the structured water content is the  
187 moisture that does not freeze under the temperature that would freeze free water  
188 (Colin and Gazbar, 1995). Based on this definition, Heukelekian and Weisberg

189 (1956) proposed the dilatometric measurement of the structured water content.  
190 This approach assumed that when the sludge was frozen to a temperature below -  
191 20°C, the volume change of the sludge would only be caused by freezing of the  
192 free water. Therefore, the free water content was determined by recording the  
193 volume change of the sludge, and the structured water content was calculated by  
194 subtracting the free water content from the total water content in the sludge (Wu,  
195 Huang and Lee, 1998).

196 Another operational determination of the structured water content was  
197 proposed by Lee and Hsu (1995), where, the structured water content was defined  
198 as the moisture that was excluding the free water. The structured water content  
199 can be obtained via a drying test (Lee and Hsu, 1995), which successfully  
200 provided a full drying curve of the sludge sample instead of a number such as the  
201 dilatometric measurement provided. A constant amount of sludge was dried under  
202 controlled temperature and relative humidity resulting in a drying curve that  
203 showed the relationship between the drying rate and the remaining moisture  
204 content in the sludge sample, and the drying rates varied for different moisture  
205 types (Figure 2.3) (Lee and Hsu, 1995). The structured water content was  
206 obtained according to the change of the drying rates. In Figure 2.3, the moisture  
207 content in the sludge at note B indicates the structured water content of the  
208 sludge. However, the determination of note B is visual and subjective, which  
209 means that interpretation of note B can lead to different structured water contents  
210 (Lee and Hsu, 1995; J. Kopp and N. Dichtl, 2000). Thus, an objective

211 measurement without subjective interpretation is necessary for determination of  
212 the structured water content in different sludge types.



213  
214 **Figure 2.3.** Drying Curve. Moisture evaporation rate vs. moisture content remains  
215 in the sludge. A-B: free water evaporation period; B-C: interstitial water  
216 evaporation period; C-D: surface water evaporation period; D-E: chemically  
217 bound water evaporation period (Lee and Hsu, 1995).

218  
219 In this thesis, structured water is defined as the moisture content in the  
220 sludge that excludes the free water similar to Lee and Hsu (1995), and the content  
221 will be determined based on the drying test results (described above). Five

222 objective approaches based on the drying test will be provided and evaluated  
223 according to their theoretical and practical interpretations.

224

## 225 **2.6 Extracellular Polymeric Substances (EPS)**

226 EPS are natural polymers secreted by the microorganisms in the sludge  
227 that provides important functional and structural properties for the biofilm/sludge  
228 flocs (Liu and Fang, 2002). EPS is mainly composed of protein (PN),  
229 polysaccharides (PS), humic substances, lipids, DNA and inorganic compounds  
230 (Sheng, Yu and Li, 2010). Bioflocculation efficiency and dewaterability of the  
231 sludge are influenced by the EPS content and composition (More et al., 2014;  
232 Neyens, 2004). The PN/PS ratio is an important parameter of the EPS, and studies  
233 indicate that a PN/PS ratio smaller than 1 might lead to poor bioflocculation and  
234 lower dewaterability (Morgan, Forster and Evison, 1990; Basuvaraj, Fein and  
235 Liss, 2015). EPS can be bound to the bacteria attached to the sludge structure thus  
236 forming a net-like structure to hold the biofilm together. EPS is often classified  
237 into two parts: 1) loosely bound EPS (LB-EPS) and 2) tightly bound EPS (TB-  
238 EPS) according to their connection with the bacteria cells and EPS extraction  
239 methodologies (More et al., 2014). The content of the LB-EPS and TB-EPS in the  
240 sludge is also an important parameter that influences sludge bioflocculation and  
241 dewaterability. Basuvaraj (2015) indicated that sludge with more TB-EPS content  
242 (TB-EPS/LB-EPS ratio >2.5) had improved settleability and dewaterability  
243 compared to sludge with less TB-EPS (TB-EPS/LB-EPS ratio <1.5). Considering  
244 the influence of EPS on the sludge dewaterability, studies on the influence of EPS

245 on the structured water content are proposed. A previous study indicated that  
246 sludge with total EPS content more than 20 mg/g VSS exhibited a higher  
247 structured water content (7-24 g H<sub>2</sub>O/ g MLSS) than sludge with less EPS content  
248 (structured water content: 6-15 g H<sub>2</sub>O/ g MLSS) (Liao et al., 2000). Therefore, in  
249 this study, it is essential to investigate the relationship between the structured  
250 water content and the sludge EPS characteristics such as PN/PS ratio, LB-EPS,  
251 TB-EPS and total EPS content.

252

253

254

255 **Chapter 3: Manuscript 1: Identification of coagulation,**  
256 **flocculation and floc strength limitations in activated sludge using**  
257 **modified jar tests**

258

259 **Keywords:** solid separation, high-rate activated sludge, branched polymer,  
260 bioaugmentation, jar test

261

262 **Abstract**

263 Floc formation is a complicated and vital process in the activated sludge system.  
264 However, elevated effluent suspended solids in activated sludge systems are  
265 common and frequently the exact cause is unknown. This study utilized multiple  
266 modified jar tests with FeCl<sub>3</sub>, polyDADMAC, linear polymer (LP) and branched  
267 polymer (BP) to assess the presence coagulation, flocculation and floc strength  
268 limitation present in high-rate activated sludge (HRAS), bioaugmented HRAS  
269 (bioHRAS) and biological nutrient removal sludge (BNR). HRAS was found to  
270 be flocculation and coagulation limited, whereas these limitations were mitigated  
271 by bioaugmentation. BioHRAS was found to be floc strength limited. BNR had  
272 no apparent limitation but benefitted from both coagulant and polymer addition.  
273 Polymers in combination with orthokinetic test are useful diagnostic tool to  
274 identify floc limitations where after appropriate measures can be taken to mitigate  
275 these limitations.

276

### 277 **3.1 Introduction**

278           Solid separation is imperative towards the success of a wastewater  
279 treatment plant (WWTP). Without it, effluent quality limits would not be  
280 obtainable. Activated sludge consists of bacteria whose density approximates  
281 water (Andreadakis, 1993). As such, activated sludge has to coagulate and  
282 flocculate in order to achieve solid separation. Solids separation is a complex  
283 process involving (1) coagulation of primary colloids into aggregates and (2)  
284 subsequent flocculation into microflocs (<50  $\mu\text{m}$ ). When exposed to tranquil  
285 conditions commonly found in clarifiers, microflocs will further flocculate into  
286 macroflocs (>50  $\mu\text{m}$ ) and settle out. Both coagulation and flocculation of  
287 activated sludge have similar mechanisms and have been used interchangeably in  
288 the past. For clarity sake, ‘floc formation’ shall henceforth be used to denote the  
289 complete process (coagulation followed by flocculation) as described above,  
290 while ‘coagulation’ and ‘flocculation’ will be used for the appropriate sub-  
291 processes (1) and (2) respectively.

292           Floc formation is most commonly described by the Derjaguin-Landau-  
293 Verwey-Overbeek (DLVO) theory (Derjaguin & Landau, 1993; Verwey et al.,  
294 1999) which describes two distinct processes: (1) double layer compression and  
295 (2) bridging (Hermasson, 1999; Langelier & Ludwig, 1949; Mer & Healy, 1963).  
296 The DVLO theory combines the attractive van der Waals interactions with the  
297 repulsive double layer interactions originating from Coulomb forces between  
298 charged particles. Activated sludge cells are negatively charged (Liao et al., 2001;  
299 Wilen et al., 2003), thus these negative repulsive forces must be overcome before

300 the attractive van der Waals forces allow for the formation of bacterial cells into  
301 aggregates. This energy barrier is function of the total surface charge of the  
302 bacterial cell. Bridging involves divalent cations ( $\text{Ca}^{2+}$ ,  $\text{Fe}^{2+}$ ,  $\text{Mg}^{2+}$ ) or high  
303 molecular weight molecules like polymers to electrostatically clump cells  
304 together. The effectiveness of this process is mediated by the surface charge and  
305 the amount of cations present and is sensitive towards changes in the monovalent  
306 to divalent (M/D) ratio. While both processes occur for both coagulation and  
307 flocculation, Mer and Healy (1963) established that coagulation is more  
308 influenced by the amount of charge to be charge neutralized while flocculation  
309 depends on successful collisions of aggregates which are subsequently held  
310 together by cationic bridges. Thus, coagulation happens perikineticly, while  
311 flocculation is orthokineticly driven. Not all collisions are successful however,  
312 with orthokinetic collision efficiency, i.e. the percentage of total collisions that is  
313 successful, being the major macroscopic metric to assess flocculation potential.  
314 Hence, mixing energy is commonly applied to promote orthokinetic over  
315 perikinetic floc formation.

316 Floc formation can be artificially induced or improved by the addition of  
317 chemicals like metal salts and synthetic polymers. Ferric chloride is commonly  
318 used in primary treatments to coagulate inorganic suspended solids into primary  
319 sludge and the removal of phosphate or as conditioning agent in dewatering.  
320 Synthetic cationic polymers are mainly used as conditioning agents in dewatering  
321 to improve total cake solids and aid solid separation in secondary clarifiers. Many  
322 types exist, depending on the application. Charge neutralization and particle

323 destabilization in the coagulation step can be achieved by adding a  
324 polyDADMAC-type polymer which typically has a very high charge density but  
325 relatively low molecular weight. Collision efficiency in the flocculation step can  
326 be improved with high molecular weight polyamide-type polymer. These  
327 polymers can be linear in structure, maximizing the molecular weight and thus  
328 minimizing optimal dosage, or branched, which improves floc strength. Given  
329 these different effects, these different types of polymer could potentially be used  
330 to pinpoint coagulation, flocculation or floc strength limitations in sludge.

331         Activated sludge floc formation is mediated through extracellular polymeric  
332 substances (EPS), which act as a biopolymer where double layer compression and  
333 bridging can take place. EPS is predominantly made out of protein,  
334 polysaccharides and to a lesser extent humic acids and DNA (Frolund et al.,  
335 1996). Multiple studies have suggested that the structure and composition of EPS  
336 is one of the main factors affecting bioflocculation, citing total amount and the  
337 protein (PN) over polysaccharide (PS) ratio being crucial to aggregation  
338 proficiency.

339         Clearly, activated sludge floc formation is a complex process involving  
340 physical (DVLO/bridging) and biological (EPS production) processes. Many  
341 limitations in the floc formation process and it is not always clear where in the  
342 floc formation process the limitation persists. As such, evaluating strategies to  
343 mitigate elevated suspended solids in secondary clarifiers due to poor floc  
344 formation is not always straightforward. Blue Plains advanced wastewater  
345 treatment plant (AWWTP) in Washington, DC, USA currently has two secondary

346 treatment trains (East and West, Solids retention time (SRT) = 1-2 days) and one  
347 biological nutrient removal (BNR, SRT = ~ 20 days) system. The East secondary  
348 system is at the time of writing being bio-augmented with BNR sludge to achieve  
349 some nitrogen removal in the secondary reactors. The West secondary reactors  
350 historically have poor effluent suspended solids (ESS) ( $33 \pm 16$  mg total  
351 suspended solids (TSS)  $L^{-1}$ ), while the East reactors perform marginally better ( $25$   
352  $\pm 22$  mg TSS  $L^{-1}$ ), although unexplained spikes in ESS persist. The BNR reactor  
353 performs excellent ( $6 \pm 2$  mg TSS  $L^{-1}$ ). Mancell-Egala et al. (2017) did a  
354 comprehensive study on the settling properties of these three systems and  
355 determined that flocs formed in these three reactors were significantly different.  
356 West produced small flocs with slow settling velocity distribution, while East  
357 produced bigger flocs with faster settling velocities, most likely due to the bio-  
358 augmentation. A good correlation with between the threshold of flocculation  
359 (TOF), a metric for collision efficiency, and ESS was found for West secondary.  
360 This gave first indications that West might be limited in floc formation, although  
361 it is unclear whether this is limited in the flocculation or coagulation step. This  
362 correlation did not hold for East, indicating another limitation is at play. Due to  
363 the size of the flocs produced, Mancell-Egala et al. (2017) suggested that floc  
364 strength might be the limiting factor, although no conclusive evidence was given.

365         In this research, the possible floc forming limitations will be further  
366 explored. Orthokinetic flocculation tests will be used to assess the sludge's floc  
367 formation. Synthetic polymers (polyDADMAC and linear and branched  
368 polyamide type) as well as  $FeCl_3$  will be used to artificially improve a part of the

369 flocculation process to pinpoint coagulation, flocculation or flocculation strength  
370 limitations present in East, West and BNR.

371

## 372 **3.2 Materials and Methods**

### 373 **3.2.1 Sample location and acquirement**

374 Blue Plains Advanced Wastewater Treatment Plant is the largest advanced  
375 wastewater treatment plant of this kind in the world, treating over 1.1 million  
376 cubic meters of sewage per day and serving District of Columbia and part of  
377 Maryland and Virginia. Samples for this study were obtained from two secondary  
378 systems (West and East; SRT = 1-2 days) and one BNR reactor (SRT = ~ 20  
379 days). A full description of aforementioned reactors can be found in Mancell-  
380 Egala et al. (2017). Samples were collected using buckets or submersible  
381 centrifugal pumps when significant amount of sludge was needed and were  
382 acquired from between June to August 2016. All experiments were performed  
383 within a few hours of sampling.

384

### 385 **3.2.2 Polymer types and preparation**

386 Ferric Chloride (Fisher Scientific, USA) and PolyDADMAC (SNF  
387 Polydyne FL-4520, USA) were used as coagulant. The polyDADMAC was a very  
388 high charge density, low molecular weight polymer. PolyDADMAC was freshly  
389 diluted to 0.2% w/w using the company provided stock media at the same day of  
390 the experiment. Linear polyamide polymer with high-molecular weight and 10%  
391 charge density (SNF Polydyne, Clarifloc SE-1163, USA) and a medium-

392 molecular weight branched polyamide polymer with 10% charge density (SNF  
393 Polydyne, Clarifloc C-3220, USA) were used as flocculent polymers. Linear and  
394 branched polymer solutions (0.2% w/w) were prepared and activated on the same  
395 day as the experiment by slowly adding the polymer granules in deionized water  
396 and stirring the solution at 300 RPM for 30 minutes.

397

### 398 **3.2.3 Modified Jar test**

399         The standardized jar test (ASTM, 1995), was modified to better represent  
400 the real conditions seen in a clarifier, while still having enough resolution to  
401 determine differences in floc formation behavior. Diluted Sludge was poured into  
402 a modified Nalgene® 4L graduated cylinder ( $\phi = 10$  cm) and mechanically mixed  
403 at  $245\text{ s}^{-1}$  (500 RPM) for 10 seconds with an IKA Eurostar 60 (IKA, USA) mixer  
404 equipped with two 4-bladed axial flow impellers when liquid prepared polymer  
405 was added. Subsequently, the sludge was further agitated at  $112\text{ s}^{-1}$  (300 RPM) for  
406 30 seconds to enmesh the polymer within the flocs. When two polymers were  
407 added, these two steps were repeated for every polymer. Mixing was throttled  
408 down to  $22\text{ s}^{-1}$  (100 RPM) for 10 minutes to allow for flocculation. Ten minutes  
409 was chosen as this was deemed sufficient for steady state floc formation to  
410 happen (Biggs & Lant, 2000; Wahlberg et al., 1994). The graduated cylinder was  
411 instantly baffled to dissipate kinetic energy and sludge was allowed to settle.  
412 After 1 minute, clamps 5 cm below the liquid level were opened and sludge was  
413 allowed to rapidly gravity drain into a sample cup. The TSS collected in this cup  
414 represent the fraction of total TSS that settled slower than  $3\text{ m h}^{-1}$ . This test was

415 used as the basic procedure for creating the orthokinetic flocculation curve (OFC)  
416 (section 3.2.3, (1)), polymer response curve (PRC) (section 3.2.3, (2)), settling  
417 velocity distribution test (SVD) (Section 3.2.3, (3)).

418 (1) Orthokinetic test

419 Orthokinetic tests were used to assess the floc formation at different  
420 concentrations under non-rate-limiting conditions. The modified jar test was used  
421 at different sludge concentrations ranging from 100 mg TSS L<sup>-1</sup> to 1500 mg TSS  
422 L<sup>-1</sup>, and thus chosen in flocculant settling range (below LOSS). Optimal polymer  
423 doses were spiked in these test after determination using the polymer response  
424 curve (Section 3.2.3, (2)). The control curve was subjected to the same protocol  
425 without the addition of polymer to include the effect of rapid mix on floc  
426 formation in the results.

427 (2) Polymer response curve

428 A polymer response curve (PRC) assessed the influence of different  
429 polymer concentrations on the floc formation. An orthokinetic curve without the  
430 addition of polymer was created prior to the test and a sludge concentration where  
431 20% of the sludge was removed was chosen. At this concentration, floc formation  
432 was limited enough to have enough resolution for the effect of polymer dosage to  
433 be observed.

434 (3) Settling velocity distribution test

435 A discreet settling velocity distribution (SVD) of the sludge was obtained  
436 by subjecting it to different settling times: 5 min (CSV = 0.6 m/h), 2 min (CSV=  
437 1.5 m/h), 1 min (CVS = 3 m/h) and 20 s (CSV = 9 m/h). SVDs were obtained at

438 the same sludge concentration as the polymer response curves. To assess the  
439 impact of shear on the SVD, both  $22 \text{ s}^{-1}$  or  $91 \text{ s}^{-1}$  (260 RPM) was applied for 10  
440 minutes as flocculation step.

441

#### 442 **3.2.4 Classic and novel settling metrics**

443 Sludge volume index (SVI) and initial settling velocity (ISV) were  
444 determined at  $3.5 \text{ g TSS L}^{-1}$  in a Nalgene® 2L settleometer according to the  
445 standard methods (APHA, 2005). Limit of Stoksian settling (LOSS) determines  
446 the sludge concentration where flocculent settling transitions into hindered  
447 settling and was measured according to Mancell-Egala et al. (2016) Threshold of  
448 flocculation (TOF) measures the minimal sludge concentration required for  
449 settleable flocs to form when subjected to a 2 min flocculation and settling time,  
450 which corresponds to a critical settling velocity (CSV) of 1.5 m/h. Six gradient  
451 concentrations from 100 mg/L to 1000 mg/L were prepared. Detailed modus  
452 operandi can be found in (Mancell - Egala et al., 2016).

453

#### 454 **3.2.5 Extracellular polymeric substances**

455 Extracellular polymeric substances were extracted using a modified heat  
456 extraction method based on Li and Yang (2007). 2.5 mg TSS of freshly sampled  
457 sludge was centrifuged at  $4000 \text{ s}^{-1}$  for 5 minutes. The pellet was resuspended in  
458 10 ml, pH adjusted (pH = 7.2), phosphate saline buffer (PBS) containing 2 mM  
459  $\text{Na}_3\text{PO}_4$ , 4 mM  $\text{KH}_2\text{PO}_4$ , 9 mM NaCl and 1 mM KCl at  $60 \text{ }^\circ\text{C}$  and immediately  
460 vortexed for 1 minute to shear of the loosely bound (LB) EPS. The sludge was

461 subsequently centrifuged at  $4000\text{ s}^{-1}$  for 10 minutes and the supernatant collected  
462 as LB-EPS. Next, the pellet was resuspended in 10 ml PBS and incubated at 60  
463 °C for 30 minutes. Lastly, the sludge was centrifuged for 15 minutes at  $4000\text{ s}^{-1}$   
464 and the tightly bound (TB) EPS fraction was recovered in the supernatant. Both  
465 LB and TB EPS were filtered through a  $1.5\text{ }\mu\text{m}$  glass microfiber filter (Whatman,  
466 USA) and stored at  $-20\text{ }^{\circ}\text{C}$  for subsequent analysis.

467 LB and TB EPS samples were analyzed for chemical oxygen demand  
468 (COD), total soluble protein (TP) and total polysaccharide (TS). COD was  
469 determined using Hach® kits. TP were determined using the The Lowry method  
470 (Lowry et al., 1951) was used using a modified Lowry Protein Assay kit (Thermo  
471 Fisher, USA) and bovine serum albumin (BSA) as standard. TS were determined  
472 using the DuBios method (DuBois et al., 1956) where glucose was used as a  
473 standard.

474

### 475 **3.3 Results**

#### 476 **3.3.1 High-rate activated sludge**

477 The West reactor at Blue Plains AWTP has been operating as a high-rate  
478 activated sludge (HRAS) reactor at short SRT (1 – 2 days) and showcased the  
479 poorest performances in terms of effluent quality and collision efficiency (as  
480 depicted by TOF) of the three reactors assessed at Blue Plains (Table 3.1).  
481 Gravitational flocculation did not create any flocs faster than  $1.5\text{ m h}^{-1}$  until the  
482 threshold of flocculation was reached, while applying orthokinetic shear at  $20\text{ s}^{-1}$   
483 induced the formation of flocs faster than  $3\text{ m h}^{-1}$  even at the lowest concentration

484 tested (Figure 3.1A). No significant difference (p-value = 0.5) was observed  
485 between the gravitational and orthokinetic slope ( $-81 \pm 28 \% \text{TSS g TSS}^{-1}$  and  $-95$   
486  $\pm 13 \% \text{TSS g TSS}^{-1}$  respectively). Steady state orthokinetic floc formation was  
487 achieved at  $558 \text{ mg TSS L}^{-1}$  (as indicated by the slope flattening out), where  $48 \pm$   
488  $1 \%$  of the sludge was unable to form flocs faster than  $3 \text{ m h}^{-1}$ . The settling  
489 velocity distribution showed that flocs predominantly (40%) settle between  $1.5 -$   
490  $3 \text{ m h}^{-1}$ . When harsher orthokinetic shear ( $90 \text{ s}^{-1}$ ) was applied, the distribution  
491 shifted to the left, with  $0.6 - 1.5 \text{ m h}^{-1}$  being the predominant settling class.  
492 (Figure 3.2A)

493 HRAS sludge did not respond well to increasing dosages of coagulants  
494 PolyDADMAC (C) and  $\text{FeCl}_3$  as indicated by the low final improvement at high  
495 dosage (C=  $16.9 \pm 2.3 \%$ ;  $\text{FeCl}_3 = 13.8 \pm 3.4 \%$ ) as shown in Figure 3.3A.  $\text{FeCl}_3$   
496 yielded an immediate improvement at low concentrations, but did not respond to  
497 an increase in dosage. C did respond to increasing dosages but failed to  
498 outcompete  $\text{FeCl}_3$ . Both linear polymer (LP) and branched polymer (BP) showed  
499 a clear increase in the formation of flocs that settle faster than  $3 \text{ m h}^{-1}$  (Figure  
500 3.3B). However, no significant difference in flocculation response was observed  
501 between both polymers' slopes ( $493 \pm 8 \% \text{ improvement (g polymer kg TSS}^{-1})^{-1}$   
502 and  $605 \pm 158 \% \text{ improvement (g polymer kg TSS}^{-1})^{-1}$  for LP and BP  
503 respectively; p-value = 0.343). Addition of  $0.5 \text{ mg polyDADMAC g TSS}^{-1}$  did  
504 not improve the polymer response at low concentrations as indicated by the  
505 similar slope to LP and BP ( $442 \pm 119 \% \text{ improvement (g polymer kg TSS}^{-1})^{-1}$ ),  
506 however steady state was reached a smaller dosage (Figure 3.3C).

507 Independent of the treatment, the percentage of sludge that formed flocs  
508 slower than  $3 \text{ m h}^{-1}$  decreased when sludge with increasing concentrations was  
509 subjected to orthokinetic shear. This decrease flattened out when steady state floc  
510 formation was achieved. C did not have observable effect on WEST sludge, and  
511 was not significantly different from the control (Figure 3.4A). LP and BP had a  
512 similar but profound effect on HRAS sludge as their slopes were nonsignificant  
513 from each other (LP =  $-14.0 \pm 0.6 \%$  improvement  $(\text{g polymer kg TSS}^{-1})^{-1}$ ; BP = -  
514  $13.5 \pm 1.3 \%$  improvement  $(\text{g polymer kg TSS}^{-1})^{-1}$ ; p-value = 0.587) (Figure  
515 3.4B). However, at  $1555 \text{ mg TSS L}^{-1}$ , BP significantly (p-value = 0.02)  
516 outperformed LP in removal percentage of flocs ( $13.0 \pm 2.7 \%$  versus  $1.7 \pm 0.3 \%$   
517 for LP and BP respectively). Combination of polymer and PolyDADMAC did  
518 not yield significant improvements over using polymer alone (Figure 3.4C).

519 Figure 3.2A shows the settling speed distribution and the effect of  
520 increased shear this distribution. Intrinsically, West flocs predominantly settled  
521 slower than  $3 \text{ m h}^{-1}$  and are resistant to shear as indicated by the small increase  
522 ( $12.5 \pm 2.51\%$ ) in flocs settling slower than  $3 \text{ m h}^{-1}$ . LP and BP performed  
523 similarly, creating flocs with settling speeds predominantly in the  $3\text{-}9 \text{ m h}^{-1}$  range  
524 and no significant change in floc strength was observed (Figure 3.5A). When  
525 polyDADMAC was combined with LP, fast settling flocs ( $> 9 \text{ m h}^{-1}$ ) were  
526 created, but were very prone to breakup when shear was increased. A  
527 Combination of polyDADMAC and BP performed worse than BP alone.

528

### 529 3.3.2 Bioaugmented high-rate activated sludge

530 Similar to the West reactor, East is operated as a high-rate activated sludge  
531 reactor with an average SRT of 1 – 2 days. East however is bioaugmented with  
532 about  $0.2 \text{ kg TSS}_{\text{BNR}} \text{ kg TSS}_{\text{East}}^{-1} \text{ d}^{-1}$ , mainly to allow for some nitrification in the  
533 secondary reactor. Effluent quality of the bioaugmented high-rate activated  
534 sludge (BioHRAS) reactor was better than the non-bioaugmented, but big  
535 fluctuations were presents as indicated by the high standard deviation (Table 3.1).  
536 Collision efficiency was better than the conventional HRAS as indicated by TOF  
537 value. The slope ( $-99 \pm 17 \% \text{ TSS g TSS}^{-1}$ ) was, while (borderline) statistically  
538 nonsignificant from HRAS (p-value = 0.09) or BNR (p-value = 0.07), higher than  
539 both (Figure 3.1B). With addition of orthokinetic shear, a consistent downwards  
540 slope was observed ( $-51 \pm 4 \% \text{ TSS g TSS}^{-1}$ ) with increasing sludge concentration  
541 and flattened out at  $1087 \text{ mg TSS L}^{-1}$  at 46% solids slower than  $3 \text{ m h}^{-1}$  remaining  
542 (Figure 3.1B). The drop of orthokinetic flocculation occurs at lower concentration  
543 around  $500 \text{ mg/L}$ . Gravitational flocculation still has its limiting percentage  
544 around 45% while orthokinetic flocculation continuously goes downwards. The  
545 settling velocity distribution is similar to the non-bioaugmented sludge with a  
546 peak showing at the  $1.5 - 3 \text{ m h}^{-1}$  class (Figure 3.2B). However, the overall  
547 distribution is more right skewed whereas the non-bioaugmented HRAS sludge is  
548 more left skewed. Applying harsher shear ( $90 \text{ s}^{-1}$ ) deteriorated the  $3 - 9 \text{ m h}^{-1}$   
549 class (from  $21 \pm 4 \%$  to  $3 \pm 3 \%$  in that respective class), while the  $0.6 - 1.5 \text{ m h}^{-1}$   
550 class became more prominent ( $13 \pm 3 \%$  to  $38 \pm 8 \%$  for  $20 \text{ s}^{-1}$  and  $90 \text{ s}^{-1}$   
551 respectively).

552 Figure 3.3D shows that neither polyDADMAC nor FeCl<sub>3</sub> had any visible  
553 improvement on bioHRAS sludge. Only at very high polyDADMAC dosage (1 g  
554 polymer kg sludge<sup>-1</sup>) a minor improvement of 18 ± 3 % over the control could be  
555 detected. LP and BP have induced a similar response on EAST sludge with  
556 similar slope (LP=229.3 ± 31.7 % improvement (g polymer kg TSS<sup>-1</sup>)<sup>-1</sup>; BP =  
557 219.8 ± 6.6 % improvement (g polymer kg TSS<sup>-1</sup>)<sup>-1</sup>; p-value = 0.660) and  
558 maximum obtainable improvement (LP = 82.2 ± 2.8 %; BP = 84.5 ± 2.5 %; p-  
559 value = 0.353). Combining 0.5 g polyDADMAC kg TSS<sup>-1</sup> with increasing  
560 concentrations of LP showed a significant improvement in response (639.8±75.7  
561 % improvement (g polymer kg TSS<sup>-1</sup>)<sup>-1</sup>) compared to LP alone (p-value = 0.001),  
562 but plateaued at a similar maximum improvement point.

563 PolyDADMAC does not has observable effect on the orthokinetic profile  
564 for bioHRAS sludge, as the slope did not differ significantly (p-value=0.077)  
565 from the control, where no polymer is dosed (Figure 3.4D). LP showed a big  
566 improvement over the control treatment, while combining both polyDADMAC  
567 with LP did not yield any additional improvement over only dosing LP (LP = 122  
568 ± 1 %TSS g TSS<sup>-1</sup>; C+LP = -119 ± 4 %TSS g TSS<sup>-1</sup>; p-value=0.347) (Figure  
569 3.4D/E). BP had a significantly bigger effect on the orthokinetic profile than LP  
570 as it obtained a steeper slope (200 ± 2 %TSS g TSS<sup>-1</sup>; p-value = 0.0001).  
571 However, this advantage disappeared when the sludge concentration reached 1000  
572 mg TSS L<sup>-1</sup>, resulting in the similar maximum removal potential (LP = 6.0 ± 0.8  
573 %, BP = 6.3 ± 0.5 %). Combining polyDADMAC with BP counteracted the  
574 observed improvements over the other polymer treatments.

575 BioHRAS showed the highest intrinsic shear sensitivity of all sludges  
576 tested (Figure 3.5B). PolyDADMAC had no effect on this. All flocculent polymer  
577 showed a clear impact on the settling distribution with an increase in the 3 – 9 m  
578  $\text{h}^{-1}$  and  $> 9 \text{ m h}^{-1}$  class. In the case of LP, the formed flocs were weak and easily  
579 broken up as indicated by the sharp increase in particles settling slower than 3 m  
580  $\text{h}^{-1}$ . BP however was able to create strong flocs that were indifferent to the  
581 increased shear. This advantage disappeared when polyDADMAC was used in  
582 combination with BP.

583

### 584 **3.3.3 Biological nutrient removal sludge**

585 Within the treatment line of Blue Plains AWTP, the BNR reactor receives  
586 the wastewater from the East and West reactors. Designed for  
587 nitrification/denitrification, the average SRT of the reactor is 20 days and receives  
588 a low loading compared to the HRAS reactors. As such, the effluent suspended  
589 solids were the lowest of the tested reactors and collision efficiency was high  
590 (Table 3.1). Gravitational settling formed flocs that settled faster than  $1.5 \text{ m h}^{-1}$  at  
591 the lowest concentration tested ( $100 \text{ mg TSS L}^{-1}$ ), but the slope ( $-70 \pm 23 \% \text{TSS g}$   
592  $\text{TSS}^{-1}$ ) was similar to HRAS sludge (Figure 3.1C). When orthokinetic shear was  
593 applied, the sludge behaved similarly to the high-rate sludge, however produced  
594 more fast settling flocs at high concentration with the slope flattening out at  $31 \pm$   
595  $4 \%$ . Finally, BNR sludge had the highest observed EPS content of the tested  
596 sludges (Table 3.1).

597           FeCl<sub>3</sub> did not show a clear response on BNR sludge except when very high  
598 dosages were applied (Figure 3.3G). PolyDADMAC (C) did show an obvious  
599 trend even at low concentrations, in contrast with both HRAS sludges. It's slope  
600 and thus response is significantly larger than HRAS' and bioHRAS' slope (p-  
601 value = 0.006 and 0.0001 respectively). LP and BP performed indifferent from  
602 eachother ( $311.9 \pm 34.2$  % improvement (g polymer kg TSS<sup>-1</sup>)<sup>-1</sup> and  $318.2 \pm 78.4$   
603 % improvement (g polymer kg TSS<sup>-1</sup>)<sup>-1</sup> respectively (Figure 3.3H). LP achieved a  
604 higher but insignificant maximum improvement compared to control ( $90.3 \pm 3.0$   
605 %) than BP ( $87.1 \pm 3.6$  %). When 0.5 g polyDADMAC was combined increasing  
606 concentrations of LP, a sharp increase in the lower dosages was observed as  
607 indicated by the high slope ( $495.2 \pm 136.8$  % improvement (g polymer kg TSS<sup>-1</sup>)<sup>-1</sup>  
608 <sup>1</sup>) (Figure 3.3I), however, the slope quickly flattened out at  $54 \pm 6$  % at 0.1 g LP  
609 kg TSS<sup>-1</sup> and remained constant.

610           Unlike the HRAS sludges, 0.5 g PolyDADMAC kg TSS<sup>-1</sup> had a profound  
611 effect when floc formation at BNR was assessed at increasing sludge  
612 concentrations ( $-123 \pm 7$  %TSS g TSS<sup>-1</sup>) (Figure 3.4G). LP has the steepest slope  
613 ( $-312 \pm 21$  %TSS g TSS<sup>-1</sup>) (Figure 3.4H) and did significantly differ from the BP  
614 slope ( $-247 \pm 30$  %TSS g TSS<sup>-1</sup>, p-value = 0.04) and the combined  
615 polyDADMAC and LP slope ( $-117 \pm 12$  %TSS g TSS<sup>-1</sup>, p-value = 0.001) (Figure  
616 3.4I). All treatments were able to reach the same steady state flocs formation ( $3.8$   
617  $\pm 0.7$  %,  $5.5 \pm 1.8$  % and  $5.4 \pm 0.3$  % for LP, BP and C + LP respectively).

618           BNR produced flocs that are strong as indicated by the indifference of the  
619 sludge's settling velocity distribution to low or high shear forces (Figure 3.2C).

620 Adding LP or BP helped achieving faster settling flocs that were more prone to  
 621 break up (Figure 3.5C). Combining polyDADMAC with LP produced slower  
 622 settling flocs than dosing polymer alone, however the flocs were completely  
 623 indifferent to higher shear forces.

624

625 **Table 3.1.** Intrinsic characteristics of the tested sludge types.

	HRAS	Bio-augmented HRAS	BNR	
<b>Reactor performance</b>				
<b>Process name</b>	West	East	BNR	
<b>Effluent TSS</b>	33.1 ± 12.4	23.8 ± 28.9	6.96 ± 4.49	mg TSS L <sup>-1</sup>
<b>Settleability parameters</b>				
<b>TOF</b>	535 ± 139	369 ± 60	295 ± 12	mg TSS L <sup>-1</sup>
<b>LOSS</b>	1706 ± 539	801 ± 259	1287 ± 307	mg TSS L <sup>-1</sup>
<b>ISV</b>	3.37 ± 1.24	1.36 ± 0.95	2.29 ± 1.05	m h <sup>-1</sup>
<b>SVI30</b>	88 ± 81	154 ± 60	122 ± 46	ml g <sup>-1</sup>
<b>specific EPS content</b>				
<b>Total EPS</b>	110 ± 37	93 ± 6	135 ± 10	mg COD g VSS <sup>-1</sup>
<b>PN/PS ratio</b>				
<b>LB-EPS</b>	0.76 ± 0.85	1.85 ± 1.47	2.03 ± 0.76	mg BSA mg glucose <sup>-1</sup>
<b>TB-EPS</b>	1.98 ± 0.57	2.23 ± 0.74	2.01 ± 0.35	mg BSA mg glucose <sup>-1</sup>
<b>Total EPS</b>	1.63 ± 0.38	2.19 ± 0.96	2.00 ± 0.13	mg BSA mg glucose <sup>-1</sup>

626

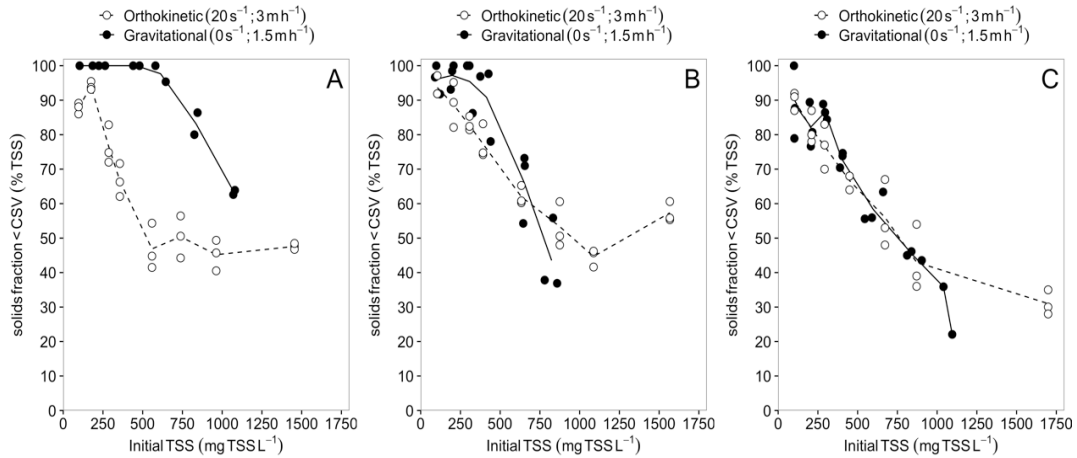
627

628

629

630

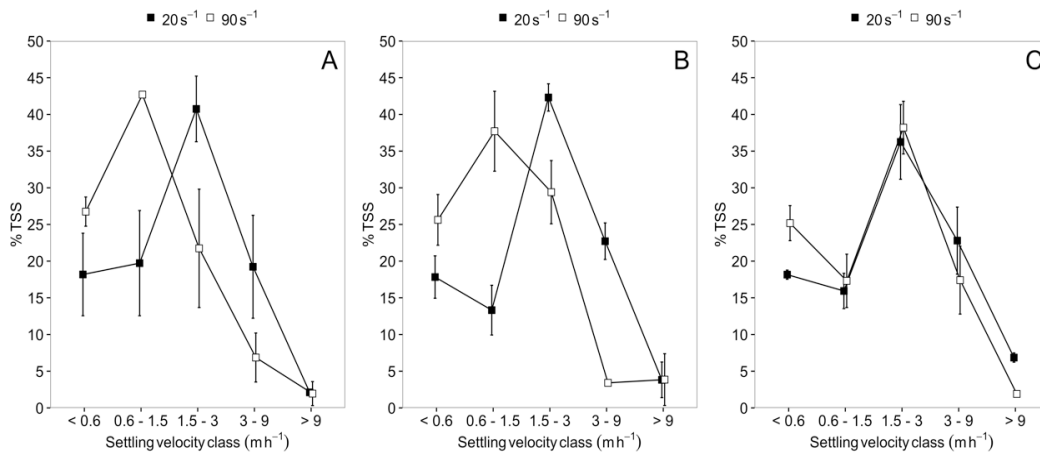
631



632 **Figure 3.1.** Orthokinetic and gravitational flocculation curves for HRAS (A)

633 bioaugmented HRAS (B) and BNR sludge (C).

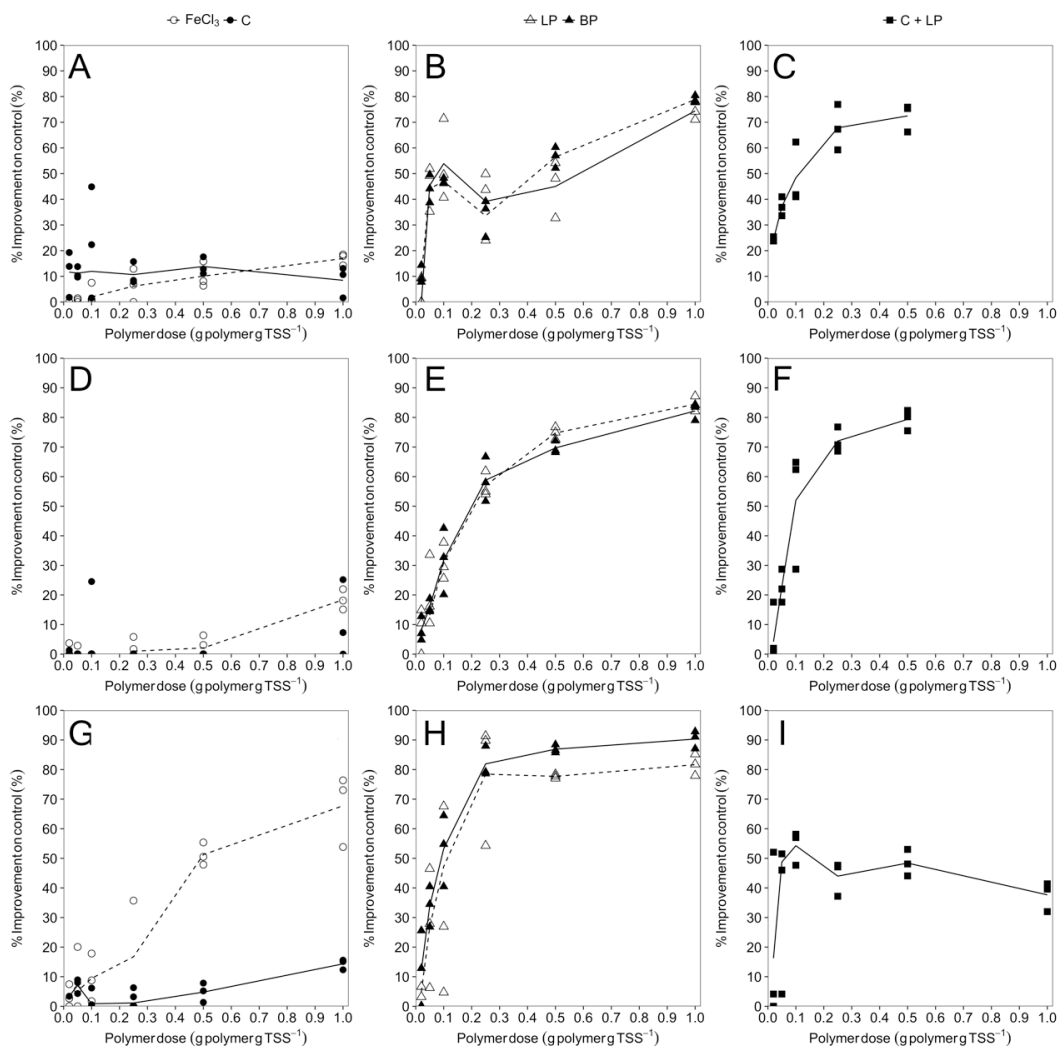
634



635

636 **Figure 3.2.** Settling velocity distribution at  $20\text{ s}^{-1}$  (solid rectangles) and  $90\text{ s}^{-1}$

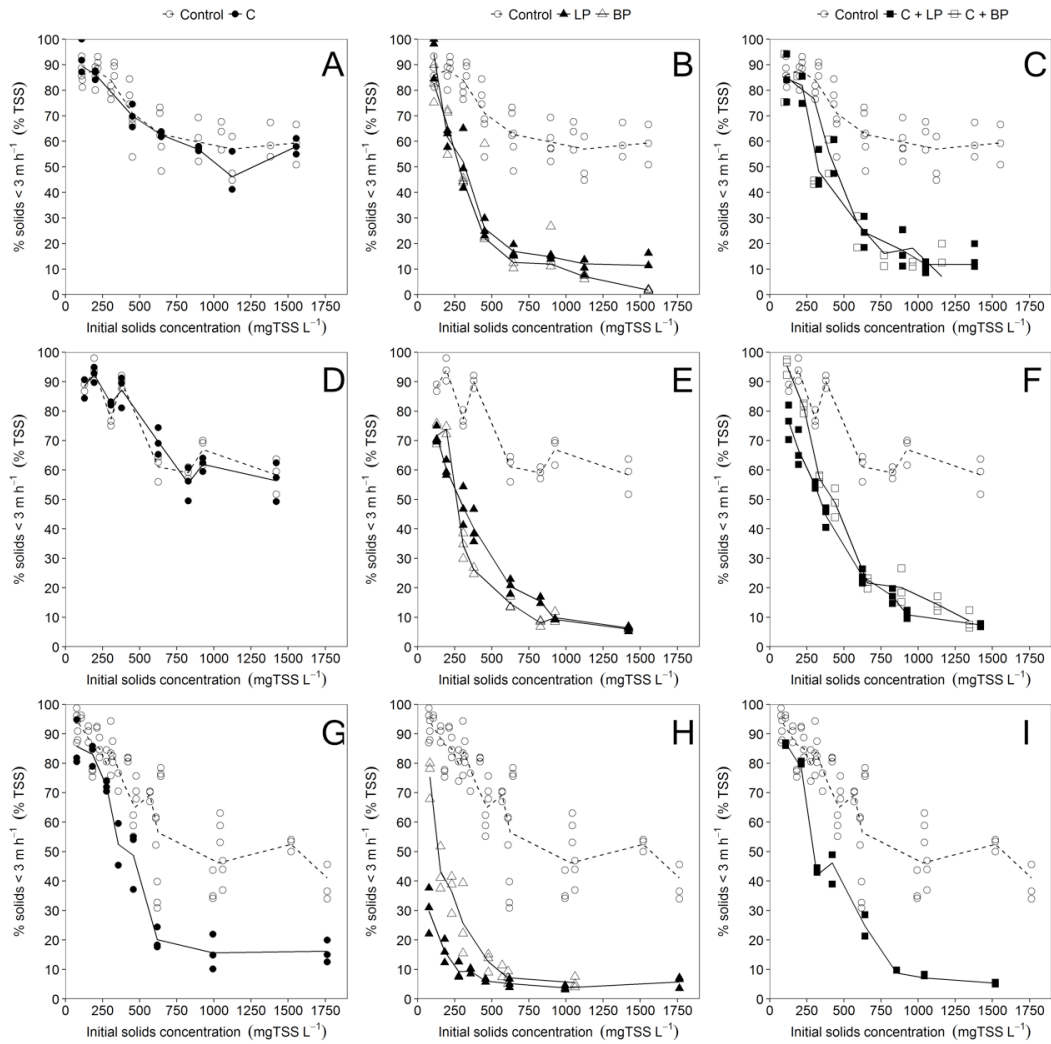
637 (hollow rectangle) for HRAS (A) bioaugmented HRAS (B) and BNR sludge (C).



639

640 **Figure 3.3.** Polymer response curves for HRAS (A-C) bioaugmented HRAS (D-

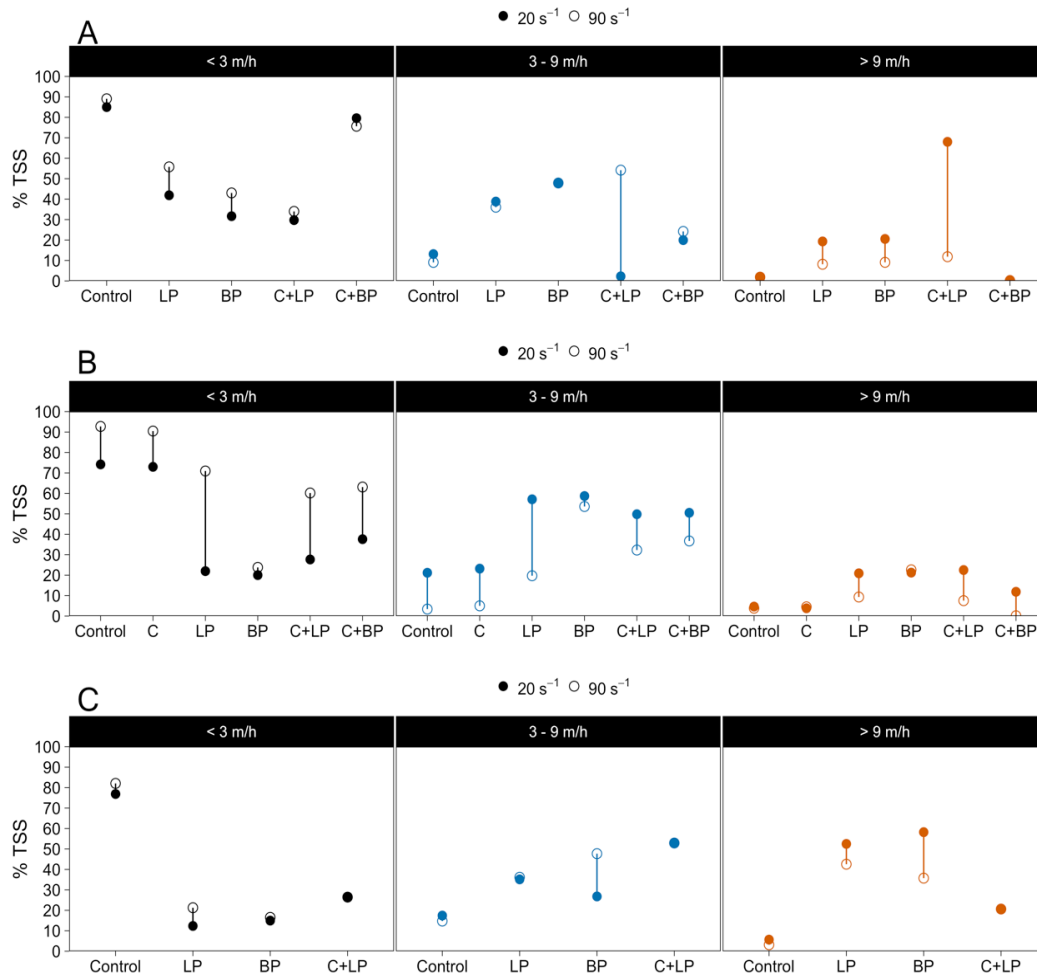
641 F) and BNR sludge (G-I).



642

643 **Figure 3.4.** Orthokinetic flocculation curves for HRAS (A-C) bioaugmented

644 HRAS (D-F) and BNR sludge (G-I).



645

646 **Figure 3.5.** Settling velocity distributions for HRAS (A), bioaugmented HRAS

647 (B) and BNR (C) sludge at 20 s<sup>-1</sup> (solid circle) and 90 s<sup>-1</sup> (hollow circle).

648

### 649 3.4 Discussion

#### 650 3.4.1 Evaluation of modified jar tests

651 Orthokinetic flocculation curves, where different concentrations of sludge

652 are subjected to a velocity gradient to promote (or obstruct at high gradients) floc

653 formation, are designed to assess steady state floc formation at different amounts

654 of collisions. As these concentrations increase, the steady state floc morphology

655 and size will change, which is represented by a change in the amount the solids  
656 traveling faster than  $3 \text{ m h}^{-1}$ . At low concentrations, less collisions happen, which  
657 resulted in smaller flocs assuming that the density of the flocs does not change.  
658 All sludges behaved similar each other below  $500 \text{ mg l}^{-1}$  as indicated by the  
659 nonsignificant difference between the sludge's OFC slopes. As such, PRC curves  
660 obtained at these concentrations only depict the influence of the polymer on  
661 collision efficiency without interference of the intrinsic stokesian characteristics of  
662 the sludge. At high concentrations, collisions are more prevalent and thus flocs  
663 were allowed to reach their maximum size as indicated by the curves in Figure 3.4  
664 to flatten out.

665

#### 666 **3.4.2 Limitations in HRAS sludge**

667 Effluent suspended solids measured in the effluent is the result of the  
668 coagulation and flocculation capabilities of the sludge. Consistent high effluent  
669 suspended solids observed in the HRAS reactor (Table 3.1) gives an indication  
670 that coagulation, flocculation, or both is limited. The control OFC curves relieved  
671 that HRAS and bioHRAS were significantly less able to form flocs faster than  $3$   
672  $\text{m h}^{-1}$  compared to BNR at high concentrations, suggesting lower collision  
673 efficiency. Furthermore, the conventional HRAS sludge has the worst TOF value  
674 of all reactors tested, indicating an intrinsic floc formation deficiency.

675 PRC curves (Figure 3.3) give valuable information on how floc formation  
676 intrinsically, i.e. independent of the amount of collisions, responds to the dosed  
677 polymer. As such, it is a direct measurement of collision efficiency of the primary

678 particles and sludge. HRAS sludge showcased the biggest response in floc  
679 formation of all sludges when LP or BP were dosed as the 50% more flocs faster  
680 than  $3 \text{ m h}^{-1}$  were formed. This strong initial response was a first indication that  
681 HRAS sludge might be limited in the flocculation step. Similarly, when  $0.5 \text{ g}$   
682 polymer  $\text{kg TSS}^{-1}$  was dosed, the OFC curves of the HRAS sludge improved,  
683 indicating that big or dense flocs were formed at lower concentration indicating  
684 improved collision efficiency. BP and LP followed the similar trend at increasing  
685 concentrations steady state flocs began to form. At this point BP created more  
686 flocs faster than  $3 \text{ m h}^{-1}$ , which became significant ( $p\text{-value} = 0.02$ ) at the final  
687 concentration tested.

688 HRAS sludge has been known to form pinpoint flocs, which are a strong  
689 indicator of a floc formation deficiency. Pinpoint flocs have been known to be  
690 denser than conventional flocs and BP with its branched structure might take  
691 advantage of that by creating compact dense flocs rather than big ones. Low SVI  
692 and high LOSS (Table 3.1) further indicated small flocs formed as the former  
693 indicates good compressibility and the latter high tolerance to hindered settling. In  
694 both cases the sludge flocs are fairly non-interactive with each other and have  
695 been described as being coagulation limited as well as adding coagulant has been  
696 proposed as a solution to pinpoint flocs.

697 If the sludge is flocculation limited, only adding coagulant might does not  
698 yield any effect as only the final floc is measured in the test. As such,  $0.5 \text{ g}$   
699 polyDADMAC  $\text{kg TSS}^{-1}$  to HRAS sludge had no effect on the floc morphology  
700 as indicated by Figure 3.4A. Assessing if a sludge is coagulation limited can

701 hence only be assessed due to indirect effect and synergies with polymer addition  
702 when flocculation is limited as well. However, the PCR curve revealed a near  
703 instantaneous improvement of 10 – 15% when FeCl<sub>3</sub> was dosed, indicating that  
704 iron did aid the coagulation process. PolyDADMAC, being a low molecular  
705 weight polymer, will act as a flocculent at higher dosage as contrary to FeCl<sub>3</sub>, it  
706 can act as a nucleation site for bridging, hence the shallow slope observed when  
707 only coagulant was dosed in Figure 3.3A. Figure 3.3C where both polyDADMAC  
708 and increasing amounts of LP were dosed did attain steady state faster than dosing  
709 polymer alone. Moreover, at 0.02 g LP g TSS<sup>-1</sup>, C + LP significantly (p-value =  
710 0.01) increased the collision efficiency compared to only LP, indicating that a  
711 coagulation was contributing to a lower overall collision efficiency. However, as  
712 0.5 g polyDADMAC per g TSS<sup>-1</sup> was dosed on top of the LP, the additional gain  
713 in collision efficiency might just be a result from the nucleation site capabilities of  
714 polyDADMAC as described above. The addition of polyDADMAC + LP did  
715 produce significantly faster flocs (> 9 m h<sup>-1</sup>) than dosing BP or LP alone,  
716 indicating that by improving coagulation and flocculation, bigger or denser flocs  
717 were created than when only polymer was dosed. These flocs were brittle, as they  
718 deteriorated once more shear was applied, which indicates that they are most  
719 likely bigger than denser, as strength of the flocs generally goes down when its  
720 size increases. The OFC curves for (bio)HRAS did not contain any information  
721 regarding coagulation limitations as coagulation is relatively independent of  
722 concentration as it more influenced by total charge than the amount collisions in  
723 contrary to flocculation. Therefore, flocculation is relatively slow compared to

724 coagulation. Hence, Figure 3.4C where both polyDADMAC and LP were used  
725 did not show any additional improvement over using polymer alone. However, at  
726 very low concentrations ( $< 150 \text{ mg TSS L}^{-1}$ ), LP nor BP had a significant  
727 improvement compared to the control ( $p\text{-value} = 0.42$  and  $0.26$  for LP and BP  
728 respectively), indicating that the polymer has no effect on the sludge. High  
729 molecular weight polymers are designed to act on bigger particles and hence  
730 require aggregates before they have any effect. As such, this is a final indication  
731 that HRAS sludge might be coagulation limited as well as flocculation limited as  
732 no aggregates were able to reach the required size for the polymer to have any  
733 effect on. In the case of bioHRAS, and BNR which show no other indication of  
734 being coagulation limited, both LP and BP did have a significant effect on the  
735 amount of the flocs formed that settled faster than  $3 \text{ m h}^{-1}$ .

736       EPS is the driver behind floc formation in activated sludge systems. The  
737 EPS of HRAS sludge did not differ significantly from the the bioaugmented  
738 variant or BNR. Most studies show a negative correlation between settleability  
739 and EPS amount, however these studies assess settleability in terms of SVI, a  
740 parameter which has recently been scrutinized to not reflect normal clarifier  
741 behavior (Mancell-Egala et al., 2016). HRAS sludge had a very low protein over  
742 polysaccharide ratio (PN/PS ratio) in the loosely bound fraction of the EPS (Table  
743 3.1). The repulsive forces between activated sludge cells have been contributed to  
744 LB-EPS (Li & Yang, 2007), while another study found that LB-EPS was  
745 responsible for attractive forces (Liu et al., 2010). However, a low PN/PS ratio  
746 has been more univocally accepted as an indicator for poor floc formation (Liao et

747 al., 2001; Morgan et al., 1990), and thus might explain the floc formation  
748 characteristics.

749

### 750 **3.4.3 Impact of bioaugmentation of HRAS on floc formation limitations**

751 Bioaugmentation of the high-rate activated sludge reactor with BNR  
752 sludge improved the overall proficiency of the solid separation as indicated by the  
753 lower effluent suspended solids (Table 3.1). However, effluent quality was quite  
754 eccentric in time as denoted by the high standard deviation, indicating a more  
755 situational limitation that might not always have an impact on effluent suspended  
756 solids. Bioaugmentation also improved the intrinsic collision efficiency of the  
757 sludge as noted by the lower obtained TOF value compared to the HRAS reactor.  
758 The shallower PCR slope for LP and BP (Figure 3.3E) indicate that  
759 bioaugmentation helped mitigating the flocculation limitation, but as no impact of  
760 polyDADMAC can be seen on the final floc formation (Section 3.4.4),  
761 flocculation assumed to be limiting. Dosing polyDADMAC and linear polymer  
762 increased the response of the latter on the sludge (figure 3.3F), however no effect  
763 of polyDADMAC nor FeCl<sub>3</sub> was observed. Hence bioaugmentation of HRAS  
764 sludge mitigated a possible coagulation limitation, and changed the floc  
765 morphology of the sludge as indicated by the higher SVI and lower LOSS and  
766 ISV. This was also observed for this particular reactor in Mancell-Egala et al.  
767 (2017), where images revealed bigger flocs than the conventional HRAS reactor  
768 tested. Next, the OFC strengthen this hypothesis as a significant different between  
769 the slope of LP and BP was observed. As final floc size increases with

770 concentration until a maximum has been achieved at high concentration, the  
771 significant slope difference between LP and BP can be explained by BP creating  
772 stronger flocs that are less prone to breakup. BP, with its branched nature, creates  
773 more compact flocs with lower fractal dimension (Hjorth et al., 2008). This  
774 advantage of BP over LP diminished when the sludge concentration was  
775 increased, which can be explained by the larger impact of macro floc formation in  
776 the (tranquil) sedimentation step. When the concentration was high, too many  
777 collisions happen to observe the effect of floc strength as everything will be  
778 allowed to reflocculate. As such, no difference between LP and BP can be  
779 observed at higher concentrations.

780 Figure 3.2B also suggests a floc strength limitation, where almost all  
781 sludge in the 3-9 m h<sup>-1</sup> class deteriorated into lower class when the sludge was  
782 subjected to 90 s<sup>-1</sup> instead of 20 s<sup>-1</sup> compared to the conventional HRAS. This was  
783 further explored in Figure 3.5B where dosing BP made the sludge very resilient to  
784 shear stress compared to LP. The linear structure of LP and high molecular weight  
785 promotes floc size which makes the flocs even more prone to breakup.  
786 Interestingly, when polyDADMAC was added in combination with BP, the  
787 benefit of the latter disappeared. One explanation is that the neutralization of  
788 charge caused an excess of positive charge, with less bridging as effect and a  
789 more brittle floc that is more sensitive to shear as result.

790

791 **3.4.4 Impact of SRT and organic loading rate on floc formation limitations**

792 The biological nutrient reactor had the lowest effluent suspended solids of  
793 the tested reactor (Table 3.1), as well as the lowest observable TOF and formation  
794 of gravitational induced flocs at the lowest concentration tested (Figure 3.1C).

795 Therefore, BNR sludge can be considered not limited in floc formation for all  
796 practical reasons. BNR was also very resilient to shear stress as no significant  
797 change in settling velocity was found when the sludge was subjected to a higher  
798 velocity gradient. Both the PCR and OFC curve showed a greater affinity for LP  
799 than BP, which was especially visible at higher polymer dosages (Figure 3.3H)  
800 and very low sludge concentrations (Figure 3.4H). Given the very good intrinsic  
801 floc forming properties of BNR sludge, BNR aggregates are most likely larger  
802 than HRAS' which explains LP's bigger affinity. Moreover, BNR is a high SRT,  
803 low organic loading rate sludge, which is for creating denser flocs as the ash  
804 levels in the sludge increases with SRT.

805 There was a clear impact of polyDADMAC in both the PRC (figure 3.3G)  
806 and OFC (Figure 3.4G) tests, which might indicate a severe coagulation  
807 limitation. However, given that coagulation is a precursor of flocculation and  
808 BNR showed very good effluent suspended solids achieved and intrinsic floc  
809 formation properties, this apparent limitation might be a side effect of the test  
810 setup. Only the final floc is measured, as such, it is hard to distinguish between a  
811 limitation in the coagulation or flocculation. BNR's flocculation might be non-  
812 limited enough for any improvement in coagulation to be seen in the final floc

813 morphology. If the sludge is (severely) flocculation limited as is the case for  
814 (bio)HRAS sludge, this is not the case as discussed above.

815

### 816 **3.5 Conclusion**

817 Three different sludge types were assessed for their possible flocculation  
818 formation limitations using modified jar tests. Three main conclusions can be  
819 summarized:

820 Conventional HRAS shows great affinity for linear polymer but is non-  
821 discriminatory towards linear or branched polymer. This sludge can be considered  
822 predominantly flocculation limited with coagulation limitation becoming apparent  
823 at low concentrations. To mitigate limitations, dosing linear polymer is advised

824 Bioaugmented HRAS shows greater affinity for branched than linear  
825 polymer. While being flocculation limited, floc strength is the main issue. As  
826 such, addition of branched polymer or careful design of clarifier headworks might  
827 be appropriate to mitigate ESS spikes.

828 BNR sludge shows no indication of a coagulation, flocculation or strength  
829 limitation. Since flocculation was not limited, low molecular weight coagulants  
830 did show an improvement in overall floc formation. Hence, cheap mannich-type  
831 coagulants might be appropriate if effluent suspended solids limits are especially  
832 stringent.

833

### 834 **3.6 References**

835 Andreadakis, A.D. 1993. Physical and Chemical-Properties of Activated-Sludge  
836 Flocculation. *Water Research*, **27**(12), 1707-1714.

- 837 APHA. 2005. *Standard methods for the examination of the water and wastewater*,  
838 Washington, DC.
- 839 ASTM. 1995. Standard Practice for Coagulation-Flocculation Jar Test of Water.  
840 in: *Annual book of ASTM standards*, ASTM International. Washington,  
841 DC.
- 842 Biggs, C.A., Lant, P.A. 2000. activated sludge flocculation: on-line determination  
843 of floc size and the effect of shear. *Water Res*, **34**(9), 2542-2550.
- 844 Derjaguin, B., Landau, L. 1993. Theory of the stability of strongly charged  
845 lyophobic sols and of the adhesion of strongly charged particles in  
846 solutions of electrolytes. *Progress in Surface Science*, **43**(1-4), 30-59.
- 847 DuBois, M., Gilles, K.A., Hamilton, J.K., Rebers, P., Smith, F. 1956.  
848 Colorimetric method for determination of sugars and related substances.  
849 *Analytical chemistry*, **28**, 350-356.
- 850 Frolund, B., Palmgren, R., Keiding, K., Nielsen, P.H. 1996. Extraction of  
851 extracellular polymers from activated sludge using a cation exchange  
852 resin. *Water Research*, **30**(8), 1749-1758.
- 853 Hermasson, B. 1999. The DLVO theory in microbial adhesion. *Colloids and*  
854 *Surfaces B: Biointerfaces*, **14**(1), 105-19.
- 855 Hjorth, M., Christensen, M.L., Christensen, P.V. 2008. Flocculation, coagulation,  
856 and precipitation of manure affecting three separation techniques.  
857 *Bioresour Technol*, **99**(18), 8598-604.
- 858 Langelier, W.F., Ludwig, H.F. 1949. Mechanism of Flocculation in the  
859 Clarification of Turbid Waters. *Journal (American Water Works*  
860 *Association)*, **41**(2), 163-181.
- 861 Li, X.Y., Yang, S.F. 2007. Influence of loosely bound extracellular polymeric  
862 substances (EPS) on the flocculation, sedimentation and dewaterability of  
863 activated sludge. *Water Res*, **41**(5), 1022-30.
- 864 Liao, B.Q., Allen, D.G., Droppo, I.G., Leppard, G.G., Liss, S.N. 2001. Surface  
865 properties of sludge and their role in bioflocculation and settleability.  
866 *Water Research*, **35**(2), 339-350.
- 867 Liu, X.M., Sheng, G.P., Luo, H.W., Zhang, F., Yuan, S.J., Xu, J., Zeng, R.J., Wu,  
868 J.G., Yu, H.Q. 2010. Contribution of extracellular polymeric substances  
869 (EPS) to the sludge aggregation. *Environ Sci Technol*, **44**(11), 4355-60.
- 870 Lowry, O.H., Rosebrough, N.J., Farr, A.L., Randall, R.J. 1951. Protein  
871 measurement with the Folin phenol reagent. *J biol Chem*, **193**(1), 265-275.
- 872 Mancell-Egala, W.A., Kinnear, D.J., Jones, K.L., De Clippeleir, H., Takacs, I.,  
873 Murthy, S.N. 2016. Limit of stokesian settling concentration characterizes  
874 sludge settling velocity. *Water Res*, **90**, 100-10.
- 875 Mancell-Egala, W.A., Su, C., Takacs, I., Novak, J.T., Kinnear, D.J., Murthy, S.N.,  
876 De Clippeleir, H. 2017. Settling regimen transitions quantify solid  
877 separation limitations through correlation with floc size and shape. *Water*  
878 *Res*, **109**, 54-68.
- 879 Mer, V.K.L., Healy, T.W. 1963. THE ROLE OF FILTRATION IN  
880 INVESTIGATING FLOCCULATION AND REDISPERSION OF  
881 COLLOIDAL DISPERSIONS. *The Journal of Physical Chemistry*,  
882 **67**(11), 2417-2420.

883 Morgan, J.W., Forster, C.F., Evison, L. 1990. A Comparative-Study of the Nature  
884 of Biopolymers Extracted from Anaerobic and Activated Sludges. *Water*  
885 *Research*, **24**(6), 743-750.

886 Verwey, E.J.W., Overbeek, J.T.G., Overbeek, J.T.G. 1999. *Theory of the stability*  
887 *of lyophobic colloids*. Courier Corporation.

888 Wahlberg, E.J., Keinath, T.M., Parker, D.S. 1994. Influence of Activated Sludge  
889 Flocculation Time on Secondary Clarification. *Water Environment*  
890 *Research*, **66**(6), 779-786.

891 Wilen, B.M., Jin, B., Lant, P. 2003. The influence of key chemical constituents in  
892 activated sludge on surface and flocculating properties. *Water Res*, **37**(9),  
893 2127-39.

894

895

896

897

898

899

900

901

902

903

904

905

906

907

908

909 **Chapter 4: Manuscript 2: Influence of extracellular polymeric**  
910 **substance (EPS) on the structured water content in the sludge and**  
911 **objective measurements of the structured water content.**

912

913 **Keywords:** Activated sludge, Biosolids, Structured water content, Extracellular  
914 polymeric substances (EPS), Dewatering properties

915

916 **Abstract**

917 Structured water is the moisture content in the sludge that cannot be removed by  
918 conventional dewatering processes and it remains in the dewatered biosolids thus  
919 causing extra cost for the storage, transportation and disposal of the biosolids. In  
920 this study, the drying test that was applied for determination of the structured  
921 water content in five sludge types (primary sludge, secondary sludge, sludge  
922 before thermal hydrolysis process (THP), sludge after THP and sludge after  
923 anaerobic digestion (AD)) were proposed and evaluated. Two baselines  
924 simulating free water evaporation (baseline A and baseline B) combined with the  
925 drying rate curve, two baselines simulating weight changed caused by free water  
926 evaporation (baseline C and baseline D) combined with the weight curve and  
927 Monod model were applied as five determinations of the structured water content  
928 in the sludge. Results indicated that baseline A and baseline D considered all  
929 experimental impactors such as temperature, relative humidity and wind speed;  
930 baseline B could be applied when experiment condition was strictly controlled.  
931 Weight curve with baseline C was limited by environmental impactors. Monod

932 model provided mathematical expression of drying rate, however it was sensitive  
933 to the experimental environment. Sludge extracellular polymeric substances  
934 (EPS) composition, floc size and dynamic viscosity were also analyzed for their  
935 impact on the structured water content. The results indicated that there was no  
936 significant correlation between the tightly bound EPS, organic matter content,  
937 protein (PN) content, polysaccharide (PS) content and PN/PS ratio of the sludge  
938 EPS and the structured water content. Structured water content was negatively  
939 correlated with loosely bound (LB)-EPS polysaccharides ( $R^2=0.57$  and  $0.64$  for  
940 baseline A and baseline B, respectively). Dynamic viscosity of the sludge did not  
941 influence the moisture evaporation, while the floc size of the sludge was  
942 positively correlated with the structured water content ( $R^2=0.77$  and  $0.60$  for  
943 baseline A and baseline B, respectively). The biosolids quality could be enhanced  
944 by reducing the moisture content in the sludge, and possible treatments involved  
945 increasing floc size and decreasing LB-EPS polysaccharide contents.

946

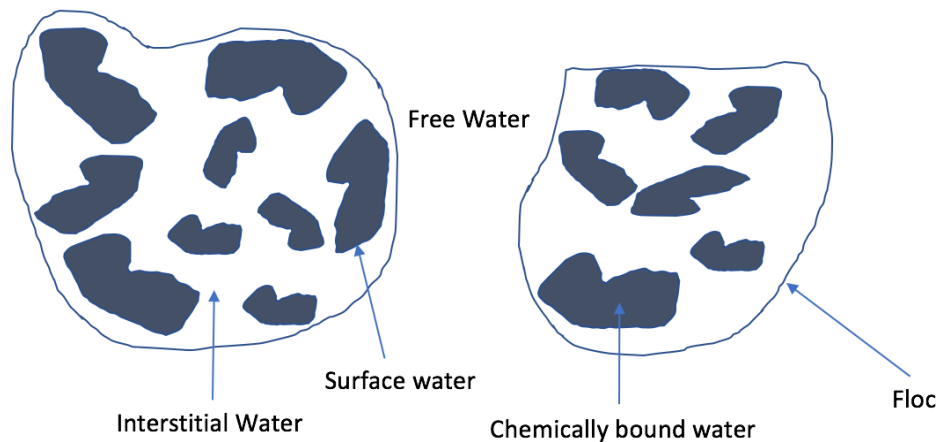
#### 947 **4.1 Introduction**

948 In wastewater treatment facilities, municipal wastewater is treated to  
949 remove the organic matters, pathogens and nutrients, and large amount of sludge  
950 is produced throughout the treatment processes. This sludge is collected and  
951 further treated to remove pathogens and moisture content. Dewatered sludge is  
952 referred to as biosolids, and it contains high level of nutrients such as organic  
953 matter, nitrogen and phosphorous, thus it has significant potential for land  
954 application (Lu, He and Stoffella, 2012). Class A biosolids that meets the US

955 Environmental Protection Agency's (USEPA) requirements has been applied in  
956 agriculture and public green places as fertilizer (Roy et al., 2011). Resource  
957 recovery facilities take charge of the waste disposal and recycling. Biosolids are  
958 produced by dewatering the sludge from the wastewater processes at multiple  
959 stages such as primary and secondary clarification. Maximum separation between  
960 the solids part and the water content is desired to achieve effluent clarity, to  
961 reduce energy consumption for biosolids handling processes at the resource  
962 recovery facility, to limit the need for storage space after the final biosolids  
963 treatment and to reduce the requirements for transportation to the land application  
964 sites (Wakeman, 2007). Sources of the biosolids are made up of primary sludge  
965 from the primary clarification as well as the biomass produced during the  
966 treatment processes, where organic carbon, nitrogen and phosphorus are removed  
967 by biological processes and precipitation. Industrial or domestic sludge can  
968 contain up to 95% water on a mass basis (Colin and Gazbar, 1995). Thus,  
969 dewatering of the sludge is applied as a process that separates water from solids.  
970 Often, more than 40% of the total cost of wastewater treatment is spent on  
971 biosolids treatment, separation and disposal (Ruiz-Hernando, Labanda and  
972 Llorens, 2010). However, current dewatering treatment approaches are still  
973 leaving the biosolids with a high moisture content ranging from 88% to 65%  
974 (Vaxelaire, 2001), and improved dewaterability is continuous challenge.

975           Dewaterability of biosolids correlates with the structured water content  
976 and the water distribution within the individual sludge flocs (Kopp and Dichtl,  
977 2000). In the sludge flocs, water can be present in different compartments

978 depending on the binding characteristics such as adsorption, capillarity forces and  
979 chemical bonds. Vesilind (1994) developed a classification of the types of water  
980 in sludge flocs, which had been applied in previous studies (Vaxelaire and Cézac,  
981 2004; Tsang and Vesilind, 1990): (1) Free water: water that is unaffected by  
982 capillary force; (2) Interstitial water: water that is trapped into interstitial places  
983 between the sludge flocs due to capillary forces; (3) Surface water: water that is  
984 attached to the surface of the sludge flocs due to adhesive forces; (4) Chemically  
985 bound water: water that is tightly bound to the sludge flocs due to chemical  
986 interactions such as hydration water (Figure 4.1). Tsang and Vesilind (1990)  
987 showed that only the free water (1) and a small proportion of the interstitial water  
988 (2) can be removed by mechanical dewatering processes, thus the combination of  
989 interstitial water, surface water and hydration water was left within the biosolids  
990 (Wu, Huang and Lee, 1998). In this study, the structured water is defined as the  
991 moisture content in the sludge excluding free water. An approach for objective  
992 measurement of the structured water content in various sludge types is required to  
993 better understand the current limitations present in sludge dewatering.  
994 Furthermore, identification of the mechanism by which water binds to the sludge  
995 flocs will provide information regarding solutions to improve dewaterability and  
996 to achieve a reduced moisture content in biosolids.



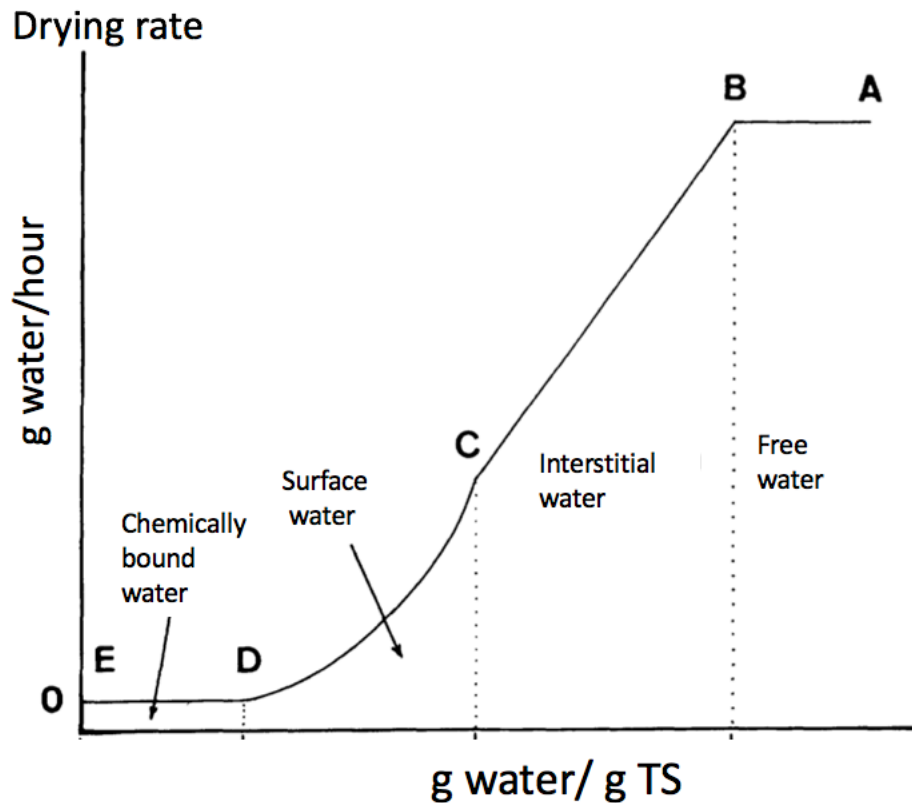
997

998 **Figure 4.1.** Moisture distribution in a sewage sludge floc (freely after Kopp and  
 999 Dichtl, 2000). Free water moved between flocs; Interstitial water was trapped in  
 1000 the interstitial places in the flocs; Surface water was adsorbed onto the surface of  
 1001 the floc particles; Chemically bound water bound to the floc particles through  
 1002 chemical bonds.

1003

1004 One approach that has been used by several research groups (Robinson  
 1005 and Knocke, 1992; Lee and Hsu, 1995; Chu and Lee, 1999) to measure the water  
 1006 distribution of biosolids is the drying test. One of the advantages of this approach  
 1007 is that the drying test provides a full curve of the drying period instead of just  
 1008 providing a number of the structured water content. Another advantage is that the  
 1009 drying test is easy to perform because it does not require the use of specialized  
 1010 equipment, thus it can be setup in any laboratory (Lee and Hsu, 1995, Matsuda,  
 1011 Kawasaki and Mizukawa, 1992). In this approach, a sludge sample is dried in a  
 1012 closed system at a constant temperature and relative humidity. The moisture loss  
 1013 is caused by evaporation of free water followed by structured water. The approach

1014 was based on a hypothesis stating that different moisture types within the sludge  
1015 have various evaporation rates (Vaxelaire and Cézac, 2004). Therefore, a change  
1016 in the evaporation rate indicates a transition between two types of water  
1017 associated with the sludge flocs. A drying curve were applied to describe the  
1018 relationship between the water content and the evaporation rate (Figure 4.2).



1019  
1020 **Figure 4.2.** Drying curve for the drying test (Lee and Hsu, 1995). The drying rate  
1021 for different water types were different: A-B indicated free water evaporation  
1022 rate; B-C indicated interstitial water evaporation rate; C-D indicated surface water  
1023 evaporation rate; D-E indicated chemically bound water evaporation rate.

1024

1025           There has been a controversy regarding the determination of the structured  
1026 water, and the content of structured water in the sludge floc depends on various  
1027 measurement technologies (Vaxelaire, 2004). One applied determination of  
1028 structured water defines it as water that does not freeze at -20 °C, at which free  
1029 water would freeze (Colin and Gazbar, 1995). A dilatometric test that is based on  
1030 this hypothesis can be applied to quantify the structured water content (Lee,  
1031 1996). In the method, a certain amount of sludge sample was subjected to freezing  
1032 temperatures until -20 °C was reached. The samples were then reheated to the  
1033 room temperature. It was hypothesized that only free water would freeze below -  
1034 20 °C, so that the volume change of the sludge sample only would be caused by  
1035 the free water freeze (Smith and Vesilind, 1995). The content of the free water in  
1036 the sludge was determined by the volume change and then subtracted from the  
1037 total water content of the biosolids to obtain the structured water content (Wu,  
1038 Huang and Lee, 1998). The dilatometric test has been applied for determination of  
1039 the structured water content because it provides contents of the structured water  
1040 content directly (Vaxelaire, 2004, Smith and Vesilind, 1995). However, a value of  
1041 the structured water content alone is not as convincing as a full curve provided by  
1042 the drying test. Furthermore, the requirements for the precision of the equipment  
1043 for the dilatometric test combines to make this method less practical.

1044           Extracellular Polymeric Substances (EPS) play an important role in the  
1045 biosolids dewatering processes (Neyens, 2004), and previous studies indicate that  
1046 the EPS content can influence the moisture distribution and dewaterability  
1047 (Houghton, 2001; Mikkelsen, 2002). Bound EPS was defined as insoluble EPS

1048 that binds with bacterial cells to form a net-like structure that is involved in  
1049 holding the sludge flocs (biofilms) together. It has further been classified as  
1050 loosely bound EPS (LB-EPS) and tightly bound EPS (TB-EPS): TB-EPS is  
1051 tightly attached on the bacterial cell surface, while LB-EPS pervades into the  
1052 surrounding environment at the outer layer of the biofilm, forming a loose  
1053 coverage of the TB-EPS (Wingender, Neu and Flemming, 1999). Proteins (PN)  
1054 and polysaccharide (PS) are two major components of EPS (Sheng, Yu and Li,  
1055 2010). TB-EPS generally contains more protein, with a PN to PS ratio of 1.6 to  
1056 2.0, whereas LB-EPS contained a higher proportion of polysaccharide, with PN to  
1057 PS ratio ranging from 0.7 to 0.9 (Basuvaraj, Fein and Liss, 2015). The later study  
1058 also showed that TB-EPS led to the formation of granular flocs, which  
1059 correlated with improved biosolids settleability and dewaterability. Meanwhile, a  
1060 high LB-EPS content caused formation of pinpoint flocs with small floc size,  
1061 which exhibited poor settleability and dewaterability (Basuvaraj, Fein and Liss,  
1062 2015). In another study, it was shown that a high LB-EPS content prevented  
1063 efficient flocculation, settleability and dewaterability of a sludge (Li and Yang,  
1064 2007). This study also found that the interstitial water content present in the LB-  
1065 EPS fraction (4.3% of total water content) was increased compared to the water  
1066 content in the TB-EPS fraction (0.2% of total water content). Therefore, LB-EPS  
1067 might result in a higher structured water content in the sludge.

1068           The establishment of an objective method for determination of the  
1069 structured water content in biosolids from DC Water was applied towards several  
1070 sample types. The main focus was put on establishing an approach based on the

1071 previously described drying test that would be capable of providing a full drying  
1072 curve to measure the different types of water present in the biosolids.  
1073 Establishment of an objective approach would represent an improvement  
1074 compared to currently applied approaches, where the determination of the  
1075 structured water content is partially subjective (Chen et al., 1997; Lee, Lai and  
1076 Mujumdar, 2006; Vaxelaire and Cézac, 2004). In this current study, objective  
1077 approaches for quantifying the structured water content were applied for sludge  
1078 with different characteristics obtained from different process steps at DC Water.  
1079 The relationships between the structured water content and sludge characteristics  
1080 like the EPS composition, floc size and the dynamic viscosity were investigated at  
1081 the same time.

1082         The samples were collected throughout the solid treatment processes.  
1083 Based on the data obtained from the drying test, five objective approaches were  
1084 developed and applied for evaluating the water content in the collected biosolids  
1085 samples. The methodologies were all assessed and evaluated according to their  
1086 theoretical and practical meanings. Analysis of the sludge viscosity and EPS  
1087 content were performed for all samples to study the relationship between them  
1088 and the structured water content.

1089

## 1090 **4.2 Materials and Methodology**

### 1091 **4.2.1 Sample locations and acquisition**

1092         The Blue Plains Advanced Wastewater Treatment Plant is the largest  
1093 advanced wastewater treatment plant in the world, treating over 1.1 million cubic

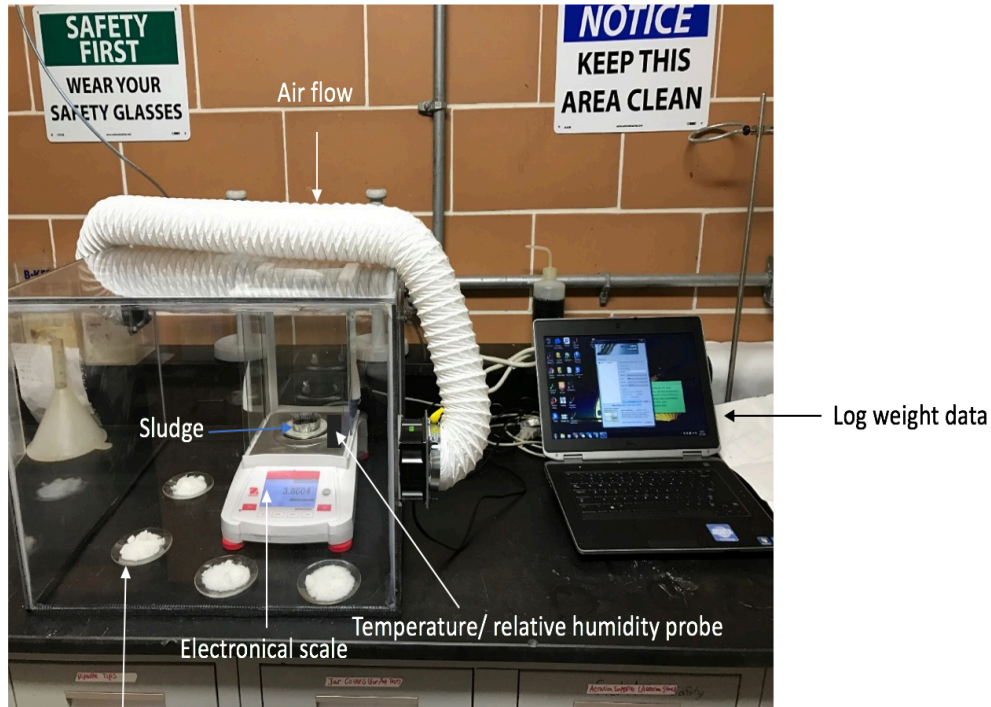
1094 meters (300 million gallons) of sewage per day and serving the District of  
1095 Columbia and parts of Maryland and Virginia (DC Water, 2017). Five sludge  
1096 types were studied in this project, following the solids treatment processes of the  
1097 Blue Plains from November 2016 to June 2017. The sampling locations were:  
1098 primary sludge collected at the primary gravity thickener (TS=5%); the biological  
1099 activated sludge (the secondary sludge) (TS=5%) collected at the secondary  
1100 thickening tank; the mix of primary and secondary sludge (40% of primary sludge  
1101 and 60% of secondary sludge based on mass) (TS=5%) collected at a blended  
1102 temporary storage tank (blending tank No. 2 in DC water) prior to the thermal  
1103 hydrolysis process (THP); the thermal-hydrolyzed mixed sludge (Cambi sludge,  
1104 the THP sludge) (TS=10%) collected after the THP process; the anaerobically  
1105 digested sludge (the AD sludge) (TS=5%) collected at a blended temporary  
1106 storage tank (blending tank No. 3 in DC water ) before dewatering. The samples  
1107 were collected using 500 ml plastic cups, and they were subjected to the drying  
1108 test immediately after collection.

1109

#### 1110 **4.2.2 Determination of the structured water content**

1111 The drying test was operated to determine the structured water content in  
1112 the sludge samples. In Figure 4.3, a closed chamber (54.5\*54.5\*38 cm) made out  
1113 of Plexi glass was set up in the laboratory at Blue Plains Advanced WWTP. The  
1114 temperature and relative humidity (RH) inside the closed chamber were controlled  
1115 by an air condition unit and magnesium nitrate ( $Mg(NO_3)_2$ ), respectively, and a  
1116 detector (OM-92 temperature/ humidity Data Logger, OMEGA) was placed in the

1117 chamber to record real-time temperature and RH every 30 seconds during the  
1118 drying period of each sample. An air flow system, fixed in two opposite walls of  
1119 the chamber, provided recycled air flow (speed= 0.52 m/s), accelerating the  
1120 drying process. An electronic scale recorded the weight changes due to water loss  
1121 from three grams of sludge sample every 30 seconds, and the data was logged  
1122 through RS232 Data Logger software (Eltima Software 2.7). Aluminum pans  
1123 (diameter=5.4 cm, height=1.5 cm) were pretreated at 550°C for at least 20 minutes  
1124 to remove potential moisture before placed on the scale. The sludge samples  
1125 covered the surface of the aluminum pan to achieve an even drying area. Air  
1126 condition and magnesium nitrate were setup at least 40 minutes before the drying  
1127 test was started to reach steady state experimental conditions: temperature of  
1128 22°C and RH of 60%. Total solids (TS) and volatile solids (VS) were measured in  
1129 duplicate at the same day for each sample by heating five grams of sludge at  
1130 105°C and 550°C for at least 24 hours and 20 minutes, respectively (Dinuccio et  
1131 al., 2010).  
1132 .



1133 magnesium nitrate solid

1134 **Figure 4.3.** Drying test set up. Electronical scale measured the weight change of  
 1135 the drying sample, and weight data was logged through the computer software  
 1136 (RS232); Magnesium nitrate controlled the relative humidity; air flow accelerated  
 1137 the evaporation of the sludge; temperature/ relative humidity probe recorded the  
 1138 experimental impactors.

1139

#### 1140 **4.2.3 Extracellular polymeric substances (EPS) extraction**

1141 EPS were extracted in triplicate by using a heat extraction method  
 1142 developed by Li and Yang (2007) where all compounds of the EPS were extracted  
 1143 simultaneously. A phosphate saline buffer solution (PBS) was applied for  
 1144 extraction of loosely bound EPS (LB-EPS) and tightly bound EPS (TB-EPS).  
 1145 PBS was prepared by mixing 2 mM  $\text{Na}_3\text{PO}_4$ , 4 mM  $\text{KH}_2\text{PO}_4$ , 9 mM  $\text{NaCl}$  and 1

1146 mM KCl, with pH adjusted to 7.2. The sludge samples were diluted until total  
1147 suspended solids (TSS) equaled to 1000 mg/L, after which 25 mg of the diluted  
1148 samples were used for EPS extraction. The samples were centrifuged at 4000 rpm  
1149 for five minutes. Then the supernatant was discarded and the concentrated solid  
1150 pellet was resuspended in 10 ml heated (60°C) PBS followed by vortexing for one  
1151 minute. The samples were then centrifuged for 10 minutes at 4000 rpm and the  
1152 liquid supernatant was collected as LB-EPS. For the TB-EPS extraction, 10 ml of  
1153 heated (60°C) PBS was added to the solid pellet and immediately vortexed for  
1154 one minute. The mixture was subsequently transported to a tube with cap and  
1155 heated at 60°C for 30 minutes. After heating, the sample was centrifuged at 4000  
1156 rpm for 15 minutes, and the supernatant was collected as TB-EPS (Li and Yang,  
1157 2007). All extracted EPS samples were labeled by the sludge type and date and  
1158 kept at -20°C until further analysis. TSS and VSS of the diluted samples were  
1159 measured in duplicate by heating at 105°C and 550°C for at least one hour and 20  
1160 minutes, respectively (El-Kamah et al., 2010).

1161

#### 1162 **4.2.4 Extracellular polymeric substances (EPS) Composition**

1163 (1) Soluble Protein Analysis:

1164 The total protein content in the extracted EPS fractions was measured  
1165 using an improved method developed from the Lowry method (Lowry et al.,  
1166 1951) because it was widely applied in previous studies (Dulley and Grieve,  
1167 1975; Markwell et al., 1978; Peterson, 1979). This method was based on the  
1168 reaction between the copper ions and peptides bound in the protein using Folin

1169 reagent (Folin and Ciocalteu, 1927). A commercial modified Lowry Protein  
1170 Assay kit (Thermo Fisher Scientific, USA) was applied for the total protein  
1171 measurement. In triplicate, EPS samples were defrosted at 25°C and 400 µL of  
1172 each EPS sample was transferred into a labeled glass tube. 400 µL of deionized  
1173 water was prepared as a control. Two ml of the Modified Lowry Protein Assay  
1174 solution (Thermo Fisher Scientific, USA) was added to each sample tube, the  
1175 tubes were then sealed and mixed completely by shaking 10 times and incubated  
1176 at 25°C for 10 minutes. At this point, 200 µL of Folin's reagent (Thermo Fisher  
1177 Scientific, USA) was added, and the tubes were immediately vortexed for one  
1178 minute and incubated at 25°C for 30 minutes. Thereafter, the total protein  
1179 concentration in each sample was determined by light transmission using a  
1180 HACH DR2800 Spectrophotometer (HACH, Loveland, Colorado) at 750 nm.

1181

1182 (2) Soluble Polysaccharide Analysis:

1183 The total polysaccharide concentration in the EPS was measured  
1184 according to an improved method developed from the DuBios method (DuBois  
1185 et al., 1956) because it was widely applied in previous studies (Cuesta et al.,  
1186 2003; Escot et al., 2001; Siddhanta et al., 1999). This approach was based on a  
1187 colorimetric method to determine polysaccharide concentration. In triplicate, EPS  
1188 samples were thawed, and two mL of each EPS sample was transferred into a  
1189 labeled glass tube. 200 mL of deionized water was prepared as a control. 0.125  
1190 mL of 80% (by weight) phenol solution was added to each test tube, after which  
1191 five mL of 98% (by weight) sulfuric acid was added immediately. Tubes were

1192 then sealed and incubated for 10 minutes without mixing at 25°C. The tubes were  
1193 then vortexed and incubated at 25°C in a water bath for 10 minutes. Thereafter the  
1194 total polysaccharide concentration was determined by light transmission  
1195 determined by using a HACH DR2800 Spectrophotometer (HACH, Loveland,  
1196 Colorado) at 485nm.

1197

### 1198 (3) Chemical Oxygen Demand (COD) Analysis:

1199 The organic matter concentration of the extracted EPS samples was  
1200 determined as the Chemical Oxygen Demand (COD). The COD concentration  
1201 was determined to study the influence of the organic matter content in the sludge  
1202 on the structured water content. For this method, HACH® COD kits (HACH,  
1203 Loveland, Colorado) were applied according to the manufacturer instructions  
1204 (HACH, COD manual, Loveland, Colorado). In this approach, the strong oxidant  
1205 potassium dichromate ( $K_2Cr_2O_7$ ) was used to oxidize organic compounds present  
1206 in the sample. During the reaction, the orange-red dichromate ion ( $Cr_2O_7^{2-}$ ) was  
1207 reduced to the green chromic ion ( $Cr^{3+}$ ). The total concentration of  $Cr^{6+}$  and  $Cr^{3+}$   
1208 were measured colorimetrically after a two-hour reaction at 150 °C. After this, the  
1209 concentration of  $Cr^{6+}$  and produced  $Cr^{3+}$  were measured by using the HACH  
1210 DR2800 Spectrophotometer (HACH, Loveland, Colorado) stored program for low  
1211 range (3–150 mg/L) and high range COD (20-1500 mg/L) measurement,  
1212 respectively.

1213

#### 1214 **4.2.5 Floc Size quantification**

1215           The floc size distribution in the five types of sludge was determined to  
1216 evaluate the influence on the structured water content. Fresh sludge samples were  
1217 collected from the Blue Plains Advanced WWTP and transported, using ice bags  
1218 to prevent bacterial growth, to the research laboratory at University of Maryland  
1219 at College Park for quantification of the sludge floc size distribution using  
1220 microscopic techniques. A capillary tube was used to take sludge samples by  
1221 slightly touching the microscope slide, and the sample was then covered by a  
1222 coverslip. The floc sizes were measured using a biological trinocular microscope  
1223 (Motic AE31 series, HongKong, China), with a 10X objective and a ruler placed  
1224 in one eye piece, where the length of each unit indicated 100  $\mu\text{m}$ . The floc size  
1225 was determined by counting 500 flocs for each sample (five randomly selected  
1226 spots on the slide, 20 flocs for each spot, five replicates). The sizes of the 500  
1227 flocs were measured and recorded in order according to their sizes. Three  
1228 characteristics of flocs were then defined using these floc size data: (1) average  
1229 floc size, which was determined as the average value of 500 floc sizes; (2)  
1230 maximum floc size, which was determined as average of the largest 10 flocs; and  
1231 (3) minimum floc size, which was determined as average of the smallest 10 flocs.

1232

#### 1233 **4.2.6 Approaches for Determination of the Structured Water Content**

1234           From the drying test, water evaporated during the whole drying period,  
1235 and the weight of the drying sample was recorded every 30 seconds. The drying  
1236 rate was defined as the mass of water that could evaporate per hour, and it was

1237 calculated by dividing the weight difference between two recordings with the time  
1238 interval (30 s). Two types of curves were applied showing the results of the  
1239 drying test. One was the drying rate (g/hr) versus moisture content (g H<sub>2</sub>O/g TS)  
1240 curve, and the other was the weight (g) versus time (hr) curve. To eliminate the  
1241 influence caused by random fluctuations from the data obtained from the drying  
1242 test and to obtain a flat curve, a rolling average was applied for the drying data  
1243 analysis (Martin, 2001). The raw data of the weight change ( $K_i$ ) was recorded  
1244 chronologically ( $K_1$  indicated the beginning of the drying test), and the average  
1245 value of proximal 20 records was calculated as a new weight change ( $S_i$ ), and the  
1246 new weight changes was applied to make curves. If  $S_i$  was calculated as the  
1247 average of date from  $K_{i-20}$  to  $K_i$ , then it was defined as the “forward rolling  
1248 average”. If  $S_i$  was calculated as the average of data from  $K_i$  to  $K_{i+20}$ , then it was  
1249 defined as the “backward rolling average”. Even though the shapes of the curves  
1250 were similar independent of applying a forward or a backward rolling average, the  
1251 results of the structured water content were different, and the difference of the  
1252 results could exceed 0.1 g.

1253

## 1254 **4.3 Results and Discussion**

### 1255 **4.3.1 Determination of the Structured Water Content**

1256 The structured water contents of the five sludge types were determined  
1257 using five objective approaches. As mentioned in section 4.2.6, drying rate curve  
1258 and weight curve were applied to represent the results of drying test.

1259

1260 **4.3.1.1 Drying Rate Curve: drying rate (g/hr) versus moisture content (g**

1261 **H<sub>2</sub>O/g TS):**

1262 The drying rate curve (Figure 4.4) started from the right end (time =0)  
1263 with a higher moisture content and moved leftward as the evaporation happened.

1264 It showed that the drying rate kept constant at the first half period of the drying  
1265 test (higher moisture content), followed by a decrease when the moisture content  
1266 reached around 3 g H<sub>2</sub>O/ g TS. The constant drying rate indicated free water  
1267 evaporation, and when the drying rate started to decrease, another moisture type,  
1268 which was structured water, began to evaporate (J. Kopp and N. Dichtl, 2000).

1269 The fluctuation of the drying rate curve made it difficult to determine the time,  
1270 when the drying rate started to decrease, which was directly correlated to the  
1271 value of structured water content. Therefore, the theoretical free water  
1272 evaporation rate was considered as a proper baseline for the real drying rate, and  
1273 the determination of drying rate drop was obtained by analysis of the difference  
1274 between the theoretical free water evaporation rate and the real drying rate.

1275 (1) Penman's Equation for the Theoretical Evaporation Rate (baseline A)

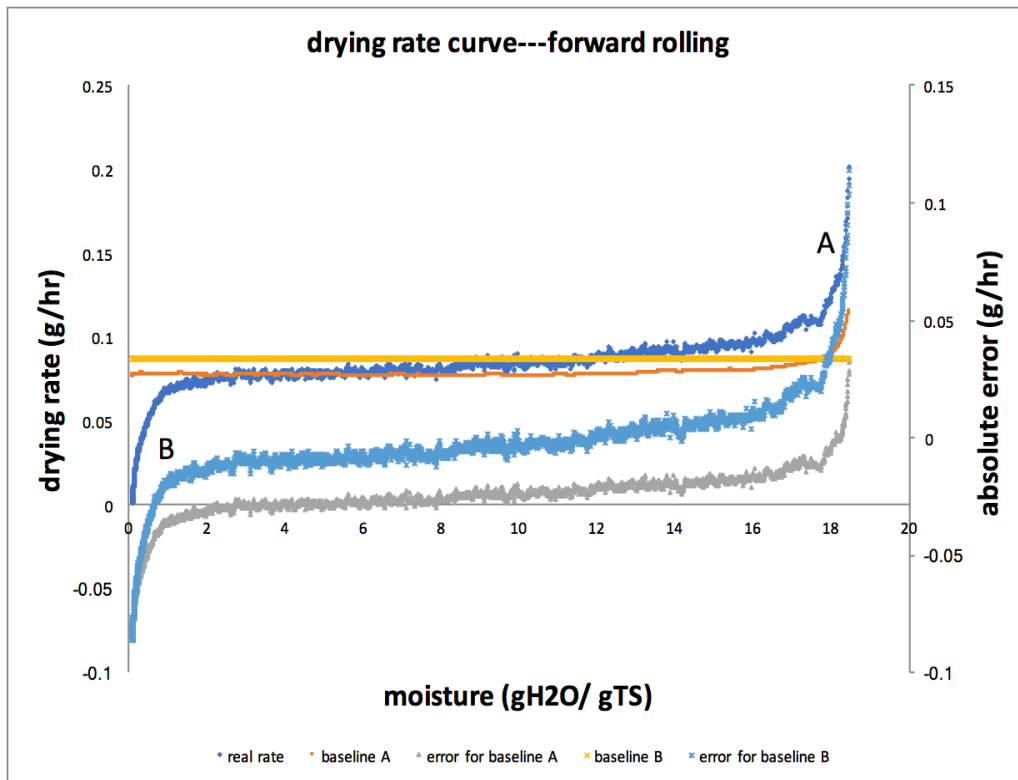
1276 Penman's equation (Eqn 1) (Penman, 1948) has been widely applied to  
1277 calculate the evaporation rate for the free water present at big surface areas like  
1278 lakes and rivers. The original Penman's equation considered solar radiation, vapor  
1279 pressure, latent heat, psychrometric coefficient and wind speed as input data  
1280 (Penman, 1948). However, not all data were available and necessary for the test of  
1281 waste water samples. A simplified Penman's equation (Eqn 2) was applied in this

1282 study for the calculated drying rate, considering only temperature, relatively  
1283 humidity (RH) and wind speed, and detailed assumption and approximation  
1284 referred to Valiantzas (2006). Free water density and pan surface area were  
1285 required for unit transition from (mm/d) to (g/hr). The calculated evaporation rate  
1286 was plotted as the baseline A for the theoretical free water evaporation rate, and  
1287 the absolute difference between real drying rate and the baseline A was defined as  
1288 the absolute error. In Figure 4.4, the orange line indicated the baseline A, and it  
1289 was a linear line that paralleled to the X-axis. During the drying period,  
1290 temperature, RH and wind speed kept constant at 22°C, 60% and 0.52 m/s  
1291 respectively, so that calculated evaporation rate from Penman's equation did not  
1292 change. The gray line (Figure 4.4) indicates the absolute error between the  
1293 baseline A and the real drying rate, and a drop was observed when the real drying  
1294 rate started to decrease. To determine when the drying rate started to decrease, a  
1295 threshold for the relatively error was set. The absolute error curve kept steady  
1296 when the data was within the moisture content ranging from 15 to 5 g H<sub>2</sub>O/g TS.  
1297 Assuming the absolute error of this range matched normal distribution, the  
1298 average and standard deviation (STDV) were calculated using this part of data,  
1299 and the threshold was set as "average - 3\*STDV". This threshold defined that  
1300 99.7% of the absolute errors closed to the average were considered as acceptable  
1301 values, and the other 0.3% absolute errors were farther away from the average so  
1302 that be considered as having big difference from the free water evaporation  
1303 (baseline A) (Benhidour and Onisawa, 2010). This threshold selected the data that  
1304 were away from the free water evaporation, and the structured water content was

1305 obtained as the average of the five smallest moisture contents, when the absolute  
 1306 error was larger than the threshold, instead of the smallest moisture content, to  
 1307 eliminate the influence of random errors.

1308 
$$E_{pen}(mm/d) = \frac{\Delta}{\Delta+\gamma} * \frac{(Rn)}{\lambda} + \frac{\gamma}{\gamma+\Delta} * \frac{6.43 (f_u)D}{\lambda} \text{ (Eqn 1)}$$

1309 
$$E_{pen}(mm/d) = 0.052(T + 20)(1-RH/100)(1-0.38 + 0.54u) \text{ (Eqn 2)}$$



1310  
 1311 **Figure 4.4.** Drying rate curve for the THP sludge when applying forward rolling  
 1312 average. Baseline A represented the free water evaporation rate from Penman’s  
 1313 equation, and it showed the influence of the environmental impactors; Baseline B  
 1314 represented the free water evaporation rate from the weight curve, and it showed a  
 1315 constant drying rate; The first drop on the right side (A) was caused by the  
 1316 experimental humidity stabilization; The second drop on the left side (B)  
 1317 indicated the structured water evaporation.

1318

1319 (2) Weight Data for the Theoretical Drying Rate (baseline B)

1320 The weight of the drying sample decreased as the drying process was  
1321 taking place, thus a weight (g) versus time (hr) curve could be applied to show the  
1322 drying test result (Figure 4.5). A proportional relationship between the weight and  
1323 the drying time was observed until the weight curve started to flatten out, and the  
1324 slope of the “weight versus time curve” indicated the drying rate. Therefore, the  
1325 proportional relationship in the weight curve and the slope of this part could be  
1326 considered as another theoretical free water evaporation rate baseline. The  
1327 proportional part, which occurred at the first half of the weight curve, indicated  
1328 the free water evaporation (J. Kopp and N. Dichtl, 2000), while the smooth part,  
1329 which occurred at the last half of the weight curve, indicated the completion of  
1330 the evaporation process. Therefore, the beginning of the structured water  
1331 evaporation should occur between the proportional part and the smooth part.  
1332 Based on the principle of making as much data as possible and at the same time,  
1333 avoiding the influence of the structured water evaporation, weight data from 3 -  
1334 20 hours of the drying period was considered as the free water evaporation and  
1335 applied for the free water evaporation rate calculation (detailed discussion could  
1336 be found in Section 4.3.1.2). Therefore, a constant evaporation rate, which was  
1337 equal to the slope of the proportional part was plotted in the “drying rate versus  
1338 moisture content curve” as baseline B (yellow line in Figure 4.4). The absolute  
1339 difference between the real drying rate and the baseline B was defined as the  
1340 absolute error (light blue line in Figure 4.4). The absolute error curve for baseline

1341 B and the real drying rate kept steady when the data was within the moisture  
1342 content ranged from 15 to 5 g H<sub>2</sub>O/g TS. Assuming the absolute data of this part  
1343 matched the normal distribution, the average and standard deviation were  
1344 calculated using this part of data, and the threshold was set as “average-  
1345 3\*STDV”. Same as baseline A, this threshold could select the real drying rate  
1346 data that were away from the free water evaporation (baseline B) (Benhidour and  
1347 Onisawa, 2010). The structured water content was obtained as the average of the  
1348 five smallest moisture contents when the absolute error was smaller than the  
1349 threshold.

1350

#### 1351 **4.3.1.2 Weight Curve: weight (g) versus time (hr)**

1352 As mentioned above (Section 4.3.1.1), the weight of the drying sample  
1353 and the drying time could be plotted and showed the result of the drying test. In  
1354 Figure 4.5, the proportional part at the beginning period of the drying test  
1355 indicated the weight change caused by free water evaporation, and the smooth  
1356 part at the terminal period of the drying test indicated the completeness of water  
1357 evaporation. The beginning of the structured water evaporation occurred between  
1358 these two parts. Similar to the drying rate curve, a theoretical weight change  
1359 caused by free water evaporation was applied as a comparison, and the structured  
1360 water content was determined by analyzing the error between the theoretical and  
1361 real weight curve.

1362 (1) Proportional Part for the Theoretical Weight Change (baseline C)

1363           The free water evaporation process was stable with a constant drying rate  
1364 (J. Kopp and N. Dichtl, 2000). Therefore, theoretically, a fixed weight difference  
1365 between adjacent recordings should be observed in the weight curve during this  
1366 process, where a proportional relationship between the weight (g) and the drying  
1367 time (hr) was shown. The drying test required three hours for experimental  
1368 environment stabilization, and during this time, the weight change was not stable  
1369 influenced by the relatively lower relative humidity (<60%), so that the weight  
1370 data within this time was not considered for data analysis. To simulate the  
1371 evaporation of free water, the weight data from 3 - 20 hours of the drying period  
1372 was considered as this proportional part because a linear relationship between the  
1373 weight and the drying time was shown during this period for all the samples. The  
1374 slope and the interception were calculated indicating the free water evaporation  
1375 rate and the moisture content in the sludge before the drying test, respectively. In  
1376 Figure 4.5, the orange line showed the modeled weight curve for the free water  
1377 evaporation as baseline C. An absolute error shown as the grey line indicated the  
1378 absolute difference between the real weight change and the baseline C. The  
1379 “absolute error” (grey line) kept stable and small for around 20 hours, then it  
1380 increased as an exponential function until reached its maximum value. During the  
1381 free water evaporation process, the real weight was similar like the baseline C,  
1382 and the “absolute error” was stable and small. When the structured water started  
1383 to evaporate, the drying rate decreased because the molecular acting force and  
1384 capillary forces between the structured water and the particles prevented the  
1385 structured water from evaporating as easily as the free water. Therefore, the real

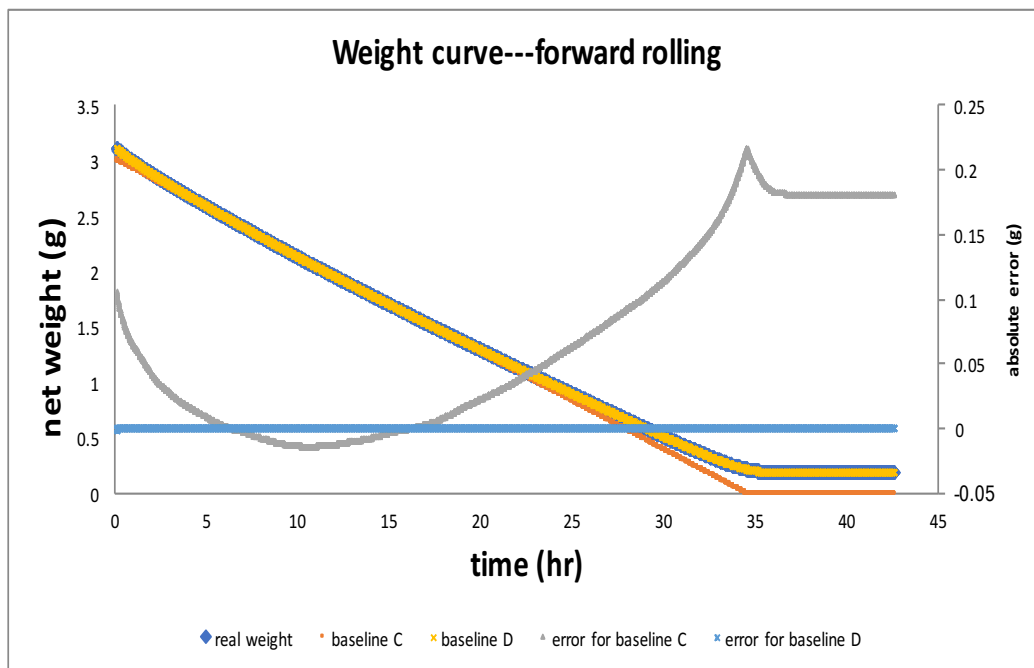
1386 weight lost became smaller than the modeled weight loss (baseline C), which only  
1387 considered the free water evaporation, causing the “absolute error” increased. The  
1388 “absolute error” increased even further when the moisture that had stronger acting  
1389 force with solid particles started to evaporate. The baseline C was set to zero  
1390 when the modeled weight was negative because the weight of sludge sample  
1391 could not be smaller than zero g. An exponential function was found to represent  
1392 the “absolute error” using weight data from 20 hours to the maximum value  
1393 ( $R^2 > 0.96$ ), and the slope was calculated using data every five minutes to show  
1394 how the “absolute error” changed. The structured water content was obtained as  
1395 the water content when the slope reached 50% of the maximum slope.

1396

1397 (2) Calculated Drying Rate for the Theoretical Weight Change (baseline D)

1398 Penman’s equation provided the calculated evaporation rate for the free  
1399 water, and it could be transited into weight change as a predicted weight change  
1400 (baseline D) for comparison with the real weight change. In Figure 4.5, the yellow  
1401 line indicated that the weight change came from the Penman’s calculated  
1402 evaporation rate, and the light blue line indicated the absolute difference between  
1403 the real weight and baseline D. For all samples, the “absolute error” was  
1404 approximately zero with the average and the standard deviation (STDV) of the  
1405 entire data both smaller than 0.005 g. The baseline D represented the weight  
1406 change caused by free water evaporation using the evaporation rate calculated by  
1407 Penman’s equation. When the structured water started to evaporate, the real  
1408 drying rate decreased, and the real weight loose would also be smaller than the

1409 baseline D. As mentioned above (Section 4.3.1.2, (1)), during the first three to 20  
 1410 hours, it was the free water that evaporated, and data of this period was applied  
 1411 for the threshold determination. Assuming the absolute error data matched the  
 1412 normal distribution, a threshold was set up as the value of the “average + 3\*  
 1413 STDV”, and it selected the data that had big difference from the baseline D. The  
 1414 structured water content was determined as the moisture content when the  
 1415 “absolute error” was bigger than threshold.



1416  
 1417 **Figure 4.5.** Weight curve for the THP sludge when the forward rolling average  
 1418 was applied. Baseline C represented the expected drying sample weight change  
 1419 for the free water evaporation; Baseline D represented the weight change from the  
 1420 Penman’s calculated evaporation rate; The error for baseline C fit an exponential  
 1421 function.

1422

### 1423 **4.3.1.3 Monod Model to Determine the Structured Water Content**

1424           The drying rate curve had the similar shape like the Monod curve (Eqn 3),  
1425 which described the mathematical relationship between the growth rate of  
1426 microorganisms ( $\mu$ ) and the concentration of limiting substrate (S) (Strigul, Dette  
1427 and Melas, 2009). Two coefficients in the equation,  $\mu_{\max}$  and  $K_s$ , indicated the  
1428 maximum growth rate of the microorganisms and the value of substrate when the  
1429 growth rate reached a half of the maximum rate, respectively. In this study, the  
1430 drying rate represented the growth rate of the microorganisms, and the moisture  
1431 content in the sludge represented the limiting substrate. The drying rate was  
1432 higher when the moisture was higher (similar to “sufficient substrate”) and then  
1433 decreased when less moisture was left in the sludge (similar to “limited  
1434 substrate”). A non-linear regression model was used to fit the Monod equation on  
1435 the data using “Rstudio” software (RStudio®, Boston, MA). The structured water  
1436 content was determined as the water content in the sludge when the slope of the  
1437 matched Monod curve equaled to 0.008. Several other thresholds were attempted,  
1438 and resulted indicated that a small change of the threshold ( $\pm 0.001$ ) could lead to  
1439 a big difference of the structured water content ( $>\pm 0.1$  g). The 0.008 was  
1440 determined as the threshold because it leaded to realistic structured water content  
1441 for all sludge types.

1442 
$$\mu = \mu_{\max} * \frac{S}{K_S+S} \text{ (Eqn 3)}$$

1443

#### 1444 **4.3.2 Structured Water Content Values**

1445           Figure 4.6 and Figure 4.7 showed the structured water content for the five  
1446 sludge types using the drying rate curve and weight curve, respectively.

1447

##### 1448 **4.3.2.1 Structured Water Content Values from the Drying Rate Curve**

1449           When applying the drying rate curve, the results of the structured water  
1450 content for a particular sludge type were similar, independent of the baselines A  
1451 and B. This was because baseline A indicated the evaporation rate of the free  
1452 water under a certain temperature and relative humidity, which was supposed to  
1453 be constant according to Kopp and Dichtl (2000). On the other hand, the baseline  
1454 B indicated the average evaporation rate of the first 20 hours, which was within  
1455 the period of the free water evaporation. Therefore, the baseline A and the  
1456 baseline B both represented the evaporation rate of the free water from two  
1457 aspects, and they had similar values (Figure 4.4, orange line for the baseline A  
1458 and yellow line for the baseline B). When the structured water started to  
1459 evaporate, the real drying rate decreased and diverged from the free water  
1460 evaporation rate. The difference between the structured water evaporation rate  
1461 and the expected free water evaporation rate became even larger when more  
1462 bound water started to evaporate, until the difference reached the threshold set  
1463 above. Since the baseline A and the baseline B had similar values and were both  
1464 paralleled to the X-axis, the time when a difference was observed between the real

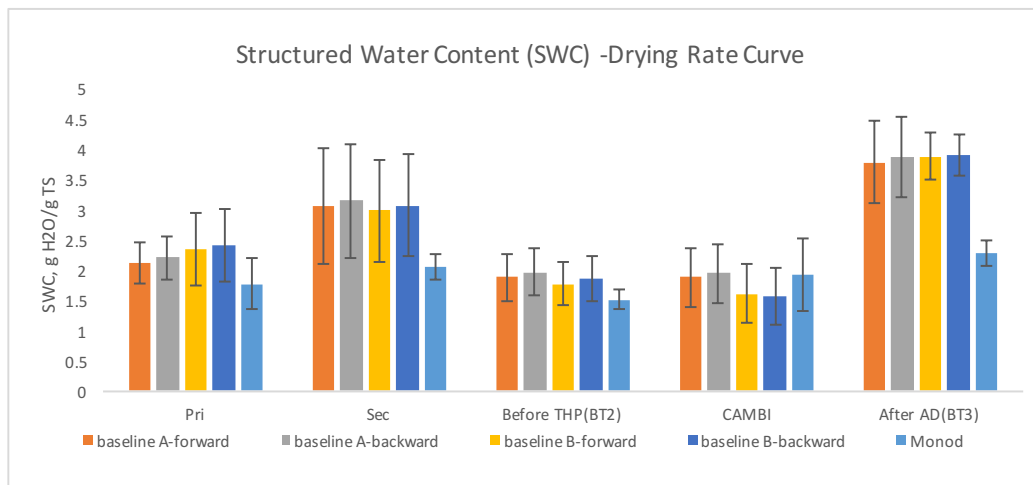
1465 drying rate and the two baselines were similar, causing similar results of the  
1466 structured water content.

1467         When applying the same baseline, no matter the Penman's calculated  
1468 drying rate (baseline A) or the constant drying rate (baseline B), the results of the  
1469 structured water content were higher when use the backward rolling average than  
1470 use the forward rolling average. That was because that when applying the rolling  
1471 average, it moved the original "drying rate versus moisture content" curve slightly  
1472 rightward and leftward for the forward rolling average and backward rolling  
1473 average, respectively. Therefore, considering the shape of the drying rate curve  
1474 (Figure 4.4), when the difference between the real drying rate and free water  
1475 evaporation rate reached the threshold, which also indicated the obvious decrease  
1476 in real drying rate caused by the transition from the free water evaporation to the  
1477 structured water evaporation, the X-axis value for backward rolling average was  
1478 slight higher than the forward rolling average.

1479         The Monod model caused the structured water content smaller than the  
1480 other measurements for all sludge types except for the Cambi sludge (after THP),  
1481 and that was caused by the choice of the threshold for the Monod model  
1482 measurement. "Rstudio" software provided a mathematical expression of the  
1483 drying rate. The curve plotted by the mathematical expression was named as the  
1484 modeled curve, and it started to indicate the drying rate instead of the real drying  
1485 rate curve. The slope of the modeled curve increased as the moisture content left  
1486 in the sludge decreased, so that a smaller threshold could lead to a higher

1487 structured water content. In this study, the threshold was determined as 0.008  
1488 because it provided realistic structured water contents for all sludge types.

1489 Figure 4.6 indicated that anaerobic sludge (AD) had highest structured  
1490 water content. Wang, Shammam and Hung (2007) proved that during the  
1491 anaerobic digestion process, while the anaerobic microorganisms break down the  
1492 organic matters, hydrous particles were produced, and that might be the reason  
1493 why the AD sludge contained higher structured water than other sludge types.  
1494 Previous studies measured even higher structured water contents for the anaerobic  
1495 digestion sludge, which were larger than five g H<sub>2</sub>O/ g TS (Tsang et al., 1990).

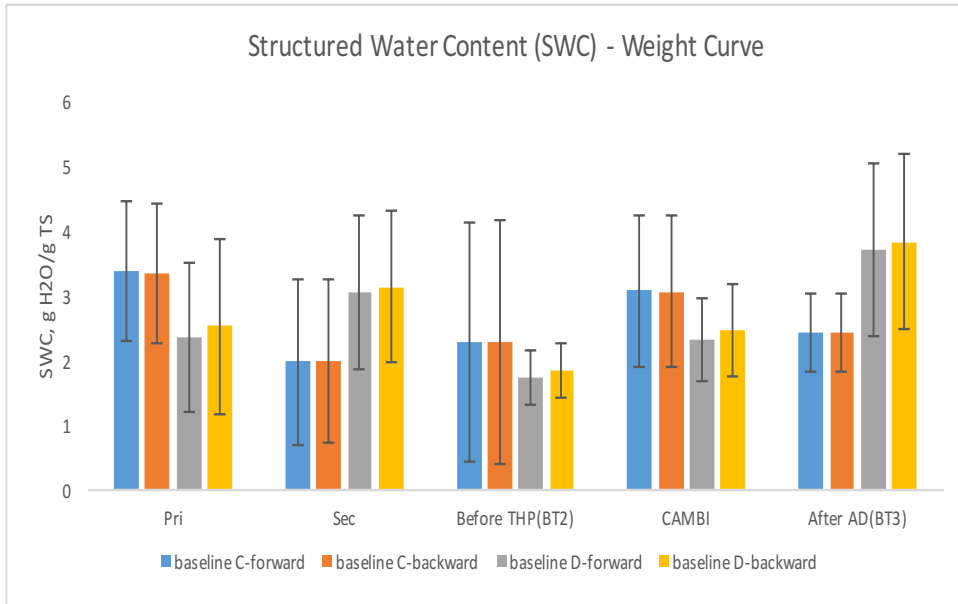


1496  
1497 **Figure 4.6.** Structured water content from the drying rate curve and Monod  
1498 model. Baseline A and B measured similar structured water content for each  
1499 sludge type, while Monod model measured smaller contents; Anaerobic digestion  
1500 sludge had highest structured water content among the five sludge types.

1501

1502 **4.3.2.2 Structured Water Content Values from the Weight Curve**

1503           Figure 4.7 showed discrepant values of the structured water content of the  
1504 sludge. When applying the weight curve, two measurements that considered the  
1505 baseline C and the baseline D caused different structured water contents,  
1506 respectively. Baseline C failed to contain the influence of environmental  
1507 conditions such as temperature, relative humidity and wind speed into calculation,  
1508 and at the same time, it assumed a constant temperature (T) and relative humidity  
1509 (RH) during the whole drying test. The temperature and relative humidity within  
1510 the Plexi chamber fluctuated slightly according to probe records. Baseline C had  
1511 large standard deviation because it was influenced by the experimental conditions  
1512 (T and RH). On the other hand, baseline D considered the environmental  
1513 impactors (T, RH and wind speed) into its calculation because its weight change  
1514 was calculated from Penman's equation. However, the standard deviation of  
1515 baseline D was still large, indicating weight curve was not as good as the drying  
1516 rate curve considering the stability of the data.



1517

1518 **Figure 4.7.** Structured water content based on results from the weight curve.

1519 Baseline C had large standard deviation because it was sensitive to the

1520 experimental environment changes; Baseline D indicated that secondary and AD

1521 sludge had higher structured water content than other sludge types.

1522

#### 1523 **4.2.3.3 Evaluation of the Structured Water Content with Cake TS**

1524 The biosolids product obtained after the dewatering process is commonly

1525 referred to as cake solids, which would be applied in land application as biosolids

1526 (Werther and Ogada, 1999). Structured water, which could not be removed by the

1527 physical dewatering process remained in the cake solids. Therefore, the TS

1528 content of the cake solids should be correlated with the structured water content,

1529 which then could be applied to predict the cake solids based on the calculated

1530 structured water content. The TS of the cake solids for each sludge types was

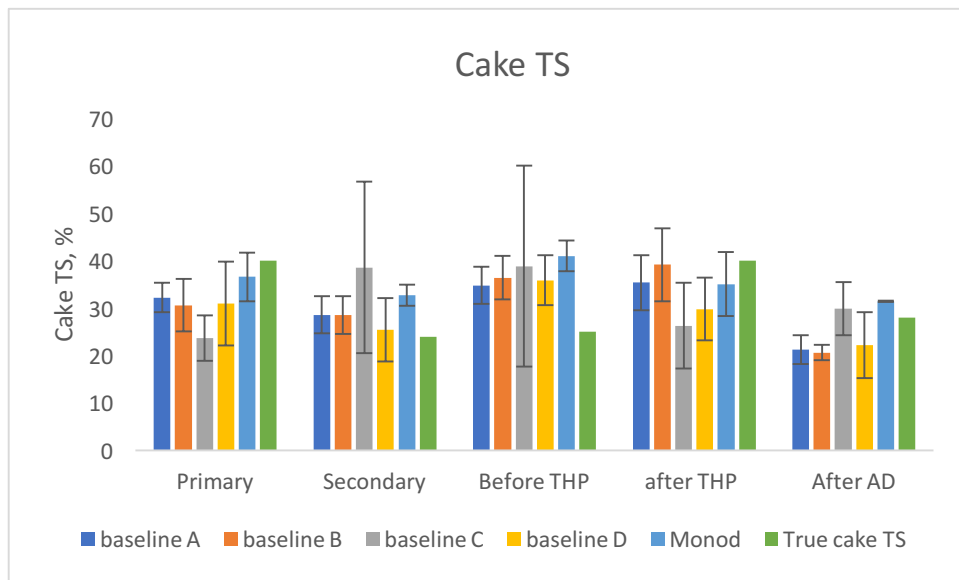
1531 measured by Zhang et al. (2017), and was applied to assess the structured water

1532 contents from this project. Zhang et al. (2017) measured the cake TS by dosing

1533 coagulant polymer, followed by centrifuge filtering and simulating the dewatering  
1534 process of DC Water. The structured water content was shown as (g H<sub>2</sub>O/g TS of  
1535 the sludge) thus the cake TS could be calculated as “1/ (1+structured water  
1536 content)”. Figure 4.8 showed the predicted cake TS based on the five approaches  
1537 for determining the structured water in this project.

1538         The results showed that the structured water content failed to accurately  
1539 predict the cake TS of the sludge for all five approaches (Figure 4.8). In this  
1540 project, the structured water was defined as the moisture in the sludge that  
1541 excluded free water, and the values of the structured water content were  
1542 determined based on the drying performance (drying rate or weight loss), which  
1543 was different from the free water evaporation. To compare the drying  
1544 performance with the free water evaporation performance, five thresholds were  
1545 determined to assess the difference between them. When the difference was larger  
1546 than the threshold, the moisture content at that point was determined as the  
1547 structured water content (see Section 4.3.1). This indicated that the predicted cake  
1548 TS based on the structured water content contained chemically bound water,  
1549 surface water and all the interstitial water. On the other hand, a previous study  
1550 indicated that the dewatering process could remove free water and a proportion of  
1551 the interstitial water from the sludge (Tsang and Vesilind, 1990). This indicated  
1552 that the “true” cake TS was determined, when the cake solids contained  
1553 chemically bound water, surface water and only part of the interstitial water. The  
1554 proportion of the interstitial water that was removed through dewatering process  
1555 was still counted as the structured according to this project, thus, the predictions

1556 overestimated the water content in the cake solids, so that they underestimated the  
 1557 cake TS. However, the cake TS of the secondary sludge and the sludge before  
 1558 THP was overestimated, indicating underestimate of the structured water content.  
 1559 These two sludge types contained more EPS than the other sludge types (Table  
 1560 4.1). The high EPS content could reduce the sludge dewaterability (More et al.,  
 1561 2014) and cause high moisture content in the cake TS.



1562  
 1563 **Figure 4.8.** Cake TS calculated by structured water contents determined by five  
 1564 objective measurements as well as true cake TS. The structured water content of  
 1565 this project failed to predict cake TS because of the influence of interstitial water  
 1566 and EPS content in the sludge.

1567

### 1568 4.3.3 Impact of EPS on the Structured Water Content

1569 Tightly bounded and loosely bounded EPS were extracted for the five  
 1570 sludge types, and COD, PN and PS were measured for further analysis of the  
 1571 relationship between the structured water content and EPS composition. The

1572 concentrations of each compounds were listed in Table 4.1. The importance of  
 1573 these results will be discussed in the subsequent sections.

1574

1575 **Table 4.1.** EPS analysis for five sludge types, based on COD, PN, PS, PN/PS  
 1576 ratio and TB-EPS/LB-EPS ratio. Average and standard deviation are shown.

		primary	Secondary	Before THP(BT2)	After THP	After AD (BT3)
<b>LB-EPS</b>	PN (mg/g VSS)	22.8±11.2	9.3±5.7	11.2±2.8	16.5±1.4	14.4±10.0
	PS (mg/g VSS)	8.9±1.9	5.4±1.9	6.7±1.1	9.4±1.3	2.7±0.8
	PN/PS ratio	2.6	1.7	1.7	1.8	5.3
	Total(PN+PS)	31.7±13.1	14.8±7.6	18.0±3.9	25.9±2.7	17.2±10.8
	% of total EPS	35	11	15	69	52
<b>TB-EPS</b>	PN (mg/g VSS)	47.7±4.3	93.4±5.4	74.4±20.3	9.1±2.5	13.9±6.1
	PS (mg/g VSS)	12.1±2.1	27.5±17.2	30.9±16.5	2.7±0.8	1.8±1.2
	PN/PS ratio	3.9	3.4	2.4	3.3	7.5
	Total(PN+PS)	59.7±6.4	120.9±22.6	105.3±36.8	11.8±3.3	15.7±7.3
	% of total EPS	65	89	85	31	48
<b>COD</b>	mg/g VSS	274±15	437±37	388±60	139±16	62±8
<b>TB-EPS/LB- EPS ratio</b>		1.9	8.2	5.8	0.4	0.9

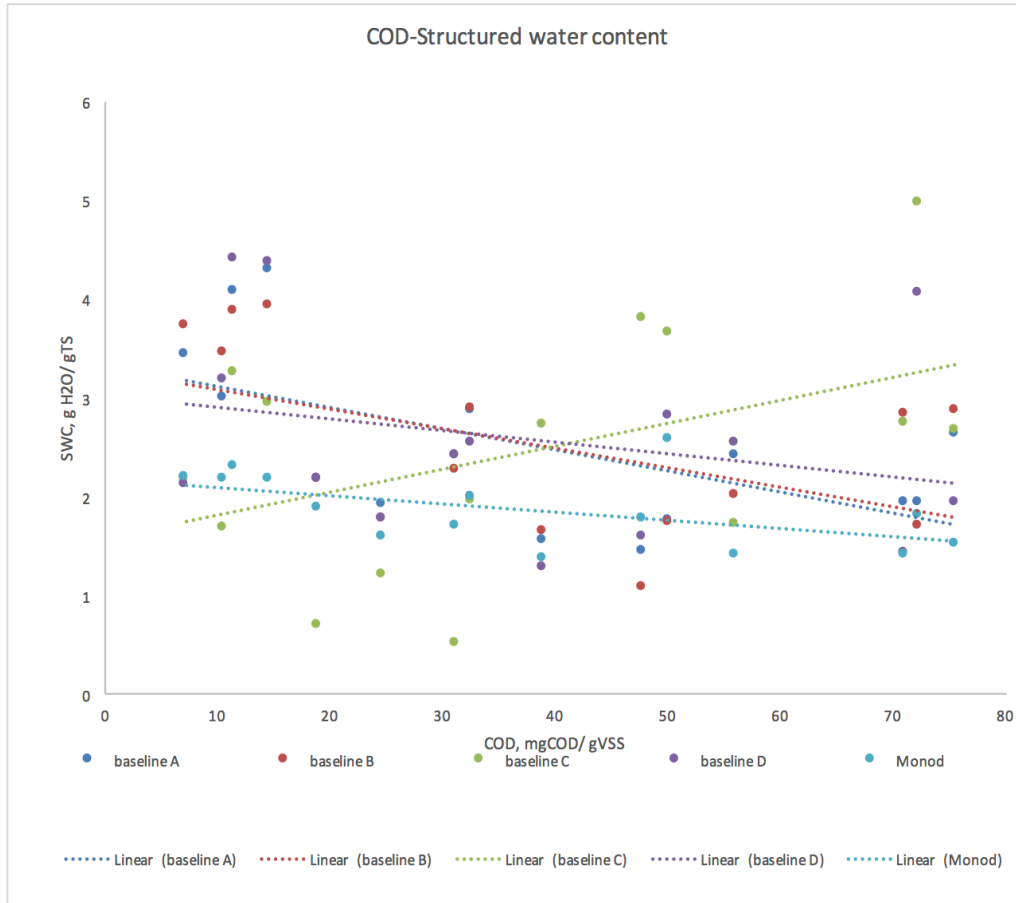
1577

1578

#### 1579 **4.3.3.1 Impact of COD on the Structured Water Content**

1580 COD values showed the content of organic matter in the sludge, and the  
1581 COD values for each sludge type could be explained by the mechanisms of  
1582 different treatment processes. Municipal sewage contained high level of organic  
1583 matters from residential drains. Therefore, the primary sludge, which captured the  
1584 suspended solids in the municipal sewage by gravitation, had higher organic  
1585 matter shown as high COD values (Table 5.1). Secondary sludge was composited  
1586 by the microorganisms that consumed the organic carbon in the primary sludge  
1587 for growth. The sludge before THP (BT2) was the mixture of the secondary and  
1588 primary sludge (primary sludge and secondary sludge count for 40% and 60% of  
1589 the total sludge by weight, respectively) by weight), so that it had the COD value  
1590 between the two sludge types. THP process made the organic compound of the  
1591 sludge more biodegradable by compressing the sludge under high temperature. In  
1592 DC Water, the THP process was achieved using Cambi technology, and the  
1593 sludge after THP was be referred as Cambi sludge to highlight this technology. In  
1594 the THP process, organic matter was degraded into smaller molecules and  
1595 inorganic matter, so that the COD value of Cambi sludge was relatively small. In  
1596 the AD process, smaller molecules of organic matter from the THP are degraded  
1597 into inorganic matters, so that smallest COD value was observed. However, the  
1598 COD value was still high in the AD sludge (Table 5.1) because the AD process  
1599 could not achieve 100% biodegradation efficiency, and the remaining organic  
1600 matters that failed to be degraded cause the COD content in the AD sludge.

1601 No significant correlation between the COD content and the structured  
 1602 water content was observed for what? ( $R^2 < 0.3$ ) (Figure 4.9). Therefore, the COD  
 1603 value of a sludge type, which represented the influence of each treatment process  
 1604 on organic matters, failed to correlate with the structured water content of a  
 1605 sludge.



1606  
 1607 **Figure 4.9.** The relationship between the COD and the structured water content.  
 1608  $R^2$  for each fitted line were all smaller than 0.3, indicating no linear relationship  
 1609 between the structured water content and the COD content of the sludge, no  
 1610 matter which approach was applied for structured water content measurement.

1611

#### 1612 **4.3.3.2 Impact of PN and PS on the Structured Water Content**

1613           PN has in other studies been shown to have a high water-holding capacity  
1614 (More et al., 2014; Sponza, 2002). Therefore, a sludge type that contained a high  
1615 PN content was supposed to have a higher structured water content. Figure 4.10-  
1616 4.14 (A) showed the impact of PN on the structured water content for the five  
1617 sludge types, but no correlation was observed between these two parameters  
1618 ( $R^2 < 0.2$ ). Figure 4.10-4.14 (B) showed the impact of PS on the structured water  
1619 content for the same five sludge types. Similar to PN content, there was no  
1620 correlation between the structured water content and the PS content ( $R^2 < 0.1$ ).  
1621 However, when the PS data were compared to the drying rate curve and baseline  
1622 A, a stronger correlation between the structured and the LB-EPS-PS was observed  
1623 ( $R^2 = 0.57$ ). A similar correlation was also observed, when a comparison between  
1624 the drying rate curve and baseline B took place ( $R^2 = 0.64$ ). Even though the  $R^2$   
1625 was smaller than 0.9 and could not indicate any significant correlation, it was still  
1626 larger than the other  $R^2$  values. It indicated that compared with any types of PN  
1627 and TB-EPS-PS, the structured water content was negatively correlated with the  
1628 LB-EPS-PS.

1629           Although neither Figures 4.10-4.114 (A) nor Figures 4.10-4.14 (B)  
1630 showed strong correlations between the structured water content of a sludge and  
1631 its PN or PS alone, there was still a possibility that the PN and PS worked  
1632 together to influence the structured water content of a sludge. Since the PN/PS  
1633 ratio was an important parameter for the EPS (Ren et al., 2016), the influence of

1634 its PN/PS proportion on the structured water content was studied for LB-EPS,  
1635 TB-EPS and total EPS (Figure 4.10-4.114 (C)). However, even though a trend  
1636 that a sludge that had a larger PN/PS ratio had a higher structured water content  
1637 was observed for all figures, it still lacked a significant correlation with a large  $R^2$ .  
1638 No matter which approach was applied to determine the structured water content,  
1639 the  $R^2$  for the fitted lines were all smaller than 0.4, indicating no significant  
1640 correlation was observed between the PN/PS ratio and the structured water  
1641 content.

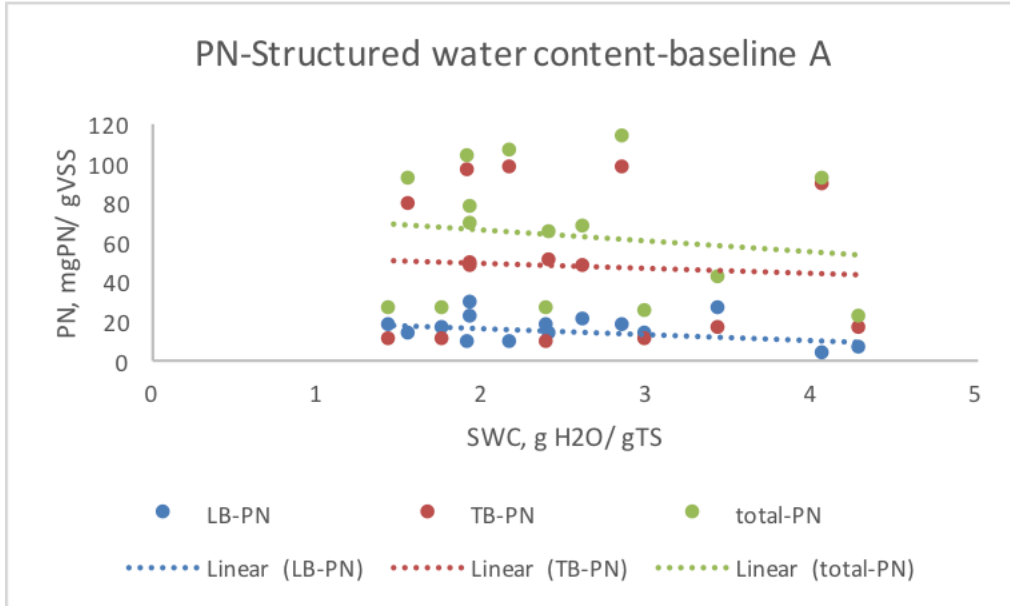
1642

#### 1643 **4.3.3.3 Impact of TB-EPS/LB-EPS Ratio on the Structured Water Content**

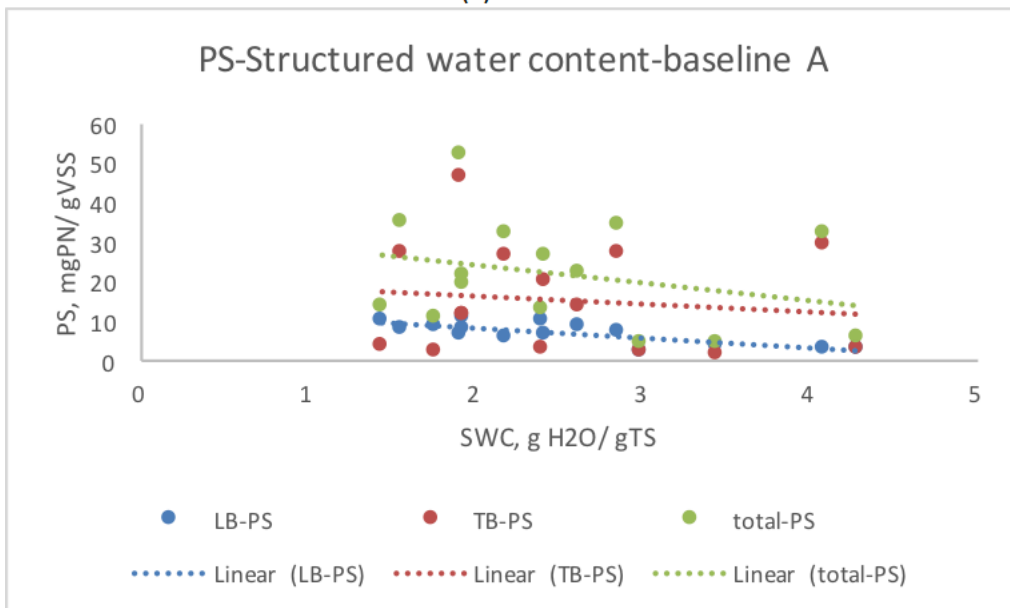
1644 TB-EPS had higher PN/PS ratio than the LB-EPS (Table 5.1), and a  
1645 sludge that had larger PN/PS ratio contained a higher structured water content  
1646 (Figure 4.10-4.14 (C)). Therefore, the content of TB-EPS, LB-EPS and TB-  
1647 EPS/LB-EPS ratio were plotted to study how they would influence the structured  
1648 water content of the sludge. Figure 4.10-4.14 (D) showed that there was no  
1649 correlation between the TB-EPS ( $R^2 < 0.1$ ) or the TB-EPS/LB-EPS ratio ( $R^2 < 0.1$ )  
1650 and the structured water content. When apply the drying rate curve and baseline  
1651 A, larger  $R^2$  value was observed between the structured water content and the  
1652 content of the LB-EPS ( $R^2 = 0.29$ ), however, it still failed to indicate any obvious  
1653 correlation.

1654 There was another fact that made it even more complicated to study the  
1655 influence of TB-EPS and LB-EPS content on the structured water content. TB-  
1656 EPS was considered to have higher water-holding capacity because it contained

1657 more PN than PS (Basuvaraj, Fein and Liss, 2015). However, for some sludge  
1658 type like the primary sludge, its LB-EPS had higher PN/PS ratio than that of the  
1659 TB-EPS of other sludge types (Table 4.1). Therefore, even the primary sludge had  
1660 smaller TB-EPS/LB-EPS ratio (1.9) (Table 4.1), its LB-EPS could be considered  
1661 as a material that had high capacity to hold moisture, making the overall  
1662 structured water content higher than other sludge types.

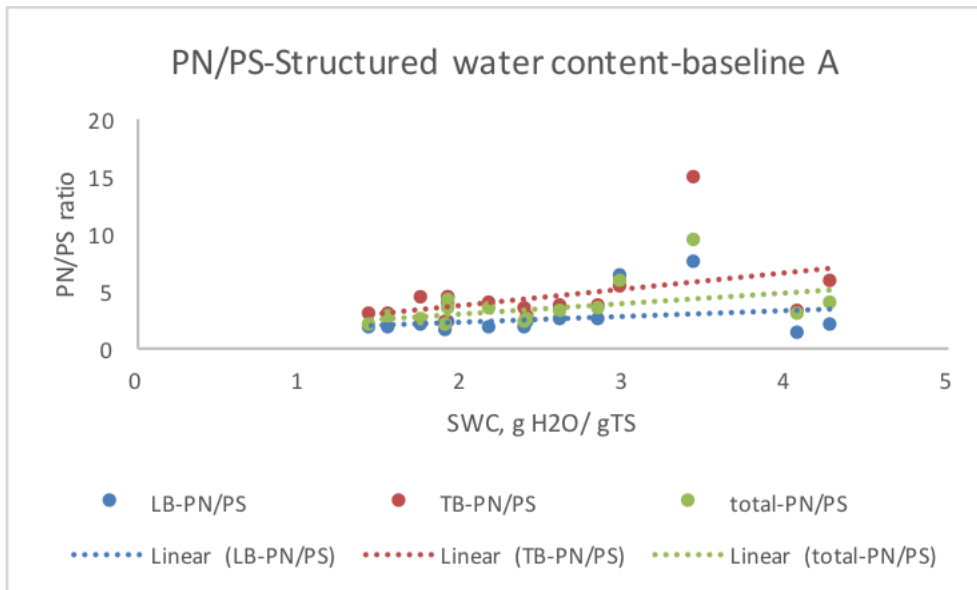


(A)

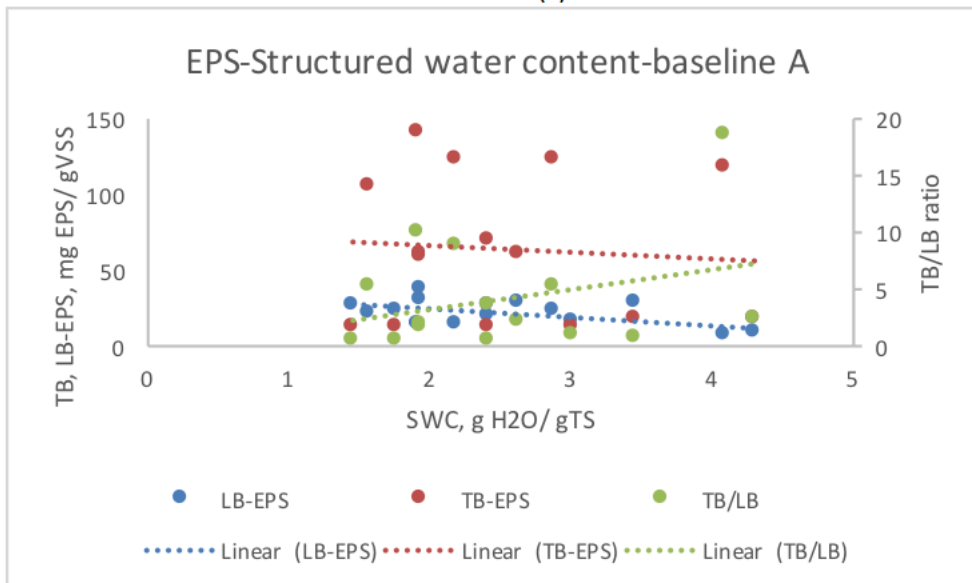


(B)

1663



(C)



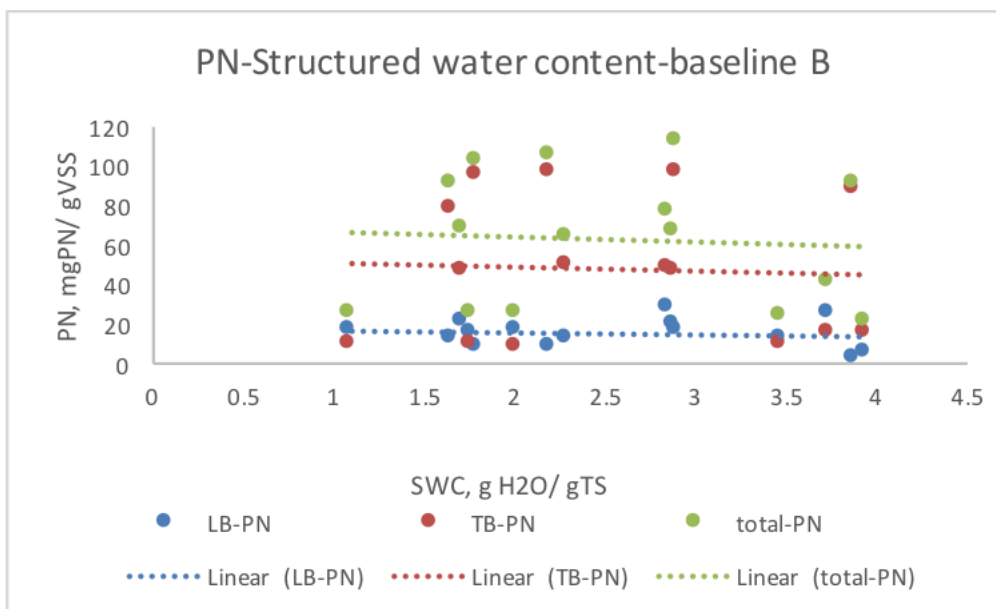
(D)

1664

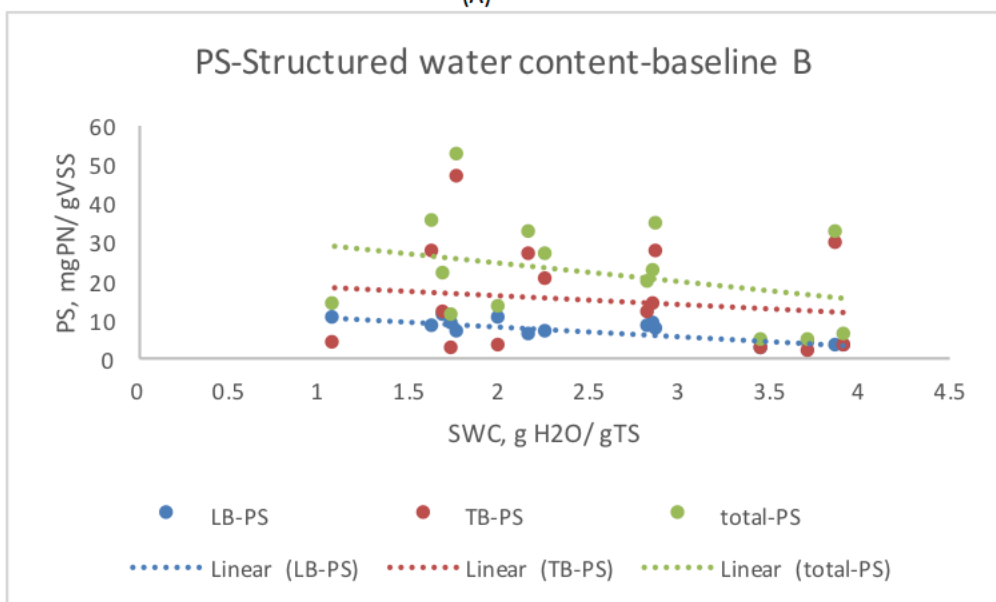
1665 **Figure 4.10.** The relationship between structured water content measured by  
 1666 drying rate curve (baseline A) and (A) PN; (B) PS; (C) PN/PS ratio; and (D) EPS.

1667

1668

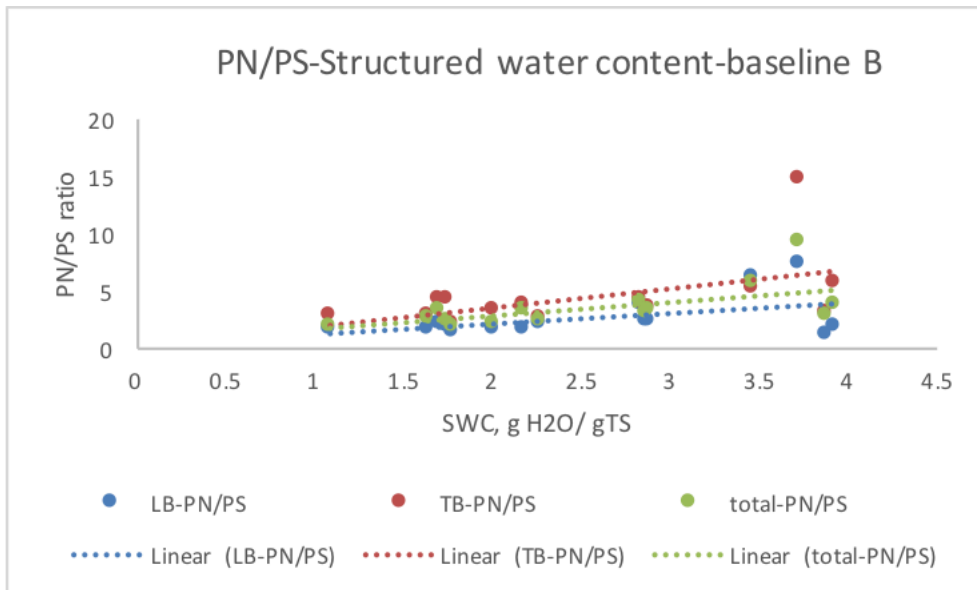


(A)

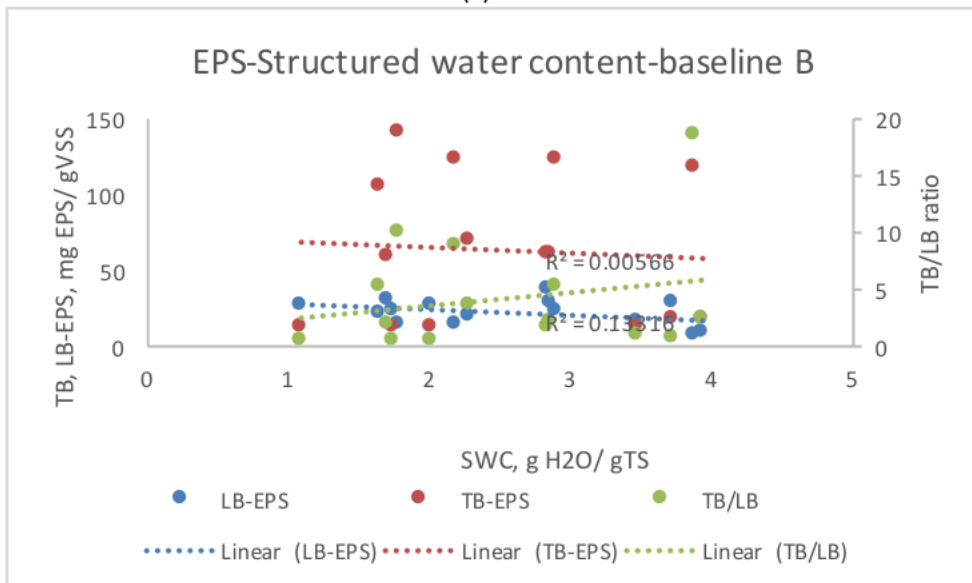


(B)

1669



(C)



(D)

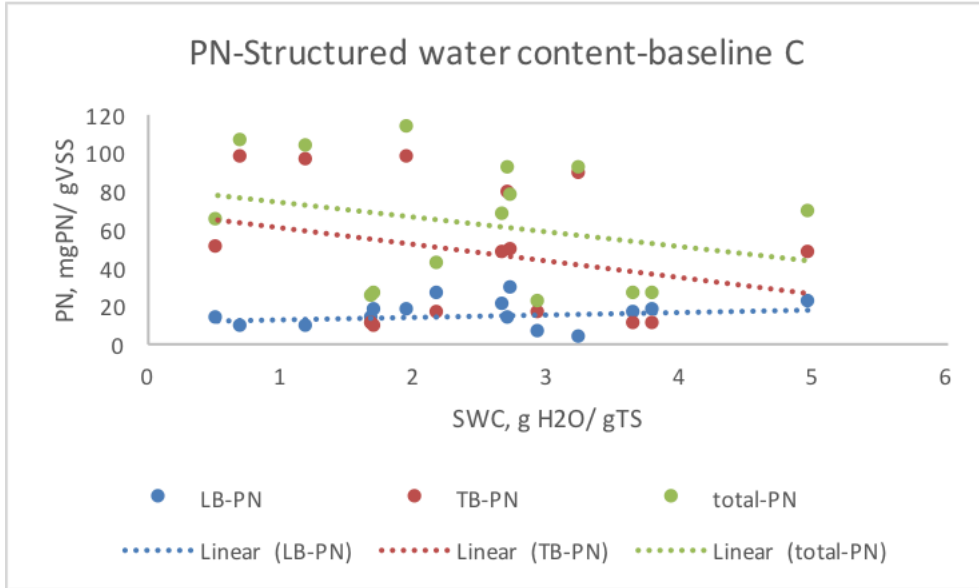
1670

1671 **Figure 4.11.** The relationship between structured water content measured by

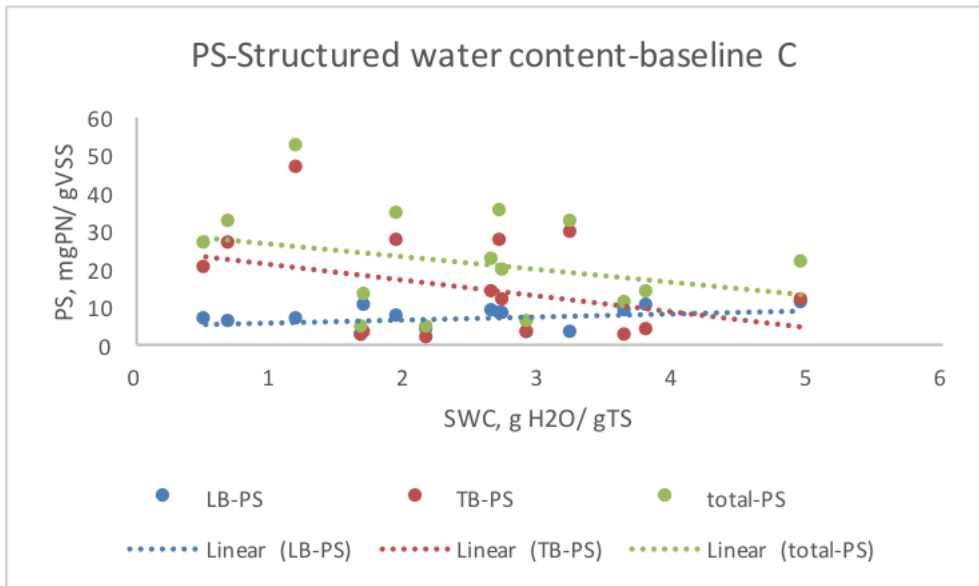
1672 drying rate curve (baseline B) and (A) PN; (B) PS; (C) PN/PS ratio; and (D) EPS.

1673

1674

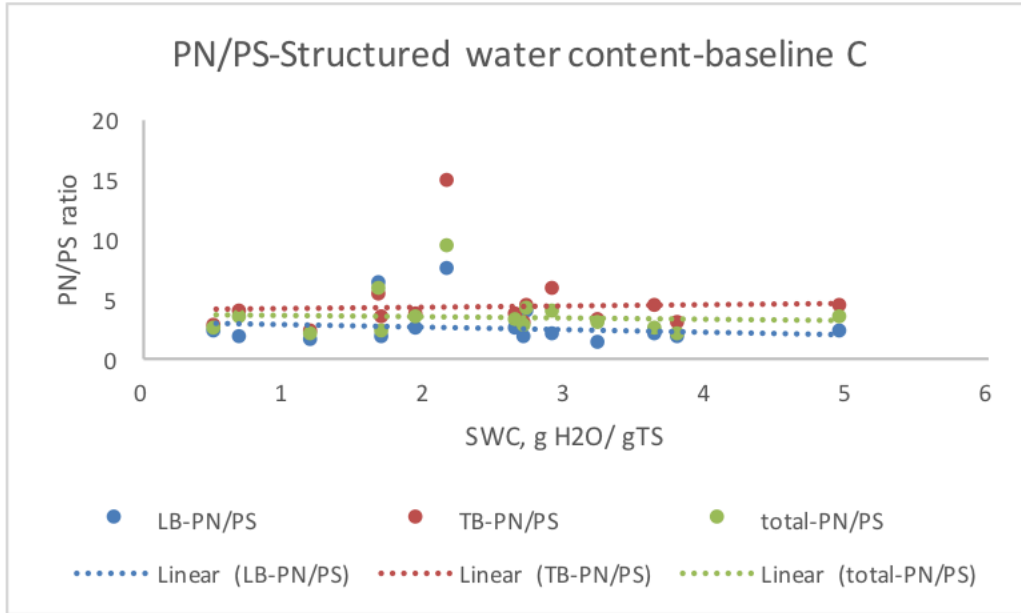


(A)

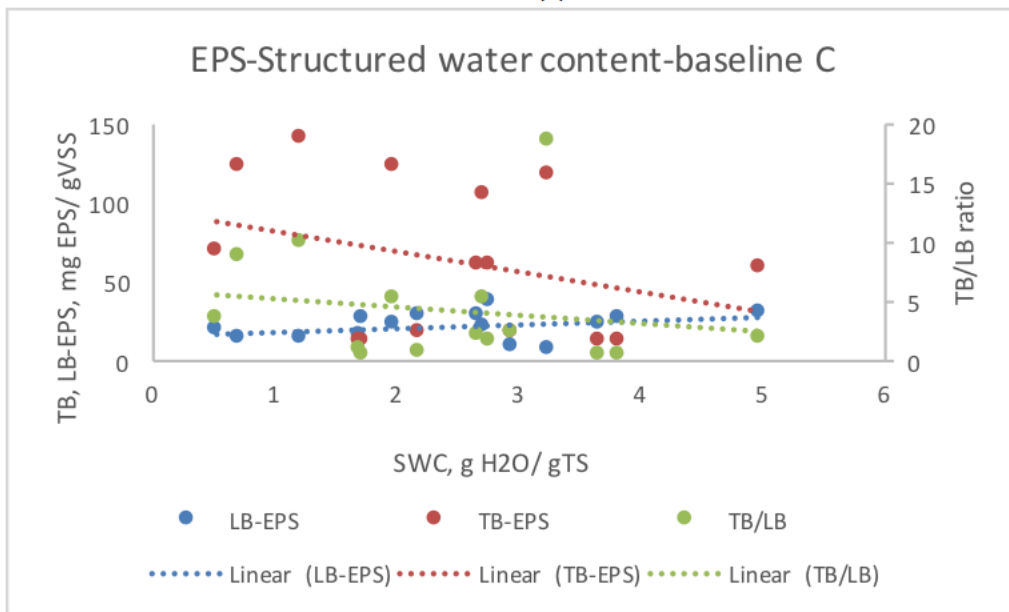


(B)

1675



(C)

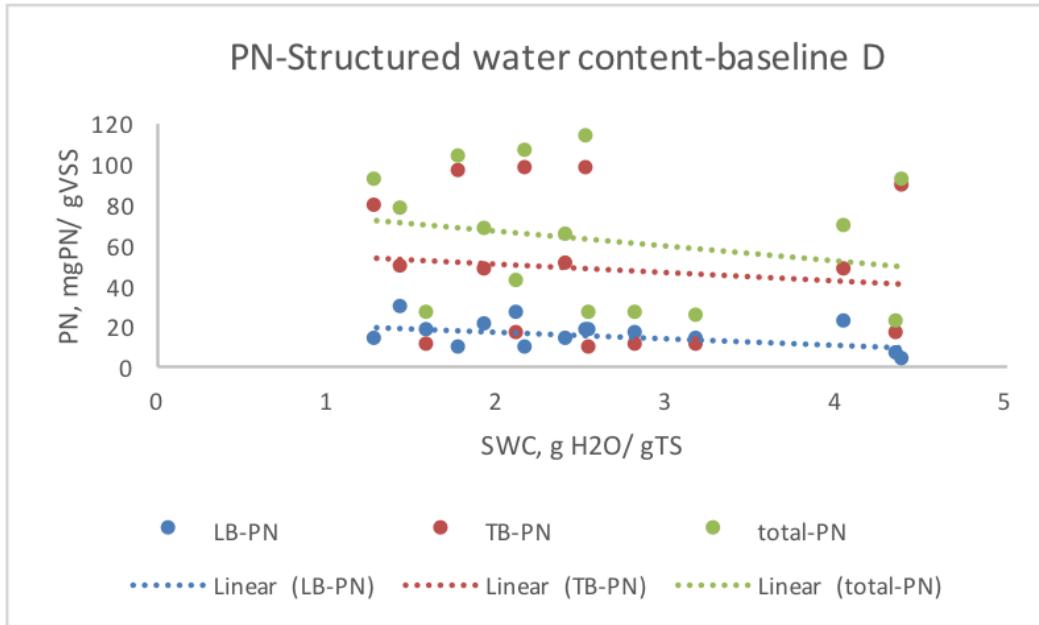


(D)

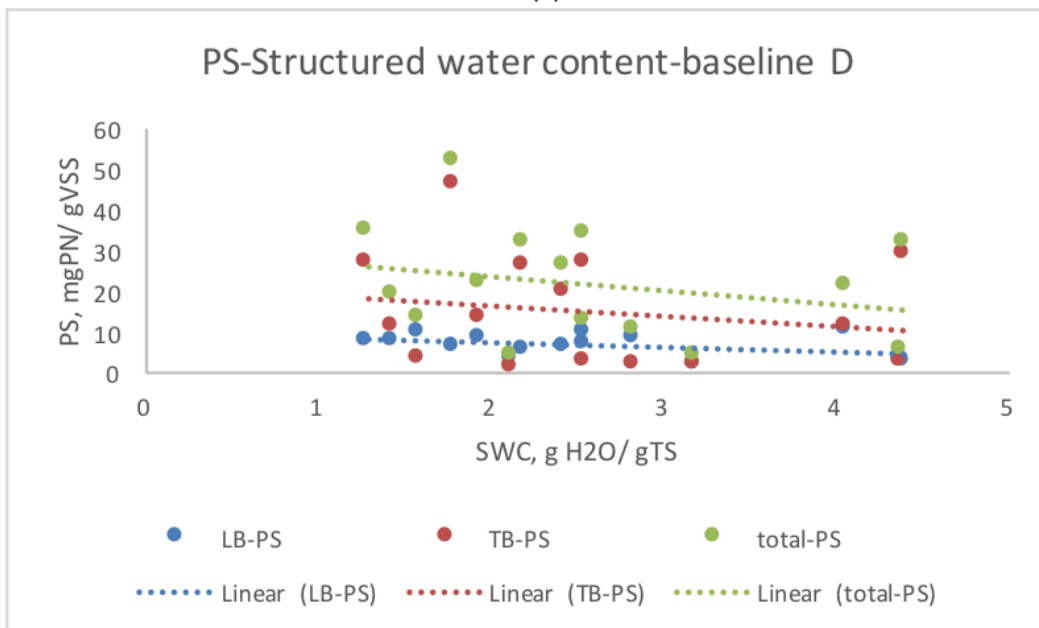
1676

1677 **Figure 4.12.** The relationship between structured water content measured by

1678 weight curve (baseline C) and (A) PN; (B) PS; (C) PN/PS ratio; and (D) EPS

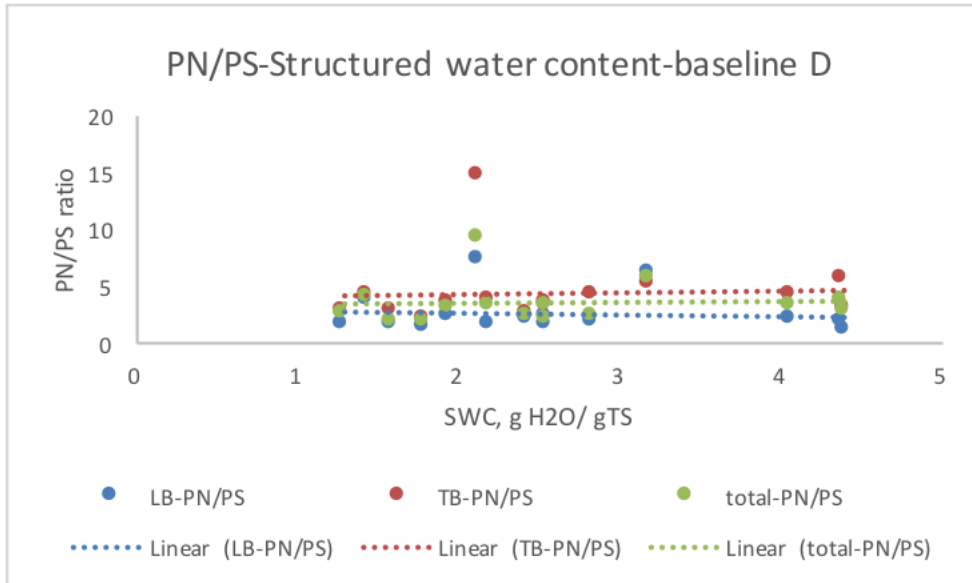


(A)

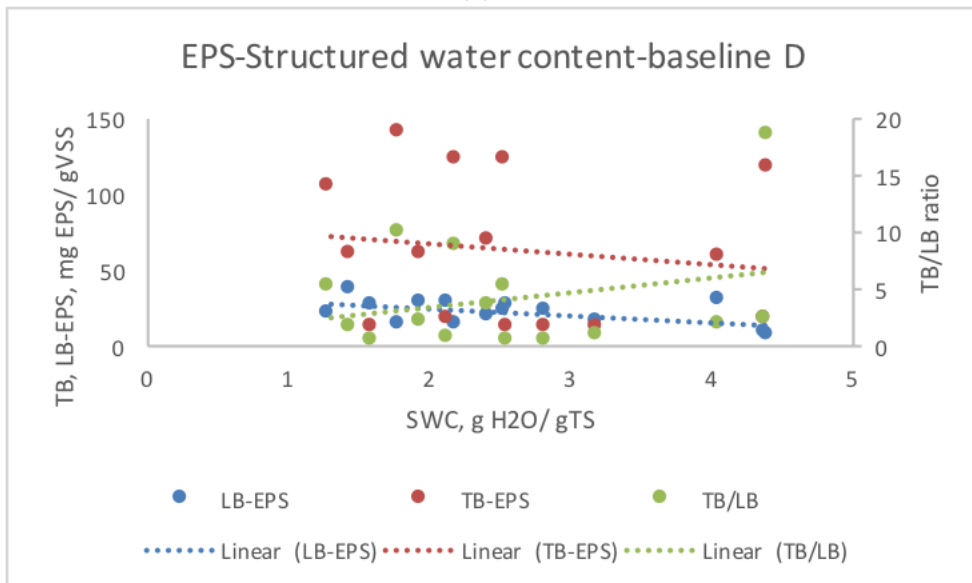


(B)

1679



(C)



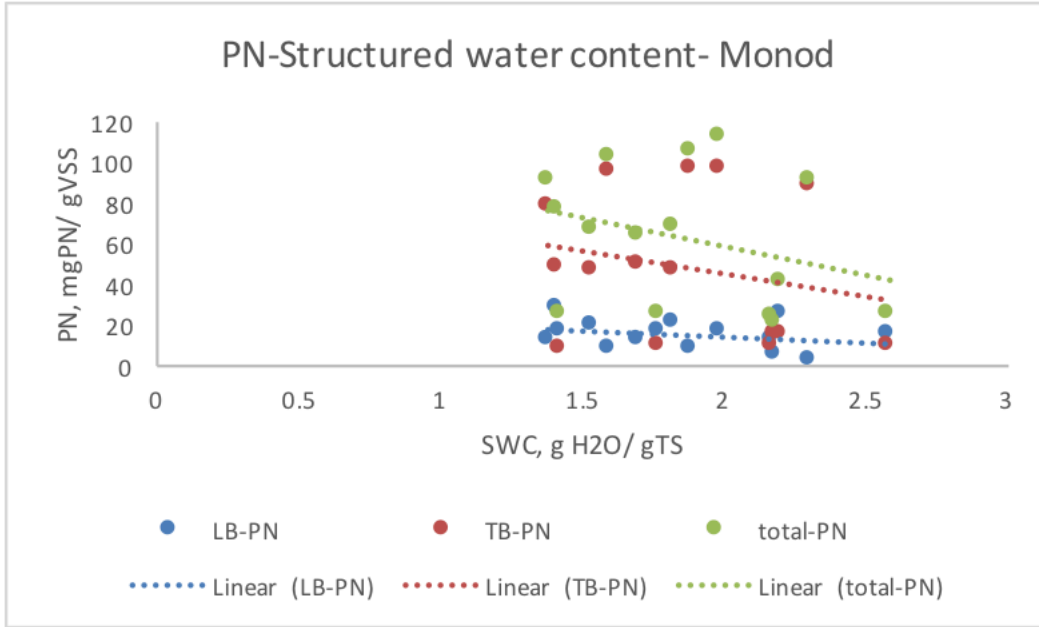
(D)

1680

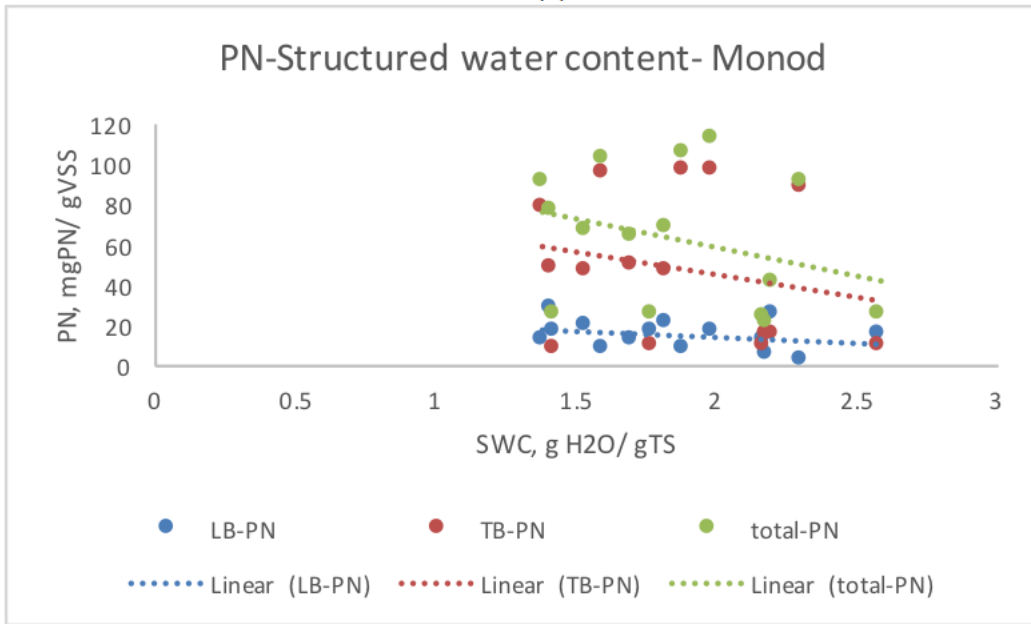
1681 **Figure 4.13.** The relationship between structured water content measured by

1682 weight curve (baseline D) and (A) PN; (B) PS; (C) PN/PS ratio; and (D) EPS.

1683

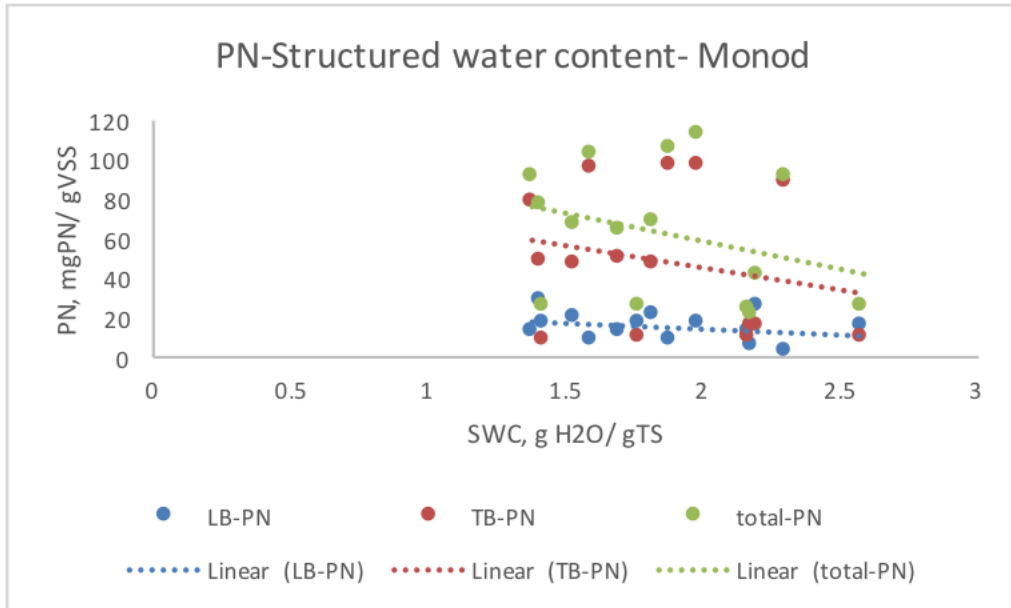


(A)

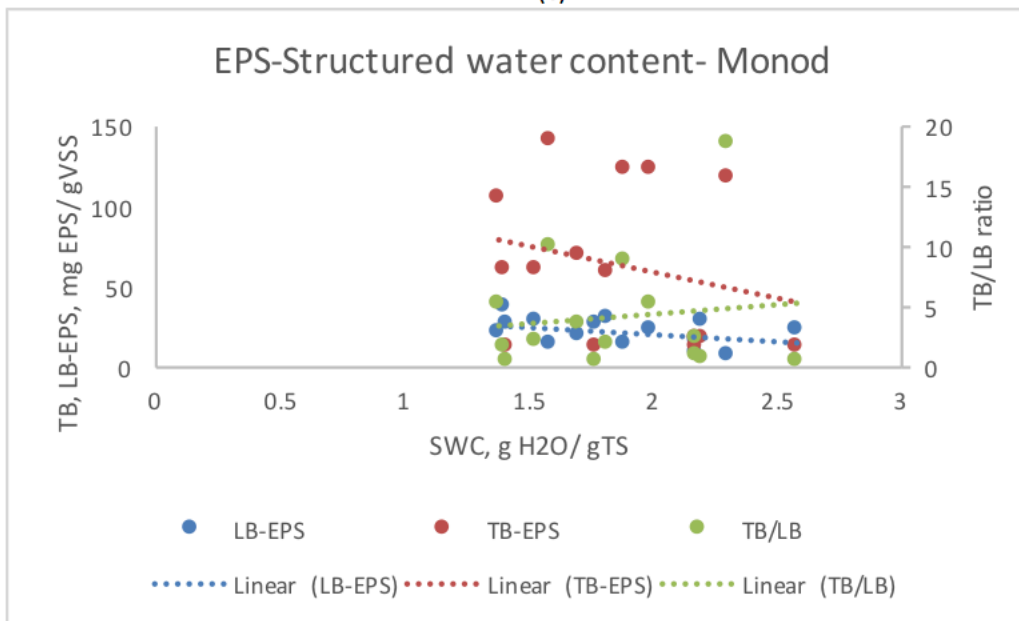


(B)

1684



(C)



(D)

1685

1686 **Figure 4.14.** The relationship between structured water content measured by

1687 Monod model and (A) PN; (B) PS; (C) PN/PS ratio; and (D) EPS.

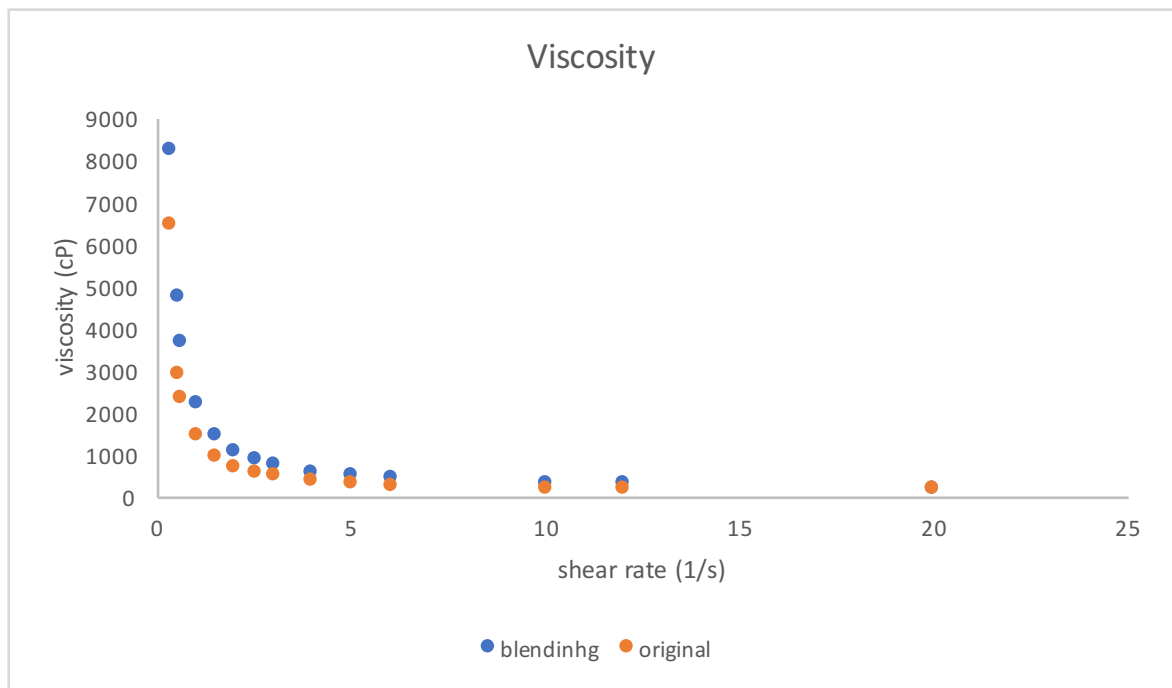
1688

#### 1689 **4.3.4 Impact of Dynamic Viscosity on the Structured Water Content**

1690 Dynamic viscosity was an important characteristic of the sludge, and a  
1691 higher dynamic viscosity indicated that the sludge was more resistant to shearing  
1692 flow. The acting force between the different levels of the sludge might also have  
1693 influence on the evaporation of free water. This study hypothesized that a sludge  
1694 type that had a higher viscosity had a higher structured water content. Blending  
1695 two letters of the primary sludge at 18,000 rpms for 1 minutes (Waring  
1696 Commercial, #WSB) successfully increased the viscosity of the sludge by 60%, as  
1697 shown in Figure 4.15. The TB-EPS was the main fraction of the net-like EPS  
1698 (Yuan, Wang and Feng, 2014) so that determined the structure of the sludge flocs  
1699 (Ding et al., 2015). The fast blending destructed the sludge flocs into smaller  
1700 pieces and released the TB-EPS so that increased the viscosity of the sludge. The  
1701 structured water content of the blended sample was determined using the  
1702 measurement that applying the drying rate curve and baseline A. The structured  
1703 water content of the primary sludge decreased from 2.12 g H<sub>2</sub>O/g TS to 1.50 g  
1704 H<sub>2</sub>O/g TS after blending test, which indicated that increasing the viscosity could  
1705 decrease the structured water content of a sludge type. The result failed to confirm  
1706 the hypothesis. Two possible explanations were raised to explain this  
1707 phenomenon. First, dynamic viscosity described the sludge resistance to the  
1708 shearing flow, however, during the whole drying test, the sample was placed in  
1709 the aluminum tank steadily, with no shearing flow occurred, so that the vertical  
1710 evaporation was not affected by the dynamic viscosity. Second, blending the  
1711 sludge sample at a high mixing speed could cause shear force and centrifugal

1712 effect. These two effects could break the flocs into smaller pieces, so that release  
1713 part of the interstitial water, which was supposed to be trapped in the cracks of the  
1714 flocs, into free water. Therefore, blending the primary sludge finally decreased the  
1715 structured water content in the sludge.

1716 Dynamic viscosity of other sludge types should be measured and analyzed  
1717 considering their TS and structured water content, so that more data would be  
1718 available to make a full curve about the relationship between the viscosity and the  
1719 structured water content.

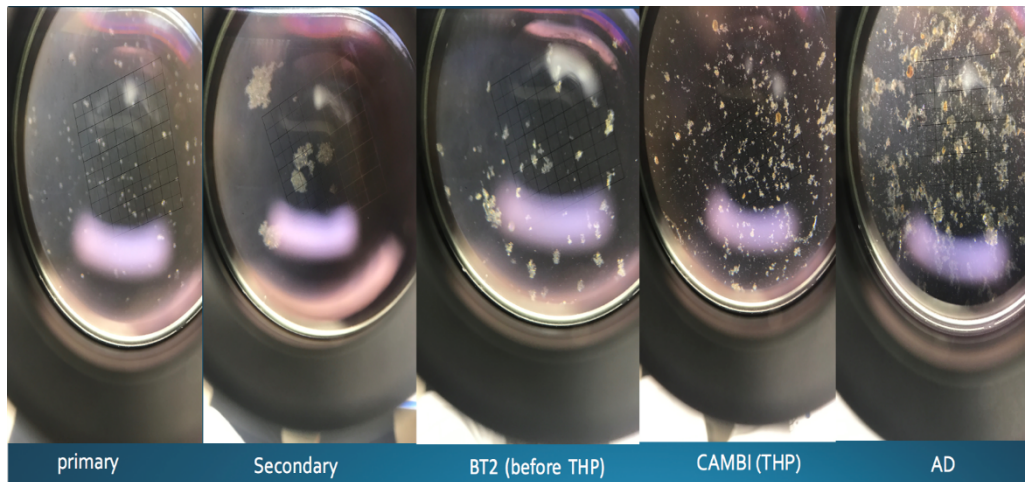


1720  
1721 **Figure 4.15.** Dynamic viscosity for the primary sludge before blending (orange)  
1722 and after blending (blue).

1723

1724 **4.3.5 Impact of Floc Size on the Structured Water Content**

1725           Flocs of the five sludge types under the microscope were shown in Figure  
1726 4.16, and the floc sizes based on 500 flocs of each sample was listed in Table 4.2.  
1727 The secondary sludge had the biggest flocs followed by the sludge before THP  
1728 and primary sludge, and the Cambi sludge had the smallest floc size. AD sludge  
1729 flocs did not show clear floc shapes under the microscope, and it was more like a  
1730 mash with pieces of particles. In the AD sludge, large flocs that connected to each  
1731 other were observed, as well as some tiny flocs that distributed in the extra places,  
1732 making it hard to determine the floc size. Considering AD and secondary sludge,  
1733 which both had big floc size also had more structure water content, floc size could  
1734 be considered as an important characteristic of a sludge that was correlated with  
1735 SWC ( $R^2=0.77$  and  $0.60$  for baseline A and baselien B, respectively).



1737 **Figure 4.16.** Flocs of five sludge types under microscope view. Secondary and  
1738 anaerobic digestion (AD) sludge had larger floc sizes than other sludge types.

1739

1740 **Table 4.2.** Floc sizes for the primary sludge, secondary sludge, sludge before  
1741 THP and sludge after THP.

unit: $\mu\text{m}$	average	max	min
primary	26.8	109	5
secondary	68.3	243	10
before THP (BT2)	41.9	108	10
Cambi (THP)	21.9	50	10

1742

1743

#### 1744 **4.3.6 Assessment of the approaches for determination of the Structured**

#### 1745 **Water Content**

1746 The five objective measurements of the structured water content all aimed  
1747 at eliminating the subjective judgement caused by visual observations or  
1748 contrived choices when determine the structured water content. The structured  
1749 water content determined when applying the drying rate curve had similar values  
1750 for each sludge type. However, applying the Monod model and weight curve  
1751 usually caused different results. Therefore, a comprehensive discussion about the  
1752 five measurements was necessary, considering both theoretical meaning and  
1753 practical meaning.

1754

#### 1755 **4.3.6.1 Penman's Equation for the free water evaporation rate (baseline A)**

1756 Penman's equation was a widely applied estimate for the free water  
1757 evaporation, however, it fitted the big surface water systems like lakes

1758 (Valiantzas, 2006). In this study, an aluminum tank (diameter=54.17 mm) was  
1759 applied as the container of the drying sample, which was apparently not a big  
1760 surface area. The fringe effect would not be neglected in this study. Simplified  
1761 Penman's equation was applied in this study because only temperature, relative  
1762 humidity and wind speed were required, which were accessible from the drying  
1763 test. This measurement was the only one that applied all the environmental  
1764 impacts into the structured water content determination among the five  
1765 measurements. The limited researches on the free water evaporation with small  
1766 surface area and their complicated model was another reason of why other model  
1767 was not applied (Koerselman and Beltman, 1988). The free water evaporation in  
1768 the environmental water system was not same as that in the sludge. The  
1769 interaction between the water molecules and the sludge flocs would influence the  
1770 free water evaporation. For all drying samples, the absolute error between the  
1771 drying rate data and the baseline A kept small and steady from 5-15 g H<sub>2</sub>O/ g TS,  
1772 indicating that it belonged to the free water evaporation period. Therefore, this  
1773 part of data was applied to set the threshold.

1774

#### 1775 **4.3.6.2 Slope of the weight curve for the free water evaporation (baseline B)**

1776 The real drying rate was the result of the weight lost with 30s divided by  
1777 the time interval, therefore, the slope of the weight vs. time curve should represent  
1778 the drying rate. During the first half of the drying test, it was free water that  
1779 evaporated, and it should have a constant drying rate theoretically, even though in  
1780 the experimental condition, the drying rate fluctuated slightly effected by the

1781 slight change of the experimental environment. The slope of the weight curve  
1782 using data from 3-20 hours could be considered as the average evaporation rate of  
1783 the free water, therefore was applied as the baseline B for the free water  
1784 evaporation. This was also a good way to combine the information of the drying  
1785 rate curve and weight curve together. The threshold of the structured water  
1786 content was set considering the data from 5-15 g H<sub>2</sub>O/ g TS to keep coincidence  
1787 with baseline A. This measurement was more influenced by the experimental  
1788 factors than the last one (baseline A). A saltation in the environmental conditions,  
1789 no matter temperature, relative humidity or wind speed changed, could cause a  
1790 variation in the drying rate. However, such variation was neutralized and could  
1791 not be shown in the baseline B when calculating the average drying rate as the  
1792 free water evaporation rate. Therefore, this measurement could only be considered  
1793 when the experimental environment was controlled scrupulously.

1794

#### 1795 **4.3.6.3 Monod model to simulate the drying test**

1796 Monod model was applied to simulate the drying rate curve, aiming to  
1797 find the mathematical expression of the complicated curve for further data  
1798 analysis. The drying rate curve had the similar figure shape of the Monod model  
1799 curve, and “Rstudio” software successfully provided the coefficients for the  
1800 function expression. This was the only measurement that provided a mathematical  
1801 expression of the drying rate. However, the Monod model did not fit all the  
1802 samples well, especially when the free water drying rate fluctuated obviously. The  
1803 threshold of the structured water content was determined as the slope of the

1804 Monod model started to be bigger than 0.08 considering the reasonable structured  
1805 water content values. Other threshold could be chosen and other mathematical  
1806 analysis of the Monod model could be considered based on particular  
1807 requirement.

1808

#### 1809 **4.3.6.4 Proportional part of weight curve for the free water evaporation**

##### 1810 **(baseline C)**

1811 As discussed above, the first half of the drying test was the free water  
1812 evaporation, and since it had constant drying rate, a proportional linear part of the  
1813 weight curve could be observed and served as the free water evaporation baseline.  
1814 The error between the baseline C and the real weight change was plotted then, and  
1815 an exponential function was determined to represent the error plot. These steps  
1816 did help to provide an objective measurement of the structured water content,  
1817 however, too many calculations on the raw data introduced multistep error  
1818 between the final data and the raw data. Also, the accomplishment of this  
1819 measurement based on the determination of the exponential function of the error  
1820 between the baseline C and the real weight change. The coefficients of the  
1821 exponential function had significant influence on the structure water content.

1822

#### 1823 **4.3.6.5 Weight change from the calculated drying rate for the free water**

##### 1824 **evaporation (baseline D)**

1825 Applying the calculated free water evaporation rate to the weight curve  
1826 was another attempt to combine the information of the two curves together. The

1827 weight change from the calculated free water evaporation rate fitted to the real  
1828 weight change best (Figure 4.5), and for most (>80%) drying tests, it was hard to  
1829 tell the difference of the baseline D and the real weight change visually. This  
1830 approach considered the experimental environmental impactors such as  
1831 temperature, relative humidity and wind speed into calculation when applying the  
1832 Penman's equation.

1833

#### 1834 **4.4 Conclusion**

1835         The five approaches for determination of the structured water content in  
1836 the sludge meet the requirements as an objective measurement with both  
1837 advantages and shortcomings. Applying the drying rate curve and baseline A  
1838 approach considered the impact of environmental conditions such temperature  
1839 and relative humidity into the calculation, so this approach could be applied when  
1840 these experimental conditions were unstable. Penman's equation estimated the  
1841 free water evaporation rate under big surface area, however, the drying test  
1842 applied aluminum pan (diameter =5.4 cm) as the sludge container, and the  
1843 influence of the fringe effect such as the adsorption interaction between the sludge  
1844 and aluminum pan could not be ignored in this case. Baseline B provided a  
1845 constant drying rate simulating the free water evaporation under fixed temperature  
1846 and humidity. However, it failed to represent the influence of the experimental  
1847 condition changes. The weight curve provided a flatter curve than the drying rate  
1848 curve, but neither baseline C nor baseline D could be considered as a good  
1849 measurement. The problems that occurred in the baseline B approach also

1850 occurred for the baseline C approach. Baseline D combined the information of the  
1851 drying rate curve and weight curve together, and it also took experimental  
1852 impactors into consideration. The Monod model was the only one that provided a  
1853 mathematical expression of the drying rate. However, results indicated that it was  
1854 influenced by the experimental conditions such as temperature and relative  
1855 humidity and could not be applied when the experimental conditions fluctuated.

1856         Structured water referred to the moisture content that could not be  
1857 removed by physical dewatering process, so that could be applied to predict cake  
1858 TS for a sludge (Werther and Ogada, 1999). However, the structured water  
1859 content determined based on the five approaches in this project could not predict  
1860 the cake TS of each sludge type accurately. The dewatering process removed the  
1861 free water as well as a proportion of the interstitial water from the sludge, which  
1862 resulted in a lower moisture content in the cake solids and a higher cake TS  
1863 compared with the results of this project. However, for the sludge types that  
1864 contained more EPS reduced dewaterability of the sludge was observed leading to  
1865 increased moisture content in the cake solids. This caused a reduced cake TS  
1866 compared with the results of this project.

1867         There was no strong correlation between the EPS sludge composition or  
1868 dynamic viscosity and the structured water content ( $R^2 < 0.5$ ) was observed.  
1869 Among the EPS compounds, a larger  $R^2$  was observed between the structured  
1870 water content and the LB-EPS-PS ( $R^2 = 0.64$ ), indicating a negative correlation,  
1871 however, it still failed to indicated a significant correlation. The structured water

1872 content was positively correlated with the floc size of the sludge ( $R^2=0.77$  and  
1873 0.60 for baseline A and baseline B, respectively).

1874

#### 1875 **4.5 Acknowledgements**

1876 The authors appreciated the support from the Blue Plains Advance  
1877 Wastewater Treatment Plant (DC Water), who funded this study and made it  
1878 possible. The Civil and Environmental Department of the University of Maryland  
1879 also provided valuable support on this project.

1880

#### 1881 **4.6 References**

- 1882 Basuvaraj, M., Fein, J. and Liss, S. (2015). Protein and polysaccharide content of  
1883 tightly and loosely bound extracellular polymeric substances and the  
1884 development of a granular activated sludge floc. *Water Research*, 82,  
1885 pp.104-117.
- 1886 Benhidour, H. and Onisawa, T. (2010). Interactive Learning of Verbal Descriptors  
1887 Meanings for Face Drawing System. *Journal of Advanced Computational  
1888 Intelligence and Intelligent Informatics*, 14(6), pp.606-615.
- 1889 Chu, C. and Lee, D. (1999). Moisture Distribution in Sludge: Effects of Polymer  
1890 Conditioning. *Journal of Environmental Engineering*, 125(4), pp.340-345.
- 1891 Colin, F. and Gazbar, S. (1995). Distribution of water in sludges in relation to  
1892 their mechanical dewatering. *Water Research*, 29(8), pp.2000-2005.
- 1893 Cuesta, G., Suarez, N., Bessio, M., Ferreira, F. and Massaldi, H. (2003).  
1894 Quantitative determination of pneumococcal capsular polysaccharide  
1895 serotype 14 using a modification of phenol–sulfuric acid method. *Journal  
1896 of Microbiological Methods*, 52(1), pp.69-73.
- 1897 Ding, Z., Bourven, I., Guibaud, G., van Hullebusch, E., Panico, A., Pirozzi, F. and  
1898 Esposito, G. (2015). Role of extracellular polymeric substances (EPS)  
1899 production in bioaggregation: application to wastewater  
1900 treatment. *Applied Microbiology and Biotechnology*, 99(23), pp.9883-  
1901 9905.
- 1902 Dinuccio, E., Balsari, P., Gioelli, F. and Menardo, S. (2010). Evaluation of the  
1903 biogas productivity potential of some Italian agro-industrial  
1904 biomasses. *Bioresource Technology*, 101(10), pp.3780-3783.
- 1905 DuBois, M., Gilles, K.A., Hamilton, J.K., Rebers, P., Smith, F. 1956.  
1906 Colorimetric method for determination of sugars and related substances.  
1907 *Analytical chemistry*, 28, 350-356.

- 1908 Dulley, J. and Grieve, P. (1975). A simple technique for eliminating interference  
1909 by detergents in the Lowry method of protein determination. *Analytical*  
1910 *Biochemistry*, 64(1), pp.136-141.
- 1911 El-Kamah, H., Tawfik, A., Mahmoud, M. and Abdel-Halim, H. (2010). Treatment  
1912 of high strength wastewater from fruit juice industry using integrated  
1913 anaerobic/aerobic system. *Desalination*, 253(1-3), pp.158-163.
- 1914 Escot, S., Feuillat, M., Dulau, L. and Charpentier, C. (2001). Release of  
1915 polysaccharides by yeasts and the influence of released polysaccharides on  
1916 colour stability and wine astringency. *Australian Journal of Grape and*  
1917 *Wine Research*, 7(3), pp.153-159.
- 1918 Folin, O. and Ciocalteu, V. (1927). On Tyrosine and Tryptophane Determinations  
1919 in Proteins. *Biological Chemistry*, (73), pp.627-650.
- 1920 Houghton, J.I., Quarmby, J., Stephenson, T. (2001). Municipal wastewater sludge  
1921 dewaterability and the presence of microbial extracellular polymer. *Water*  
1922 *Sci. Tech.* (44). pp.373-379.
- 1923 J, Kopp. and N, Dichtl. (2000). Prediction of full-scale dewatering results by  
1924 determining the water distribution of sewage sludges. *Water Science and*  
1925 *Technology*, 42(9), pp.141-149.
- 1926 Koerselman, W. and Beltman, B. (1988). Evapotranspiration from fens in relation  
1927 to Penman's potential free water evaporation (EO) and pan  
1928 evaporation. *Aquatic Botany*, 31(3-4), pp.307-320.
- 1929 Lee, D. (1996). Interpretation of bound water data measured via dilatometric  
1930 technique. *Water Research*, 30(9), pp.2230-2232.
- 1931 Lee, D. and Hsu, Y. (1995). Measurement of bound water in sludges: A  
1932 comparative study. *Water Environment Research*, 67(3), pp.310-317.
- 1933 Lee, D., Lai, J. and Mujumdar, A. (2006). Moisture Distribution and Dewatering  
1934 Efficiency for Wet Materials. *Drying Technology*, 24(10), pp.1201-1208.
- 1935 Li, X. and Yang, S. (2007). Influence of loosely bound extracellular polymeric  
1936 substances (EPS) on the flocculation, sedimentation and dewaterability of  
1937 activated sludge. *Water Research*, 41(5), pp.1022-1030.
- 1938 Lowry, O.H., Rosebrough, N.J., Farr, A.L., Randall, R.J. 1951. Protein  
1939 measurement with the Folin phenol reagent. *J biol Chem*, 193(1), 265-275
- 1940 Lu, Q., He, Z. and Stoffella, P. (2012). Land Application of Biosolids in the USA:  
1941 A Review. *Applied and Environmental Soil Science*, 2012, pp.1-11.
- 1942 Markwell, M., Haas, S., Bieber, L. and Tolbert, N. (1978). A modification of the  
1943 Lowry procedure to simplify protein determination in membrane and  
1944 lipoprotein samples. *Analytical Biochemistry*, 87(1), pp.206-210.
- 1945 Martin, R. (2001). Noise power spectral density estimation based on optimal  
1946 smoothing and minimum statistics. *IEEE Transactions on Speech and*  
1947 *Audio Processing*, 9(5), pp.504-512.
- 1948 Matsuda, A., Kawasaki, K. and Mizukawa, Y. (1992). Measurement of bound  
1949 water in excess activated sludges and effect of freezing and thawing  
1950 process on it. *J. Chem. Eng. Japan / JCEJ*, 25(1), pp.100-103.
- 1951 Mikkelsen, L. (2002). Physico-chemical characteristics of full scale sewage  
1952 sludges with implications to dewatering. *Water Research*, 36(10),  
1953 pp.2451-2462.

- 1954 More, T., Yadav, J., Yan, S., Tyagi, R. and Surampalli, R. (2014). Extracellular  
 1955 polymeric substances of bacteria and their potential environmental  
 1956 applications. *Journal of Environmental Management*, 144, pp.1-25.
- 1957 Neyens, E. (2004). Advanced sludge treatment affects extracellular polymeric  
 1958 substances to improve activated sludge dewatering. *Journal of Hazardous*  
 1959 *Materials*, 106(2-3), pp.83-92.
- 1960 Penman, H. (1948). Natural Evaporation from Open Water, Bare Soil and  
 1961 Grass. *Proceedings of the Royal Society A: Mathematical, Physical and*  
 1962 *Engineering Sciences*, 193(1032), pp.120-145.
- 1963 Peterson, G. (1979). Review of the folin phenol protein quantitation method of  
 1964 lowry, rosebrough, farr and randall. *Analytical Biochemistry*, 100(2),  
 1965 pp.201-220.
- 1966 Ren, B., Young, B., Variola, F. and Delatolla, R. (2016). Protein to  
 1967 polysaccharide ratio in EPS as an indicator of non-optimized operation of  
 1968 tertiary nitrifying MBBR. *Water Quality Research Journal of Canada*,  
 1969 51(4), pp.297-306.
- 1970 Robinson, J. and Knocke, W. (1992). Use of dilatometric and drying techniques  
 1971 for assessing sludge dewatering characteristics. *Water Environment*  
 1972 *Research*, 64(1), pp.60-68.
- 1973 Roy, M., Dutta, A., Corscadden, K., Havard, P. and Dickie, L. (2011). Review of  
 1974 biosolids management options and co-incineration of a biosolid-derived  
 1975 fuel. *Waste Management*, 31(11), pp.2228-2235.
- 1976 Ruiz-Hernando, M., Labanda, J. and Llorens, J. (2010). Effect of ultrasonic waves  
 1977 on the rheological features of secondary sludge. *Biochemical Engineering*  
 1978 *Journal*, 52(2-3), pp.131-136.
- 1979 Sheng, G., Yu, H. and Li, X. (2010). Extracellular polymeric substances (EPS) of  
 1980 microbial aggregates in biological wastewater treatment systems: A  
 1981 review. *Biotechnology Advances*, 28(6), pp.882-894.
- 1982 Siddhanta, A., Shanmugam, M., Mody, K., Goswami, A. and Ramavat, B. (1999).  
 1983 Sulphated polysaccharides of *Codium dwarkense* Boergs. from the west  
 1984 coast of India: chemical composition and blood anticoagulant  
 1985 activity. *International Journal of Biological Macromolecules*, 26(2-3),  
 1986 pp.151-154.
- 1987 Smith, J. and Vesilind, P. (1995). Dilatometric measurement of bound water in  
 1988 wastewater sludge. *Water Research*, 29(12), pp.2621-2626.
- 1989 Sponza, D. (2002). Extracellular polymer substances and physicochemical  
 1990 properties of flocs in steady and unsteady-state activated sludge systems.  
 1991 *Process Biochemistry*, 37(9), pp.983-998.
- 1992 Strigul, N., Dette, H. and Melas, V. (2009). A practical guide for optimal designs  
 1993 of experiments in the Monod model. *Environmental Modelling &*  
 1994 *Software*, 24(9), pp.1019-1026.
- 1995 Tsang, K.R. and Vesilind, P.A. (1990). Moisture distribution in sludges. *Wat.*  
 1996 *Sci.Tech.*, 22(12), 135-142.
- 1997 Vaxelaire, J. (2001). Moisture sorption characteristics of waste activated sludge.  
 1998 *Journal of Chemical Technology & Biotechnology*, 76(4), pp.377-382.
- 1999 Valiantzas, J. (2006). Simplified versions for the Penman evaporation equation

2000 using routine weather data. *Journal of Hydrology*, 331(3-4), pp.690-702.

2001 Vaxelaire, J. and Cézac, P. (2004). Moisture distribution in activated sludges: a

2002 review. *Water Research*, 38(9), pp.2215-2230.

2003 Vesilind, P. (1994). The role of water in sludge dewatering. *Water Environment*

2004 *Research*, 66(1), pp.4-11.

2005 Wakeman, R. (2007). Separation technologies for sludge dewatering. *Journal of*

2006 *Hazardous Materials*, 144(3), pp.614-619.

2007 Wingender, J., Neu, T. and Flemming, H. (1999). *Microbial extracellular*

2008 *polymeric substances*. 1st ed. Berlin: Springer.

2009 Wu, C., Huang, C. and Lee, D. (1998). Bound water content and water binding

2010 strength on sludge flocs. *Water Research*, 32(3), pp.900-904.

2011 Yuan, D., Wang, Y. and Feng, J. (2014). Contribution of stratified extracellular

2012 polymeric substances to the gel-like and fractal structures of activated

2013 sludge. *Water Research*, 56, pp.56-65.

2014

2015

2016

2017

2018

2019

2020

2021

2022

2023

2024

2025

2026

2027

2028

2029

2030

2031

2032

2033

2034

2035

2036

2037

2038

2039

## 2040 **Chapter 5: Conclusion**

2041 Biosolids production is important to the solid treatment process in the  
2042 wastewater treatment facilities. It contains high content of nutrients beneficial for  
2043 soil reclamation thus biosolids have been widely applied in land applications as  
2044 fertilizer. This study investigated the enhancement of the biosolids production  
2045 from two aspects: 1) sludge clarification, which increased the source of the  
2046 biosolids and enhanced the biosolids production quantitatively, and 2) sludge  
2047 dewaterability, which determined the moisture content in the biosolids and  
2048 enhanced the biosolids production qualitatively. Removing moisture content from  
2049 the biosolids reduced its volume, so that saved cost and energy consumption of  
2050 the biosolids storage, transportation and disposal.

2051 Bioflocculation was an important step for the activated sludge  
2052 clarification. The high-rate activated sludge bioflocculation limitations were  
2053 studied by modified jar tests and polymer dosing. Polymer dosing involving  
2054 coagulant, linear polymer and branched polymer enhanced the coagulation,  
2055 flocculation and floc strength, respectively. The results indicated that the three  
2056 activated sludge types that were tested at DC Water exhibited different limitations  
2057 (Chapter 3). High-rate activated sludge (HRAS) was flocculation limited as well  
2058 as coagulation limited, and dosing experiments with coagulant and polymers both  
2059 caused improvements of the sludge bioflocculation. Bioaugmentation with sludge  
2060 from biological nutrient removal (BNR) reactor mitigated the flocculation  
2061 limitation in the HRAS. However, bioaugmented high-rate activated sludge  
2062 (BioHRAS) was floc strength limited, and branched polymer enhanced its

2063 bioflocculation by strengthening the sludge flocs (Chapter 3, Figure 3.5). BNR  
2064 sludge showed the best bioflocculation behavior among the three activated sludge  
2065 types, with least effluent total suspended solids (TSS) ( $6.96 \pm 4.49$  mg/L),  
2066 indicating no flocculation and floc strength limitations.

2067         The structured water content is important for the dewaterability of the  
2068 sludge, since it determines the moisture content in the biosolids. To test this  
2069 parameter, a drying test was evaluated using five sludge types (primary sludge,  
2070 secondary sludge, sludge before thermal hydrolysis process (THP), sludge after  
2071 THP and sludge after anaerobic digestion (AD)) in the Blue Plains WWTP. Based  
2072 on these experiments five approaches were assessed in this study. The results  
2073 showed that the five approaches could be used under different circumstances:

- 2074         • The drying rate curve and baseline A could be applied when the influence  
2075             of the experiment temperature (T), relative humidity (RH) or wind speed  
2076             was significant because the equation of baseline A took these  
2077             environmental impactors into consideration.
- 2078         • Baseline B could be applied only when the experimental environment (T,  
2079             RH and wind speed) was constant.
- 2080         • The weight curve and baseline C also depended on the experimental  
2081             conditions such as T, RH and wind speed. The data analysis of this  
2082             approach involved multistep calculation such as rolling average, curve  
2083             fitting and slope calculation, where multiple errors caused by each step  
2084             could not be avoided for this measurement.

- 2085       • Baseline D fitted the real weight change best with small absolute  
2086       difference between the real weight change and the baseline D (range from  
2087       0.0001g to 0.001g). It also took environmental impactors (T, RH and  
2088       wind speed) into consideration because of the calculated evaporation  
2089       using Penman's equation.
- 2090       • The Monod model provided a mathematical expression of the drying rate.  
2091       However, it could only be applied when experimental conditions such as  
2092       T, RH and wind speed were constant, under which the real drying rate  
2093       curve had an approximate shape of the Monod model.

2094

2095       The structured water content determined by these five objective  
2096       determinations did not match the cake TS of the five sludge types because  
2097       different from this project, which considered all the interstitial water as the  
2098       structured water, the dewatering process removed a proportion of interstitial water  
2099       from the anaerobic sludge, so that reduced the moisture content in the cake solids,  
2100       causing a higher cake TS than the calculated cake TS using the structured water  
2101       content from this project. For the sludge that contains high content of EPS such as  
2102       the secondary sludge, which reduced the dewaterability of the sludge, more  
2103       moisture content was left in the cake solids, resulting in a smaller cake TS compared  
2104       with the calculated cake TS using the structured water content from this project.

2105       The relationship between the structured water content and the sludge EPS  
2106       composition, dynamic viscosity and floc size were also studied, and no strong  
2107       correlation was observed between either of them (Chapter 4). However, when

2108 apply the drying rate curve, an obvious stronger correlation between the soluble  
2109 polysaccharide content in the loosely bound extracellular polymeric substances  
2110 (LB-EPS-PS) and the structured water content ( $R^2=0.57$  and  $0.64$  for baseline A  
2111 and B, respectively) was observed, and increased LB-EPS-PS content caused a  
2112 decrease in the structured water content. The size of the sludge flocs was also  
2113 influencing the structured water content ( $R^2=0.77$  and  $0.60$  for baseline A and  
2114 baseline B, respectively). Larger flocs provided more space within the flocs, so  
2115 they could trap more interstitial water than smaller flocs. From another aspect,  
2116 small flocs could be considered as the result of breaking up of the larger flocs.  
2117 During the break up, the floc structure was destroyed, and interstitial water that  
2118 was used to be trapped inside the flocs was released into free water. Therefore,  
2119 increased sludge floc size caused increase in the structured water content.

2120 In the Blue Plains Advanced Wastewater Treatment Plant (DC Water),  
2121 500 tons of wet biosolids are produced every day, with total solid content around  
2122 30% (DC Water, 2017). The facility spends money, manpower and energy on the  
2123 management of these biosolids. 350 tons of water were disposed along with 150  
2124 tons of dry biosolids. The cost caused by storage and transportation of the wet  
2125 biosolids could be reduced by reducing the moisture content in the biosolids and  
2126 enhancing the biosolids production quality. Conventional dewatering processes  
2127 successfully remove free water from the sludge, so that it is the structured water  
2128 that remains in the biosolids (Tsang and Vesilind, 1990). Finding out the sludge  
2129 characteristics that determine its structured water content could provide solutions  
2130 that reduce the structured water content of the sludge, so that achieve less

2131 moisture content in the biosolids and contribute to the biosolids disposal of  
2132 wastewater treatment facilities.

2133

#### 2134 **Future Research Perspectives**

2135 The five approaches of the structured water content measurement all  
2136 achieve the objective of the thesis (objective (2)). However, the data analysis of  
2137 these measurement could be further improved: 1) The Penman's equation used for  
2138 calculating the free water evaporation rate was estimated based on a big surface  
2139 area. Instead, water evaporation on small surface area models (Birdi, Vu and  
2140 Winter, 1989; Erbil, McHale and Newton, 2002) could be applied to match the  
2141 real drying test condition (diameter of drying sample=5.4 cm); 2) The  
2142 determination of the thresholds applied for the five approaches all use the  
2143 combination the "average" and the "standard deviation", assuming the data  
2144 matched normal distribution. Instead, particular distribution of the data should be  
2145 determined for all approaches, such as Chi-square distribution and multimodal  
2146 distribution, and the threshold determination for each approach should consider its  
2147 data distribution characteristics. Therefore, improvement on the data analysis  
2148 mathematically and statistically should be proposed to improve the objective  
2149 measurements of the structured water content.

2150 In this study, a negative correlation between the LB-EPS-PS and  
2151 structured water content was observed. However, the mechanism of how the  
2152 polysaccharide content influenced the structured water content is still unclear. A  
2153 possible hypothesis is that some functional groups or special structure in the LB-

2154 EPS-PS might impact the water-holding capacity of the sludge (Reeves et al.,  
2155 1996). Fluorescent dyes can stain various structures in the EPS according to the  
2156 target of the dye (Madea and Ishida, 1967; Wood and Fulcher, 1983). For  
2157 example, Fluorescein Labeled Concanavalin A (Con A) stains the “ $\beta$ -D-PS”  
2158 structure in the polysaccharide (Lawrence, Neu and Swerhone, 1998). Therefore,  
2159 qualitative and quantitative staining experiments could be applied in a further  
2160 study to detect whether particular structures in the polysaccharide cause the  
2161 influence on the structured water content. A study investigating the LB-EPS-PS  
2162 composition, structure and its influence on the sludge structured water content  
2163 should be proposed for this aspect.

2164         This study also indicated that the structured water content in the sludge  
2165 was positively correlated with its floc size. More detailed research that evaluates  
2166 whether it is the interstitial space within the flocs or other conditions such as the  
2167 floc structure or the composition of the microorganisms in the flocs that cause the  
2168 influence on the structured water content should also be proposed (Basuvaraj,  
2169 Fein and Liss, 2015).

2170         This study could lead to another project that focus on how LB-EPS-PS and  
2171 floc size influence the structured water content in the sludge and what sludge  
2172 characteristics determine the floc size. Therefore, the objectives of the project  
2173 could be determined as: 1) Investigate which structure of the polysaccharide in the  
2174 loosely bound extracellular polymeric substances that influences the sludge  
2175 structured water content; 2) Investigate how sludge floc size influences the sludge  
2176 structured water content; 3) Study which characteristics of the sludge that

2177 determines the floc size. Staining test using fluorescent dyes could detect various  
2178 structures in the polysaccharide, so that investigate whether particular structures  
2179 in the LB-EPS-PS determined the structured water content in the sludge.  
2180 Biological trinocular microscope measures the floc size of various sludge types,  
2181 and floc morphology and smaller structure within the flocs such as its interstitial  
2182 space could be determined using even more precise microscopes. The relationship  
2183 between the structured water content and these floc characteristics could be  
2184 studied to study how floc size influences the structured water content. Thereafter,  
2185 how the floc morphology and size be determined could be investigated. EPS is an  
2186 important compound of the sludge, and its composition such as protein (PN)  
2187 content, polysaccharide (PS) content and PN/PS ratio should be analyzed to study  
2188 its influence on the floc size.

2189

2190

2191

2192

2193

2194 **References (Chapter 1, 2 and 5, excluding manuscript references)**

- 2195 Basuvaraj, M., Fein, J. and Liss, S. (2015). Protein and polysaccharide content of  
2196 tightly and loosely bound extracellular polymeric substances and the  
2197 development of a granular activated sludge floc. *Water Research*, 82,  
2198 pp.104-117.
- 2199 Busch, P. and Stumm, W. (1968). Chemical interactions in the aggregation of  
2200 bacteria bioflocculation in waste treatment. *Environmental Science &*  
2201 *Technology*, 2(1), pp.49-53.
- 2202 Chao, A. and Keinath, T. (1979). Influence of process loading intensity on sludge  
2203 clarification and thickening characteristics. *Water Research*, 13(12),  
2204 pp.1213-1223.
- 2205 Colin, F. and Gazbar, S. (1995). Distribution of water in sludges in relation to  
2206 their mechanical dewatering. *Water Research*, 29(8), pp.2000-2005.
- 2207 Deng, Y., Xu, J., Liu, Y. and Mancl, K. (2014). Biogas as a sustainable energy  
2208 source in China: Regional development strategy application and decision  
2209 making. *Renewable and Sustainable Energy Reviews*, 35, pp.294-303.
- 2210 Derjaguin, B., Landau, L. 1993. Theory of the stability of strongly charged  
2211 lyophobic sols and of the adhesion of strongly charged particles in  
2212 solutions of electrolytes. *Progress in Surface Science*, 43(1-4), 30-59.
- 2213 Basuvaraj, M., Fein, J. and Liss, S. (2015). Protein and polysaccharide content of  
2214 tightly and loosely bound extracellular polymeric substances and the  
2215 development of a granular activated sludge floc. *Water Research*, 82,  
2216 pp.104-117.
- 2217 Birdi, K., Vu, D. and Winter, A. (1989). A study of the evaporation rates of small  
2218 water drops placed on a solid surface. *The Journal of Physical Chemistry*,  
2219 93(9), pp.3702-3703.
- 2220 Erbil, H., McHale, G. and Newton, M. (2002). Drop Evaporation on Solid  
2221 Surfaces: Constant Contact Angle Mode. *Langmuir*, 18(7), pp.2636-2641.
- 2222 Esteller, M., Martínez-Valdés, H., Garrido, S. and Uribe, Q. (2009). Nitrate and  
2223 phosphate leaching in a Phaeozem soil treated with biosolids, composted  
2224 biosolids and inorganic fertilizers. *Waste Management*, 29(6), pp.1936-  
2225 1944.
- 2226 Heukelekian, H. and Weisberg, E. (1956) Bound Water and Activated Sludge  
2227 Bulking, *Sewage and Industrial Wastes*, 28(4), pp. 558–574.
- 2228 Higgins, M., Tom, L. and Sobeck, D. (2004). Case Study I: Application of the  
2229 Divalent Cation Bridging Theory to Improve Biofloc Properties and  
2230 Industrial Activated Sludge System Performance—direct Addition Of  
2231 Divalent Cations. *Water Environment Research*, 76(4), pp.344-352.
- 2232 Jin, B., Wilén, B. and Lant, P. (2003). A comprehensive insight into floc  
2233 characteristics and their impact on compressibility and settleability of  
2234 activated sludge. *Chemical Engineering Journal*, 95(1-3), pp.221-234.
- 2235 J, Kopp. and N, Dichtl. (2000). Prediction of full-scale dewatering results by  
2236 determining the water distribution of sewage sludges. *Water Science and*  
2237 *Technology*, 42(9), pp.141-149.
- 2238 Lastella, G., Testa, C., Cornacchia, G., Notornicola, M., Voltasio, F. and Sharma,

- 2239 V. (2002). Anaerobic digestion of semi-solid organic waste: biogas  
2240 production and its purification. *Energy Conversion and Management*,  
2241 43(1), pp.63-75.
- 2242 Lawrence, J., Neu, T. and Swerhone, G. (1998). Application of multiple  
2243 parameter imaging for the quantification of algal, bacterial and  
2244 exopolymer components of microbial biofilms. *Journal of Microbiological*  
2245 *Methods*, 32(3), pp.253-261.
- 2246 Lee, D. and Hsu, Y. (1995). Measurement of bound water in sludges: A  
2247 comparative study. *Water Environment Research*, 67(3), pp.310-317.
- 2248 Lee, D., Lai, J. and Mujumdar, A. (2006). Moisture Distribution and Dewatering  
2249 Efficiency for Wet Materials. *Drying Technology*, 24(10), pp.1201-1208.
- 2250 Li, Z., Lu, P., Zhang, D., Chen, G., Zeng, S. and He, Q. (2016). Population  
2251 balance modeling of activated sludge flocculation: Investigating the  
2252 influence of Extracellular Polymeric Substances (EPS) content and zeta  
2253 potential on flocculation dynamics. *Separation and Purification*  
2254 *Technology*, 162, pp.91-100.
- 2255 Liu, H. and Fang, H. (2002). Extraction of extracellular polymeric substances  
2256 (EPS) of sludges. *Journal of Biotechnology*, 95(3), pp.249-256.
- 2257 Maeda, H. and Ishida, N. (1967). Specificity of Binding of Hexopyranosyl  
2258 Polysaccharides with Fluorescent Brightener. *The Journal of*  
2259 *Biochemistry*, 62(2), pp.276-278.
- 2260 More, T., Yadav, J., Yan, S., Tyagi, R. and Surampalli, R. (2014). Extracellular  
2261 polymeric substances of bacteria and their potential environmental  
2262 applications. *Journal of Environmental Management*, 144, pp.1-25.
- 2263 Morgan, J.W., Forster, C.F., Evison, L. 1990. A Comparative-Study of the Nature  
2264 of Biopolymers Extracted from Anaerobic and Activated Sludges. *Water*  
2265 *Research*, 24(6), 743-750.
- 2266 Murthy, S., Novak, J. and Holbrook, R. (2000). Optimizing Dewatering of  
2267 Biosolids from Autothermal Thermophilic Aerobic Digesters (ATAD)  
2268 Using Inorganic Conditioners. *Water Environment Research*, 72(6),  
2269 pp.714-721.
- 2270 Neyens, E. (2004). Advanced sludge treatment affects extracellular polymeric  
2271 substances to improve activated sludge dewatering. *Journal of Hazardous*  
2272 *Materials*, 106(2-3), pp.83-92.
- 2273 Novak, J. (2006). Dewatering of Sewage Sludge. *Drying Technology*, 24(10),  
2274 pp.1257-1262.
- 2275 Painter, H. and Viney, M. (1959). Composition of a domestic sewage. *Journal of*  
2276 *Biochemical and Microbiological Technology and Engineering*, 1(2),  
2277 pp.143-162.
- 2278 Parkin, G. and Owen, W. (1986). Fundamentals of Anaerobic Digestion of  
2279 Wastewater Sludges. *Journal of Environmental Engineering*, 112(5),  
2280 pp.867-920.
- 2281 Poduska, R. and Hicks, J. (1979). Polymer Addition for Effluent Quality  
2282 Control. *Water Pollution Control Federation*, 51(11), pp.2615-2615.
- 2283 Reeves, P., Hobbs, M., Valvano, M., Skurnik, M., Whitfield, C., Coplin, D., Kido,  
2284 N., Klena, J., Maskell, D., Raetz, C. and Rick, P. (1996). Bacterial

2285 polysaccharide synthesis and gene nomenclature. *Trends in Microbiology*,  
2286 4(12), pp.495-503.

2287 Sheng, G., Yu, H. and Li, X. (2010). Extracellular polymeric substances (EPS) of  
2288 microbial aggregates in biological wastewater treatment systems: A  
2289 review. *Biotechnology Advances*, 28(6), pp.882-894.

2290 Singh, R., Nayak, B., Biswal, D., Tripathy, T. and Banik, K. (2003). Biobased  
2291 polymeric flocculants for industrial effluent treatment. *Materials Research*  
2292 *Innovations*, 7(5), pp.331-340.

2293 Smith, J. and Vesilind, P. (1995). Dilatometric measurement of bound water in  
2294 wastewater sludge. *Water Research*, 29(12), pp.2621-2626.

2295 Stasta, P., Boran, J., Bebar, L., Stehlik, P. and Oral, J. (2006). Thermal processing  
2296 of sewage sludge. *Applied Thermal Engineering*, 26(13), pp.1420-1426.

2297 Tsang, K.R. and Vesilind, P.A. (1990). Moisture distribution in sludges. *Wat.*  
2298 *Sci.Tech.*, 22(12), 135–142.

2299 Urbain, V., Block, J. and Manem, J. (1993). Bioflocculation in activated sludge:  
2300 an analytic approach. *Water Research*, 27(5), pp.829-838.

2301 Vaxelaire, J. (2001). Moisture sorption characteristics of waste activated sludge.  
2302 *Journal of Chemical Technology & Biotechnology*, 76(4), pp.377-382.

2303 Vaxelaire, J. and Cézac, P. (2004). Moisture distribution in activated sludges: a  
2304 review. *Water Research*, 38(9), pp.2215-2230.

2305 Verwey, E.J.W., Overbeek, J.T.G., Overbeek, J.T.G. 1999. Theory of the stability  
2306 of lyophobic colloids. Courier Corporation.

2307 Vesilind, P. (1994). The role of water in sludge dewatering. *Water Environment*  
2308 *Research*, 66(1), pp.4-11.

2309 Vorosmarty, C. (2000). Global Water Resources: Vulnerability from Climate  
2310 Change and Population Growth. *Science*, 289(5477), pp.284-288.

2311 Wakeman, R. (2007). Separation technologies for sludge dewatering. *Journal of*  
2312 *Hazardous Materials*, 144(3), pp.614-619.

2313 Wang, H., Brown, S., Magesan, G., Slade, A., Quintern, M., Clinton, P. and Payn,  
2314 T. (2008). Technological options for the management of  
2315 biosolids. *Environmental Science and Pollution Research - International*,  
2316 15(4), pp.308-317.

2317 Wang, L., Shamma, N. and Hung, Y. (2007). Biosolids treatment processes.  
2318 Totowa, N.J.: Humana Press.

2319 Werther, J. and Ogada, T. (1999). Sewage sludge combustion. *Progress in Energy*  
2320 *and Combustion Science*, 25(1), pp.55-116.

2321 Wood, P. and Fulcher, R. (1983). Dye interactions. A basis for specific detection  
2322 and histochemistry of polysaccharides. *Journal of Histochemistry &*  
2323 *Cytochemistry*, 31(6), pp.823-826.

2324 Wu, C., Huang, C. and Lee, D. (1998). Bound water content and water binding  
2325 strength on sludge flocs. *Water Research*, 32(3), pp.900-904.

2326  
2327  
2328  
2329